

“Gilberto Vlaic” XVII School on Synchrotron Radiation: Fundamentals, Methods and Applications

Muggia (Italy), 16 - 26 September 2024



Analysis of diffraction data

Marco Merlini

Earth Science Department
Università degli Studi di
Milano (Italy)

1) GEOMETRY of diffraction (powder diffraction experiments)

- 1.1) Monochromators
- 1.2) Calibration of beamline parameters
- 1.3) Use of unit cell volume for determination of bulk properties (i.e. thermal expansion, etc.)
- 1.4) Microstructure (i.e. crystallite size)

2) INTENSITY of diffraction

- 2.1) Quantitative analysis
- 2.2) Structure determination (powder and single crystals)

3) EXAMPLES

- 3.1) Diffraction tomography
- 3.2) Single crystal at extreme conditions
- 3.3) Single crystal data processing

1) GEOMETRY of diffraction (powder diffraction experiments)

- 1.1) Monochromators
- 1.2) Calibration of beamline parameters
- 1.3) Use of unit cell volume for determination of bulk properties (i.e. thermal expansion, etc.)
- 1.4) Microstructure (i.e. crystallite size)

Bragg's law

Laue equations

Rietveld fit

Structure factor

2) INTENSITY of diffraction

- 2.1) Quantitative analysis
- 2.2) Structure determination (powder and single crystals)

3) EXAMPLES

- 3.1) Diffraction tomography
- 3.2) Single crystal at extreme conditions
- 3.3) Single crystal data processing

Software:

1) GEOMETRY of diffraction (powder diffraction experiments)

- 1.1) Monochromators
- 1.2) Calibration of beamline parameters
- 1.3) Use of unit cell volume for determination of bulk properties (i.e. thermal expansion, etc.)
- 1.4) Microstructure (i.e. crystallite size)

Bragg's law

Fit2D

Dioptas

Laue equations

Rietveld fit

GSAS

GSAS-II

2) INTENSITY of diffraction

- 2.1) Quantitative analysis
- 2.2) Structure determination (powder and single crystals)

Structure factor

3) EXAMPLES

- 3.1) Diffraction tomography
- 3.2) Single crystal at extreme conditions
- 3.3) Single crystal data processing

Software:

1) GEOMETRY of diffraction (powder diffraction experiments)

- 1.1) Monochromators
- 1.2) Calibration of beamline parameters
- 1.3) Use of unit cell volume for determination of bulk properties (i.e. thermal expansion, etc.)
- 1.4) Microstructure (i.e. crystallite size)

Bragg's law

Fit2D

Dioptas

2) INTENSITY of diffraction

- 2.1) Quantitative analysis
- 2.2) Structure determination (powder and single crystals)

Laue equations

Rietveld fit

GSAS

GSAS-II

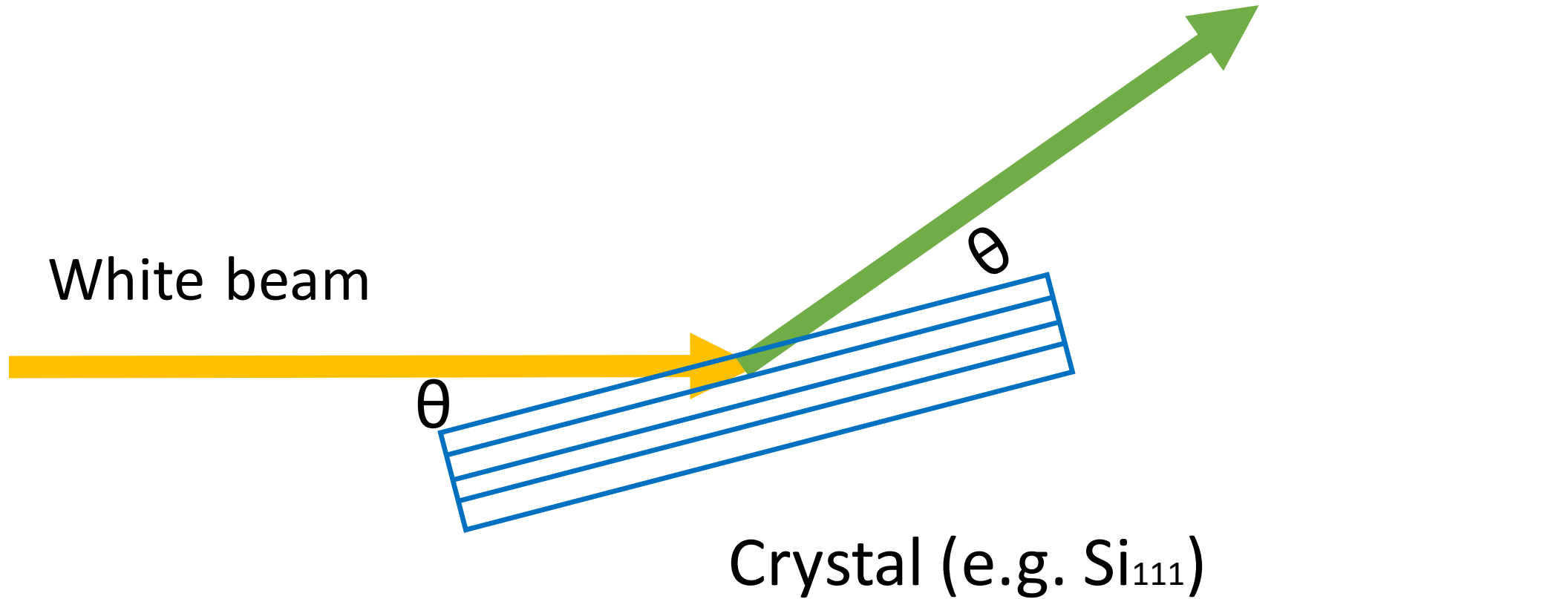
3) EXAMPLES

- 3.1) Diffraction tomography
- 3.2) Single crystal at extreme conditions
- 3.3) Single crystal data processing

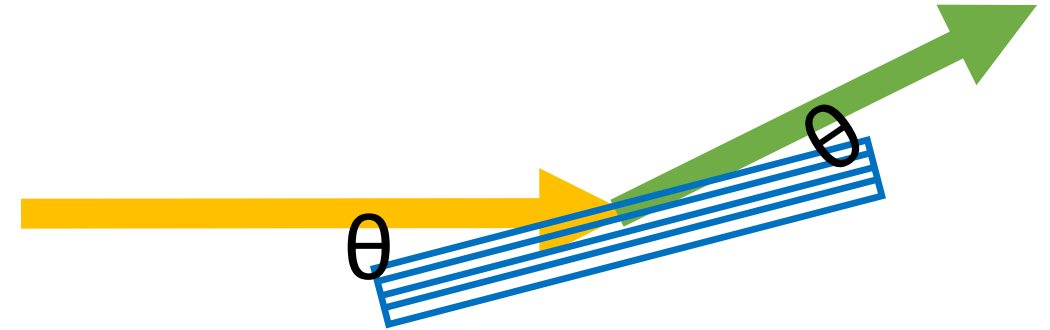
*Crystal structure database
(American Mineralogist database)*

*Single crystal data reduction
(multipurpose – inorganic)*

1.1) Monochromators

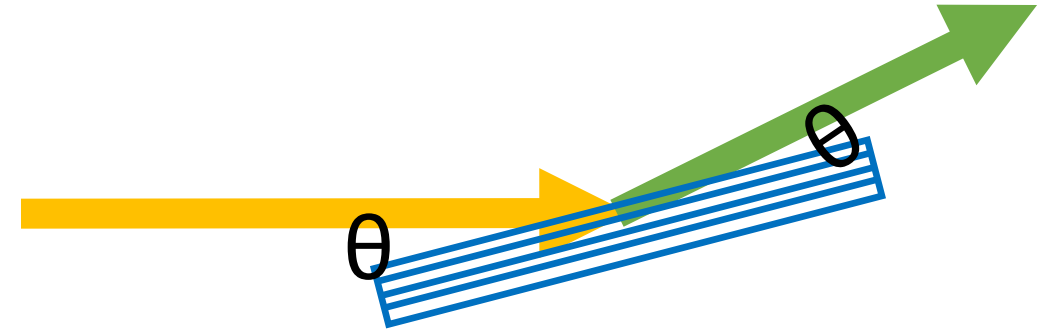


1.1) Monochromators



At which theta angle should be set a Si₁₁₁ monochromator to get 30keV ?

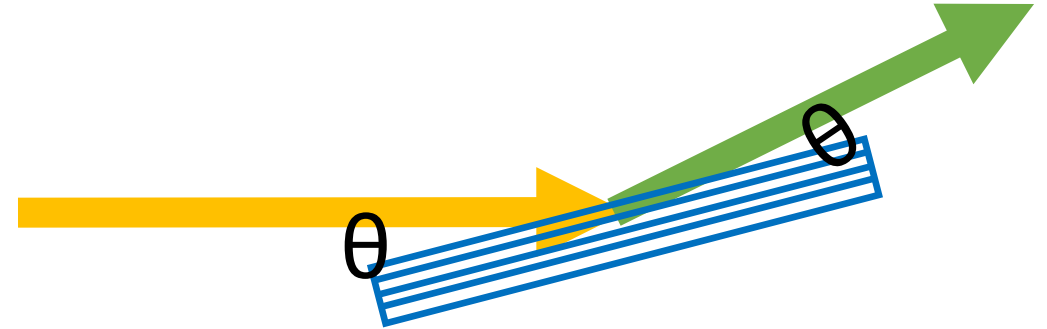
1.1) Monochromators



At which theta angle should be set a Si₁₁₁ monochromator to get 30keV ?

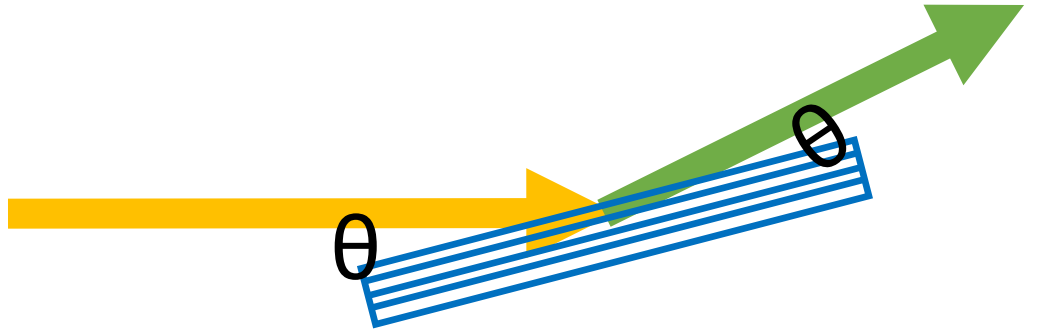
- Need Bragg's law and crystallographic (unit cell) parameters of crystalline silicon

1.1) Monochromators



Bragg's law: $2d_{hkl} \sin\theta = (n)\lambda$

1.1) Monochromators



Bragg's law: $2d_{hkl} \sin\theta = (n)\lambda$

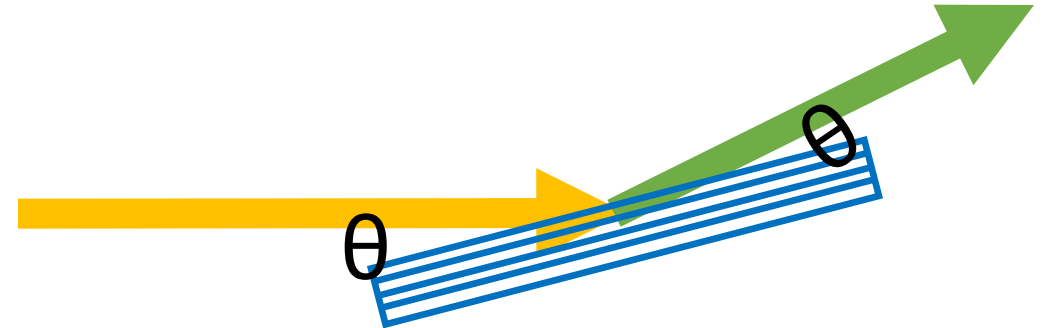
$$E=h\nu=hc/\lambda$$

$$E(\text{keV})=12.4 / \lambda(\text{\AA})$$

12.398...

12.39841930...

1.1) Monochromators



Bragg's law: $2d_{hkl} \sin\theta = (n)\lambda$

$$E=h\nu=hc/\lambda$$

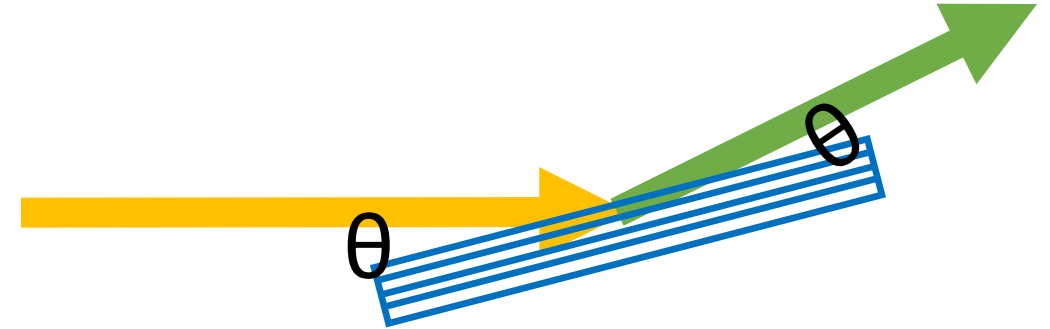
$$E(\text{keV})=12.4 / \lambda(\text{\AA})$$

12.398...

12.39841930...

$$30 \text{ keV} : \lambda = 0.41328 \text{ \AA}$$

1.1) Monochromators



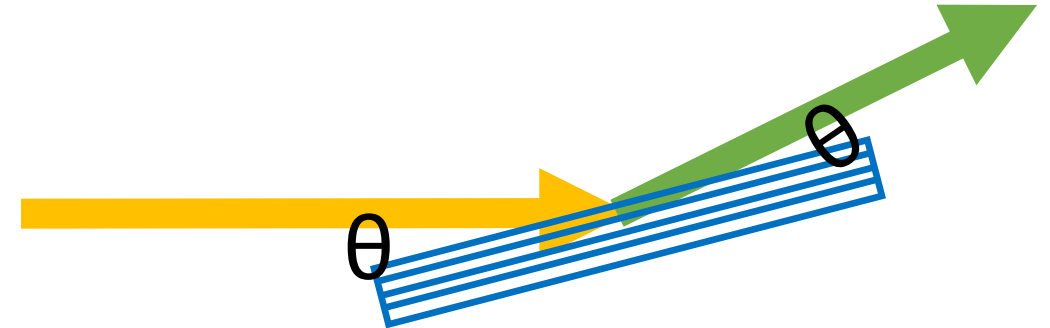
Bragg's law: $2d_{hkl} \sin\theta = (n)\lambda$

Silicon: cubic, $a = 5.43102 \text{ \AA}$

$$1/d^2 = (h^2 + k^2 + l^2)/a^2$$

$$d_{111} = 3.13560 \text{ \AA}$$

1.1) Monochromators



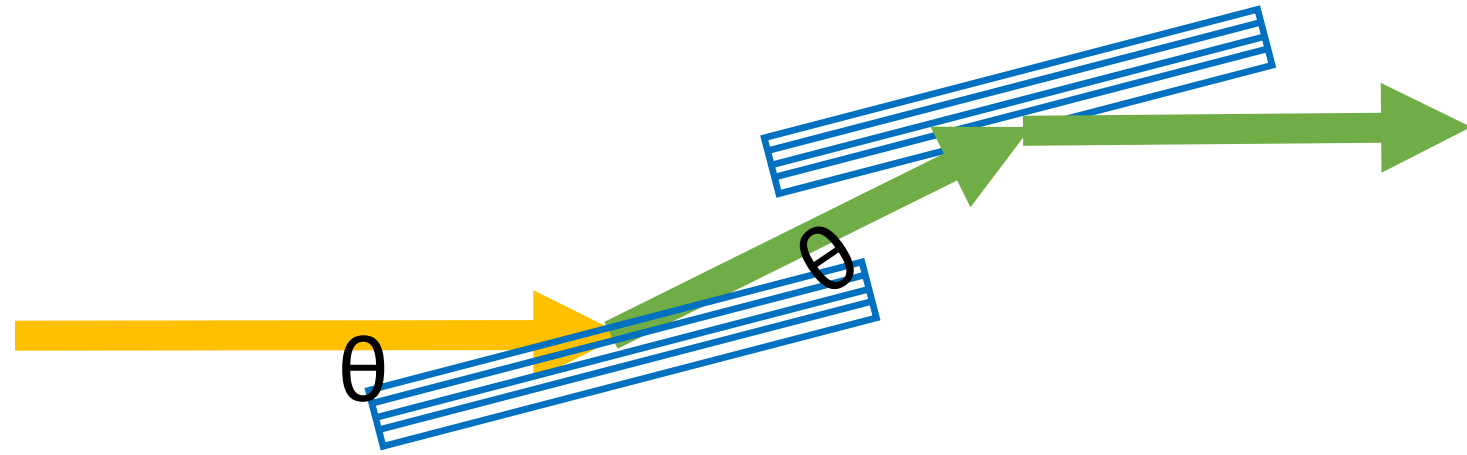
Bragg's law: $2d_{hkl} \sin\theta = (n)\lambda$

$$\lambda = 0.41328 \text{ \AA}$$

$$\Theta=3.7786^\circ$$

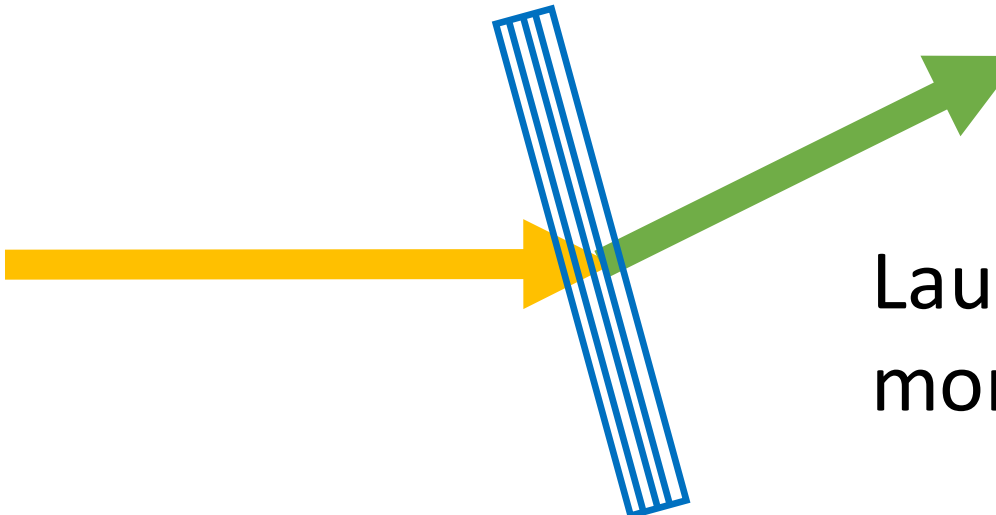
$$d_{111} = 3.13560 \text{ \AA}$$

1.1) Monochromators



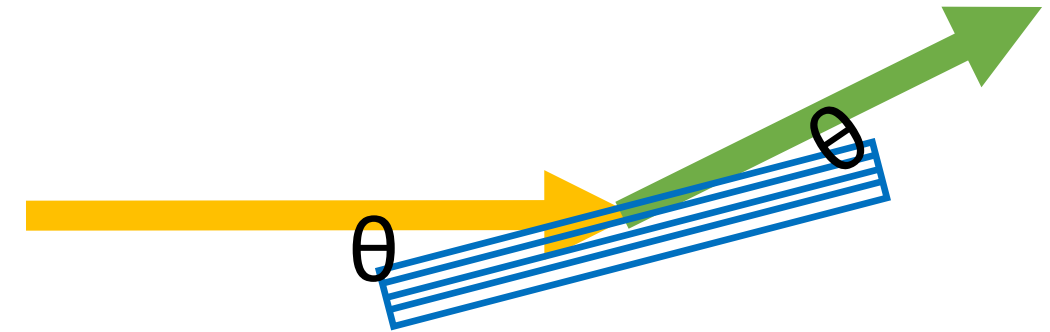
Double parallel monochromators

1.1) Monochromators

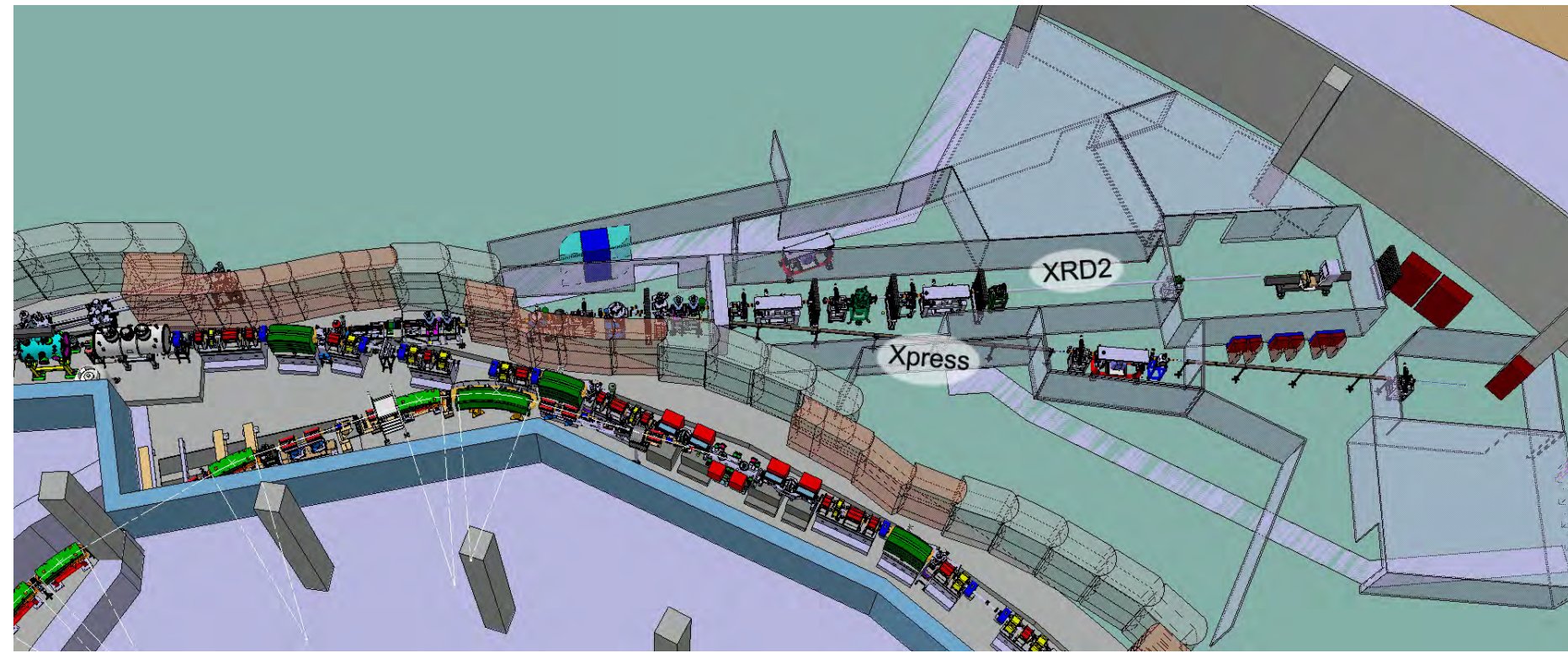
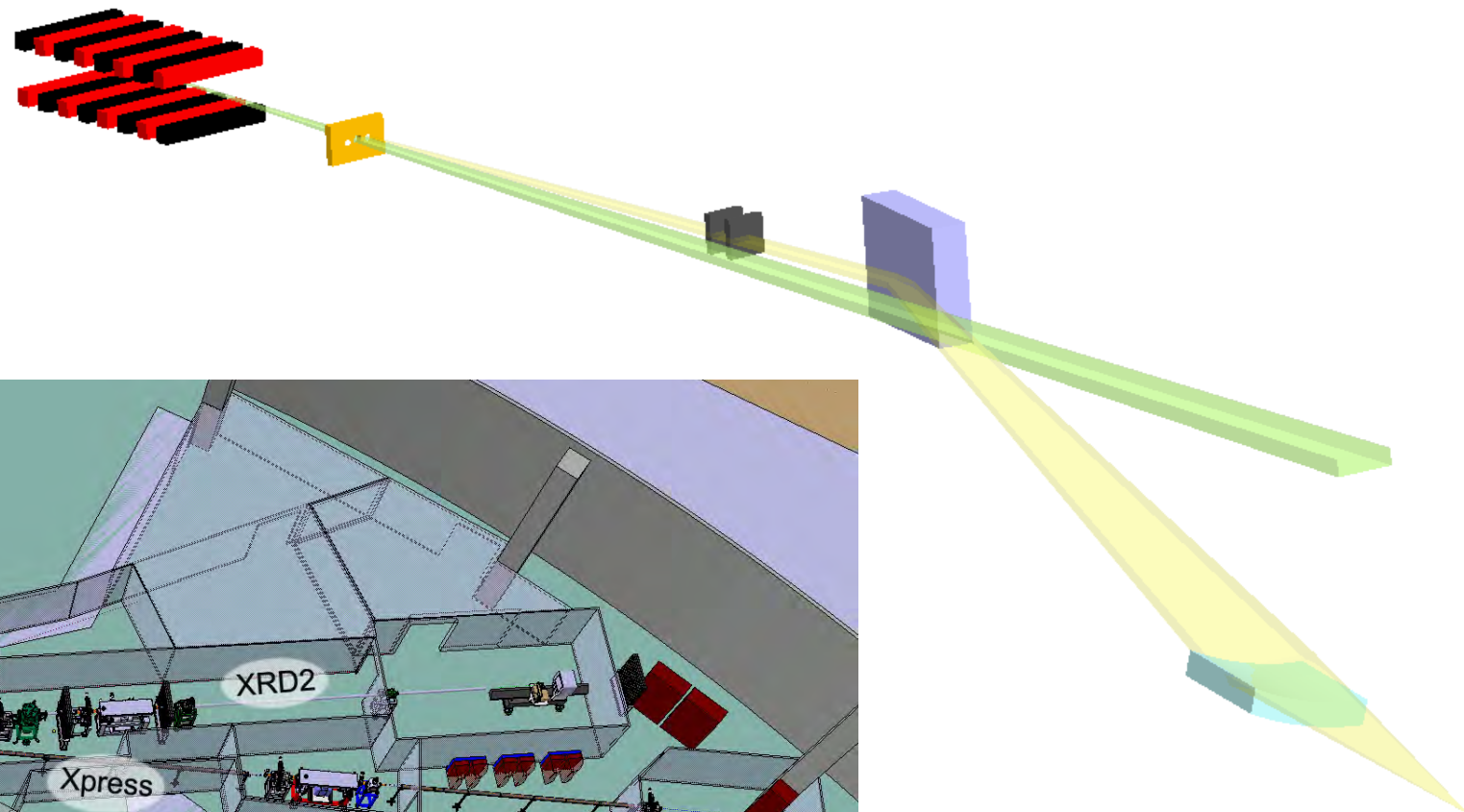


Laue geometry
monochromator

Or single monochromator for
specific purposes (i.e. two
beamlines on single source)

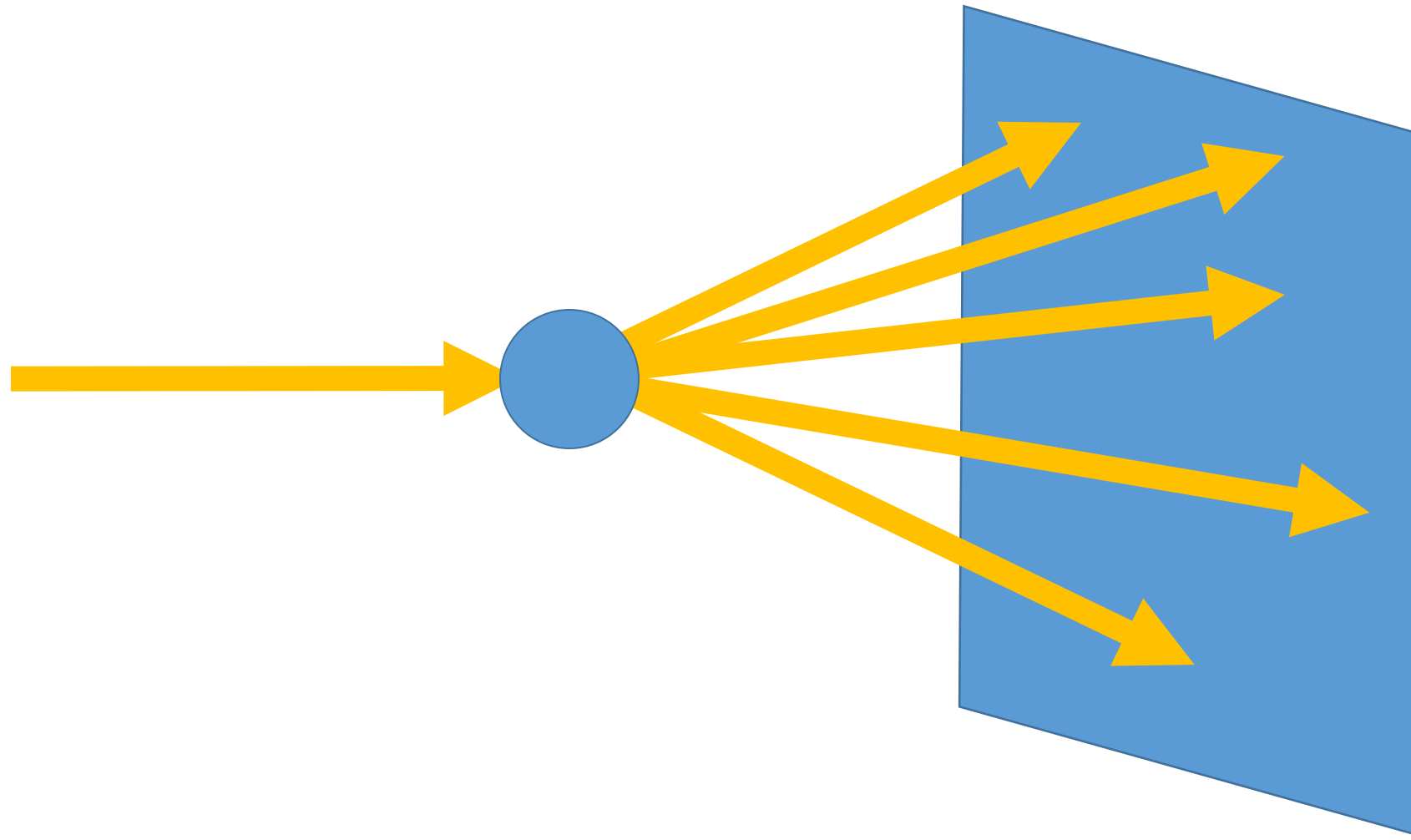


1.1) Monochromators

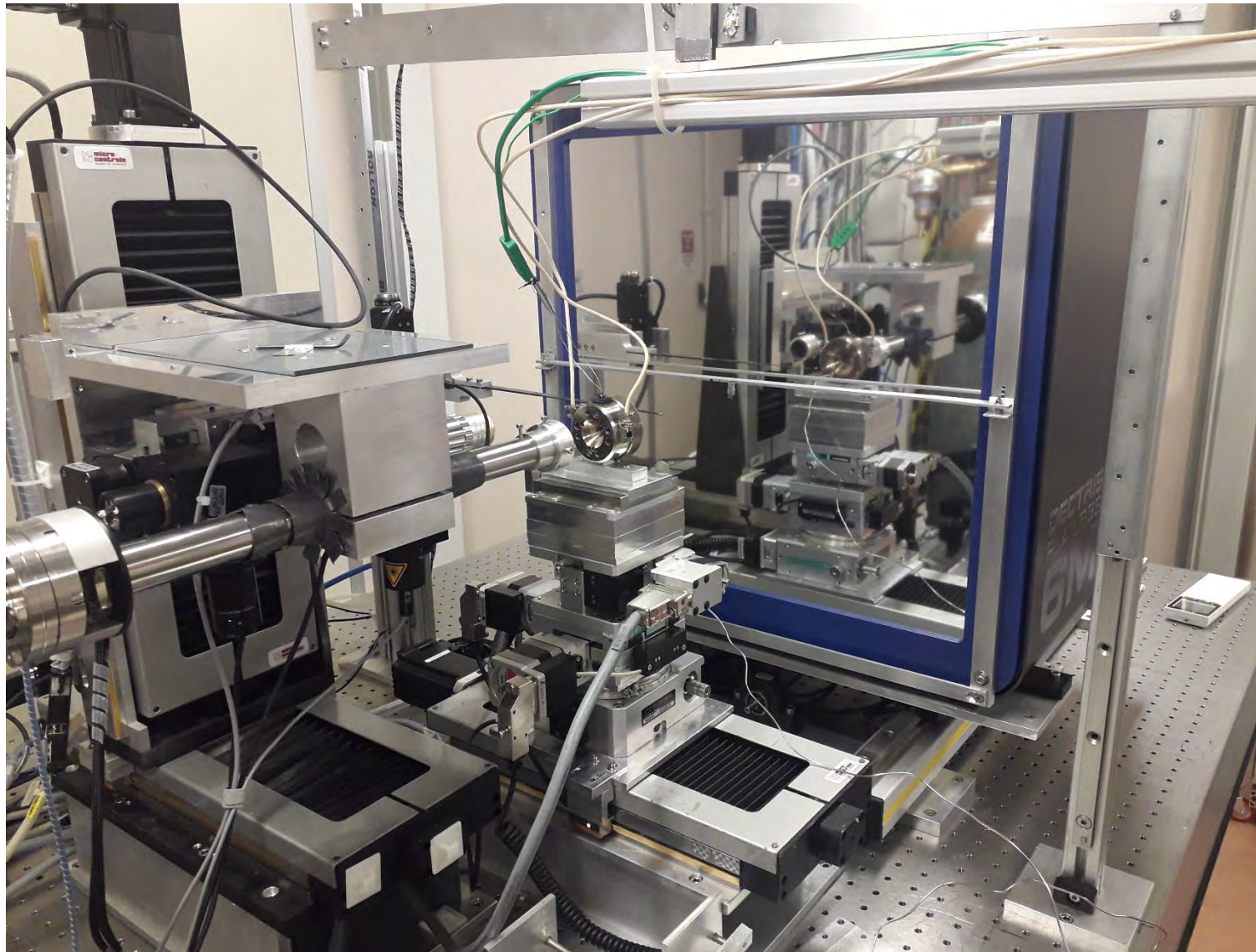


Courtesy of A. Lausi & P. Lotti

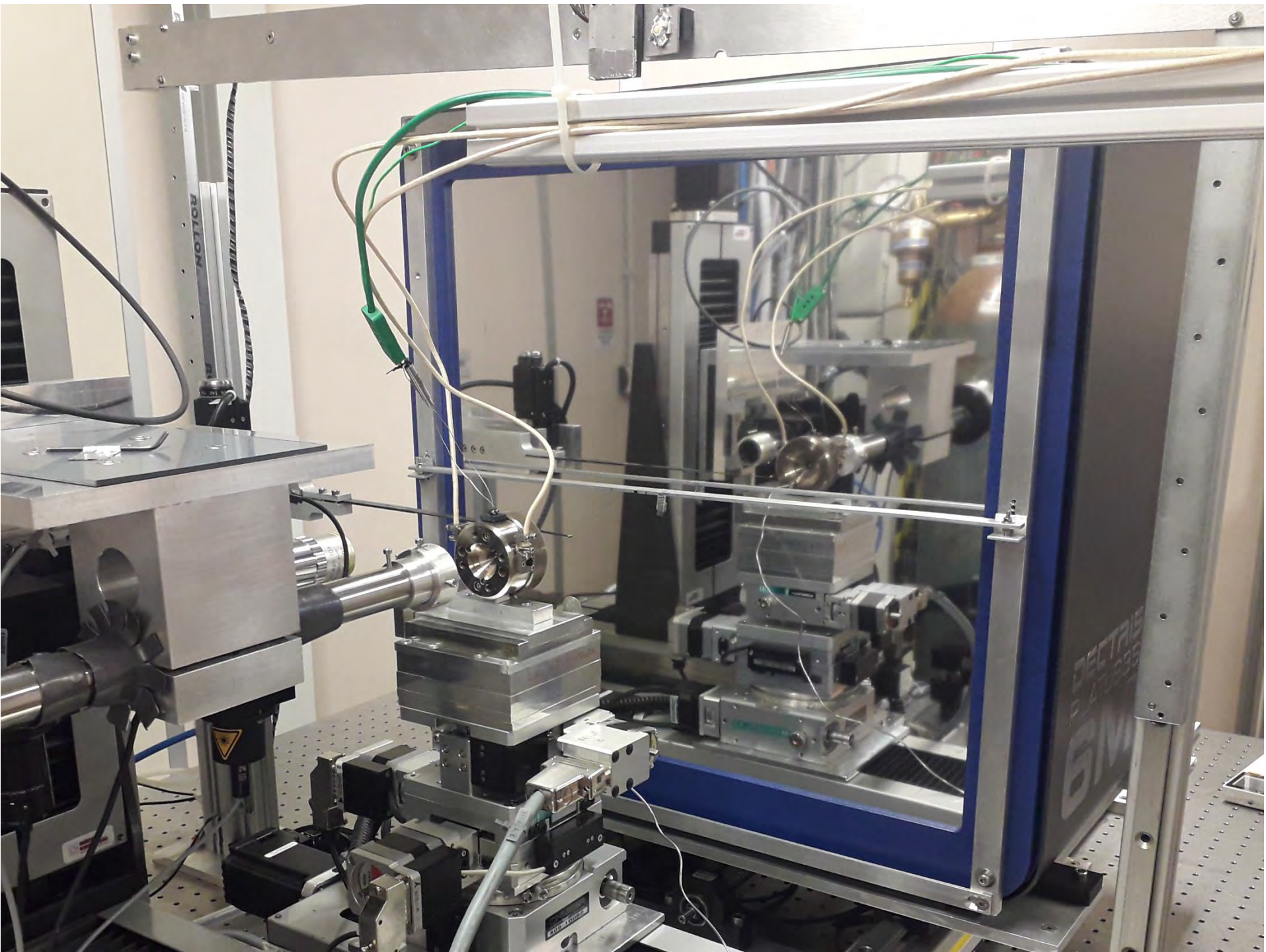
1.2) Calibration of beamline parameters

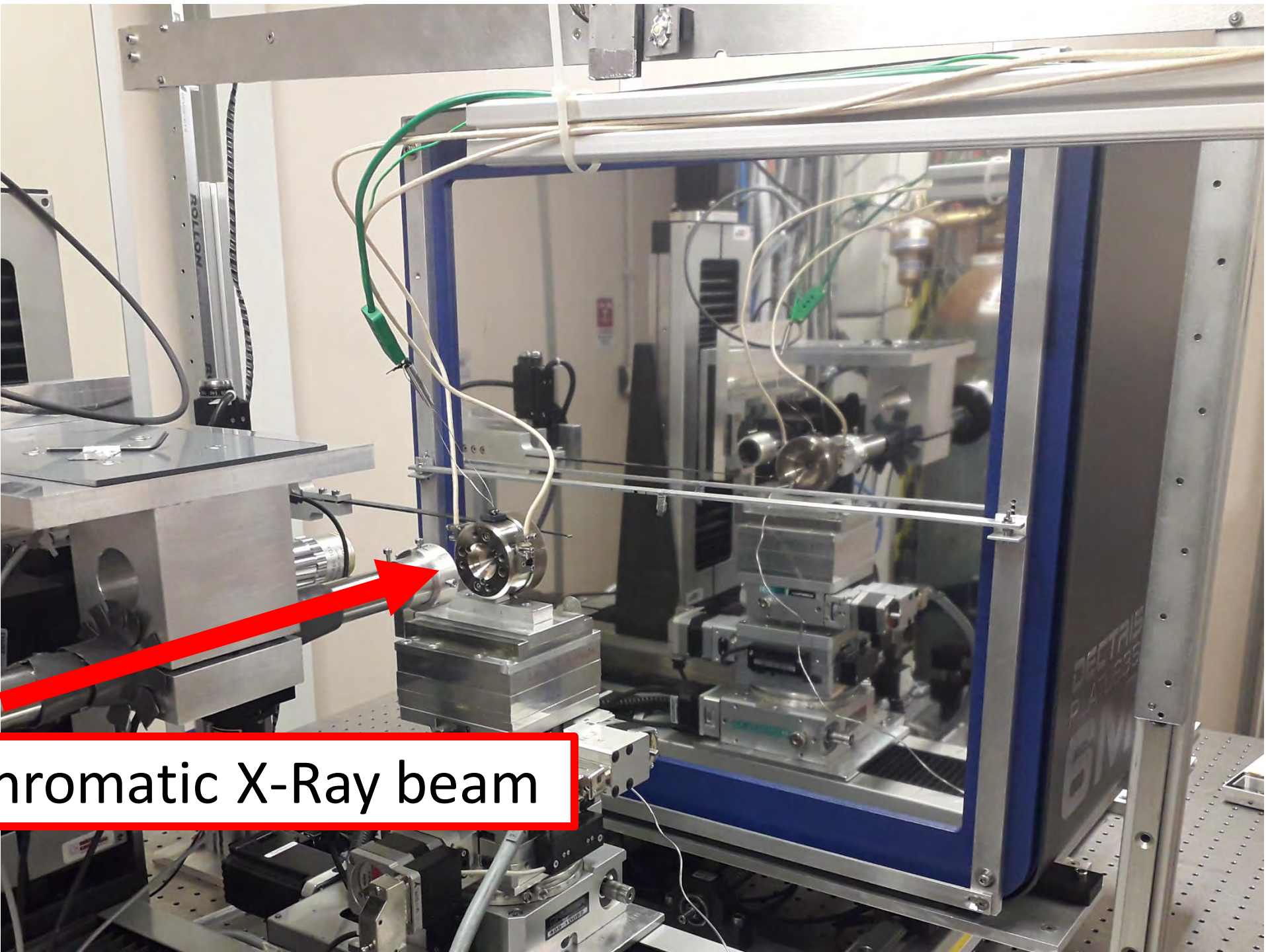


1.2) Calibration of beamline parameters

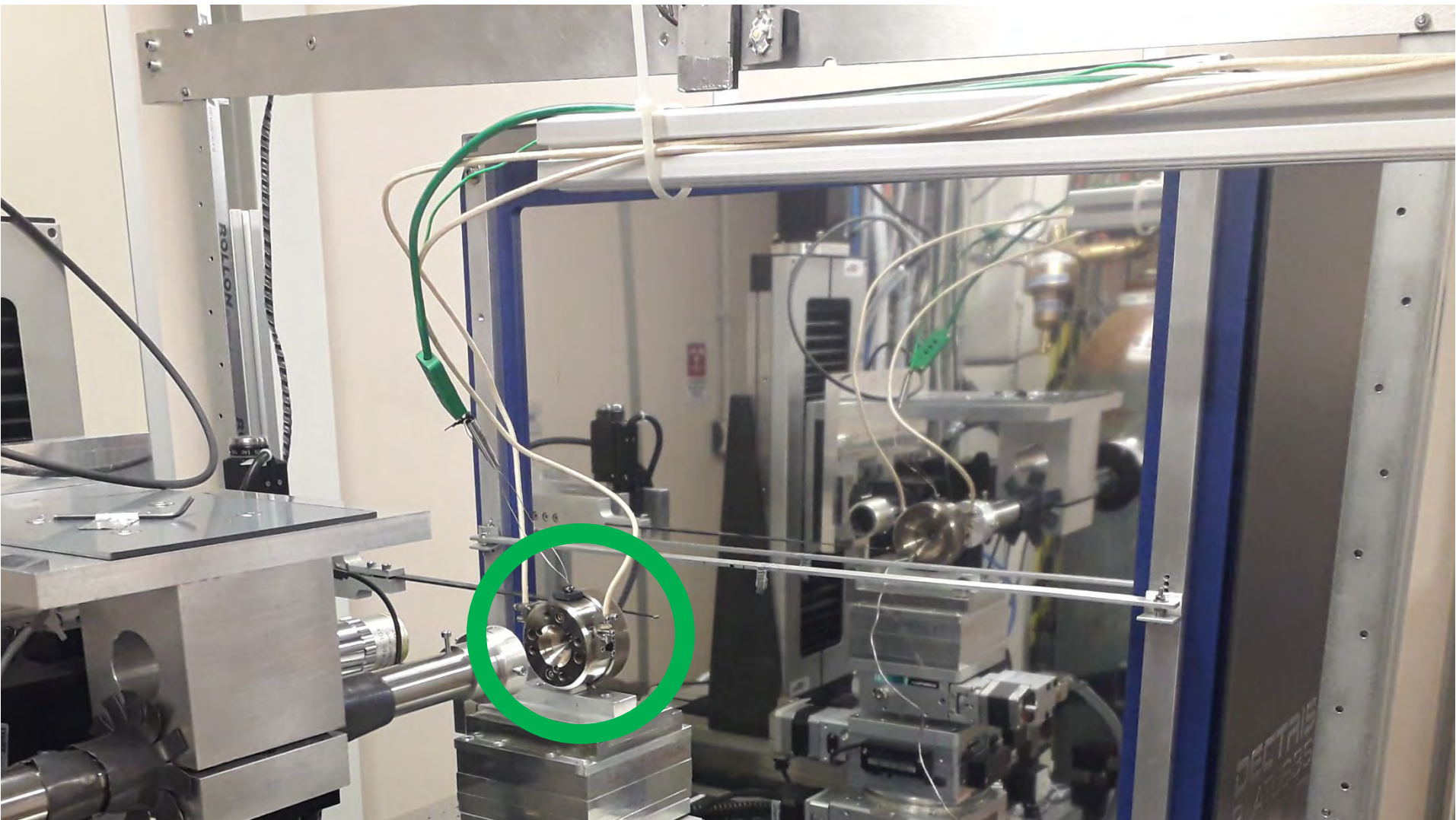


XPRESS @ Elettra



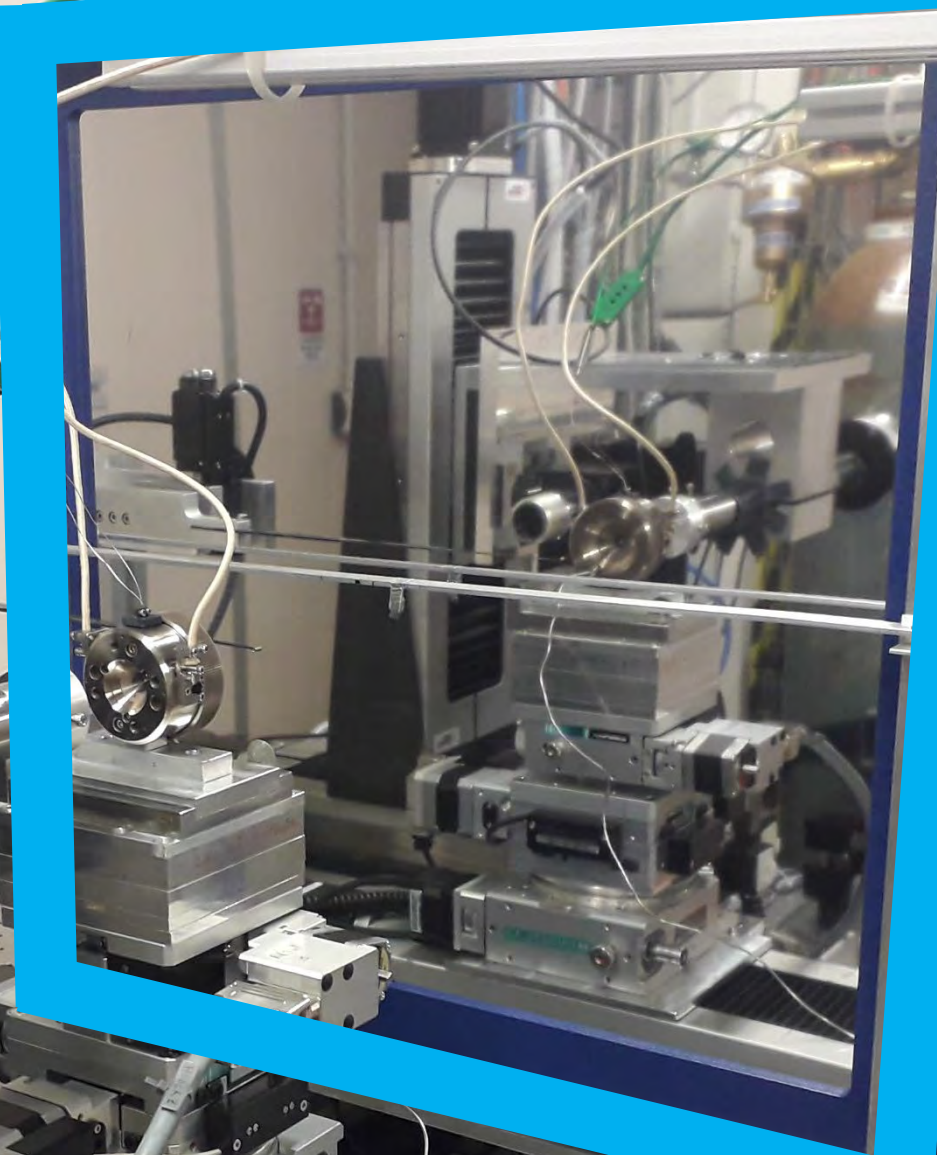
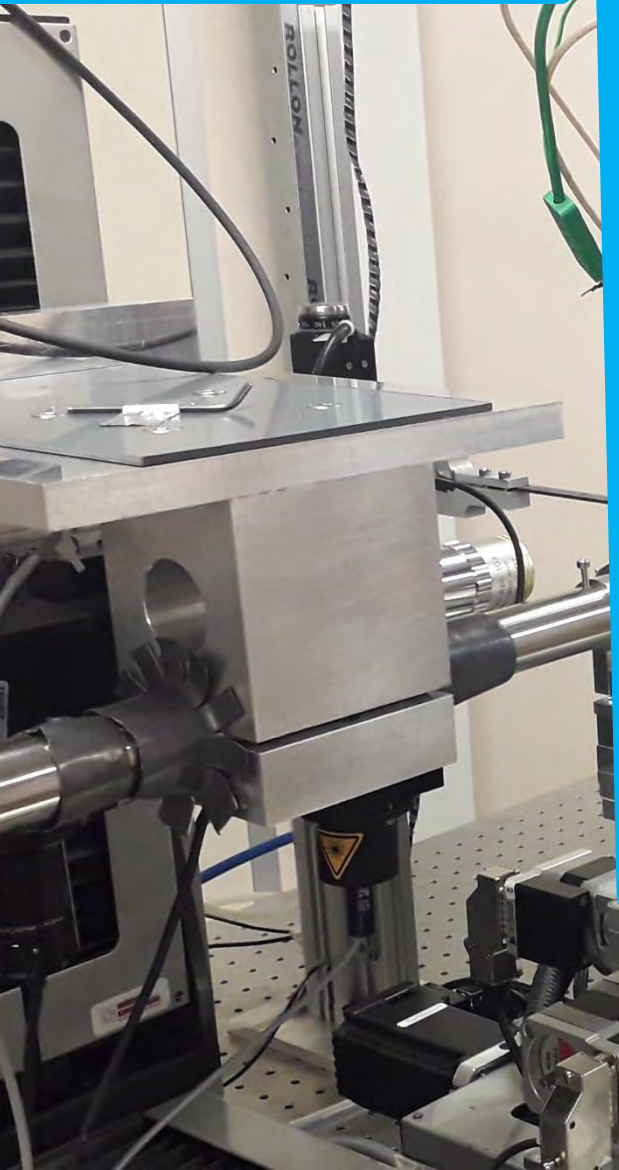


Monochromatic X-Ray beam

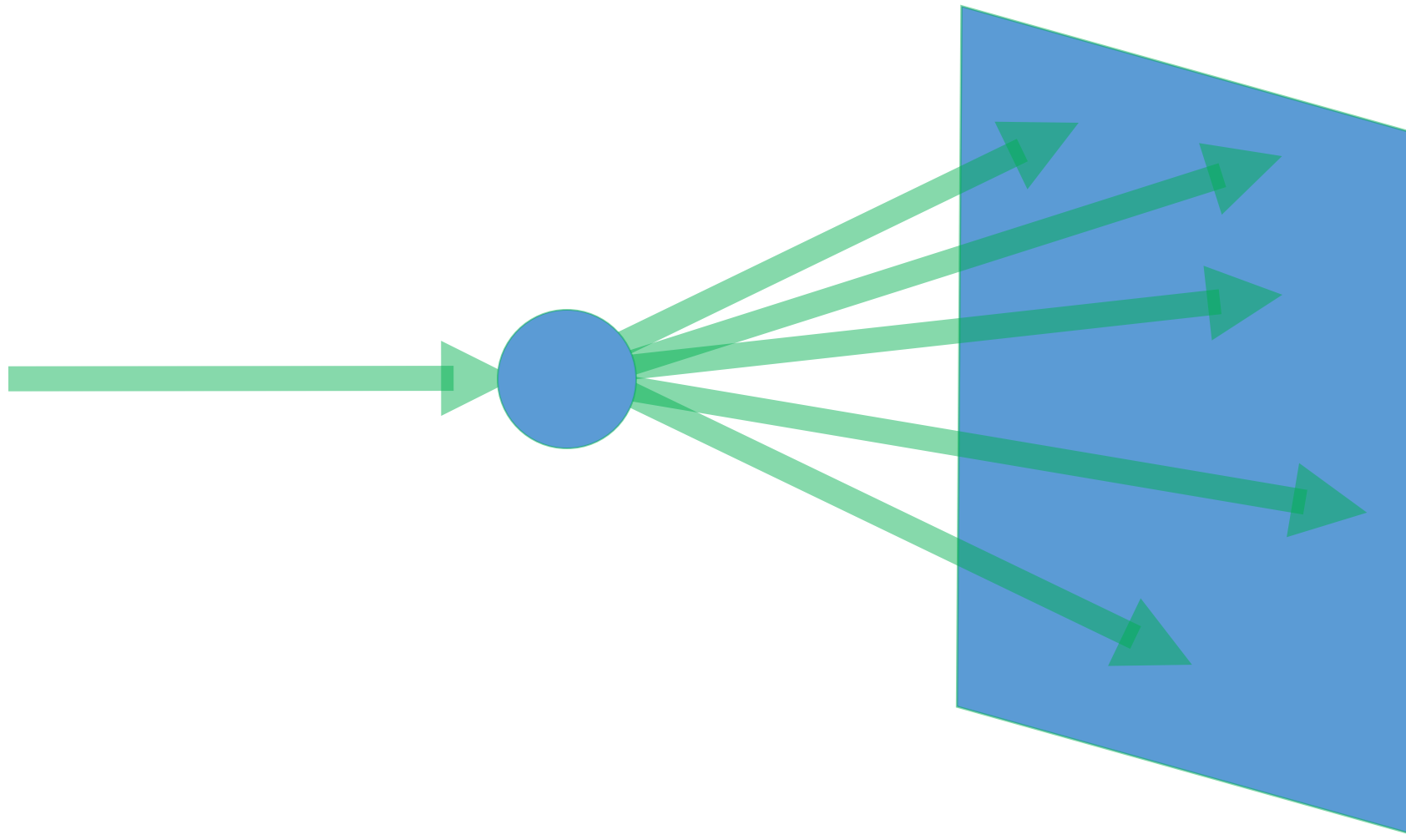


Sample
(High pressure / High temperature Diamond Anvil Cell)

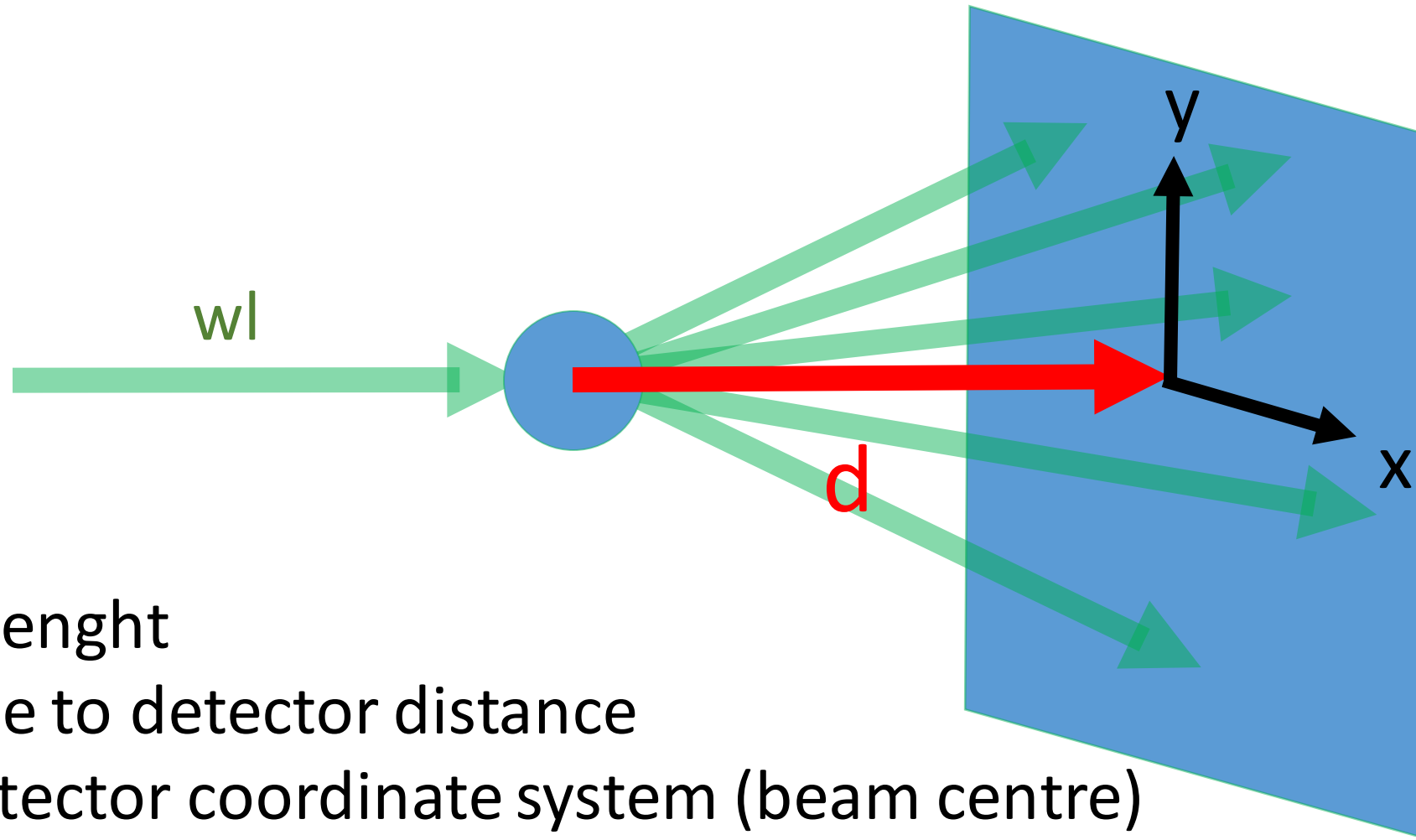
Area detector



1.2) Calibration of beamline parameters



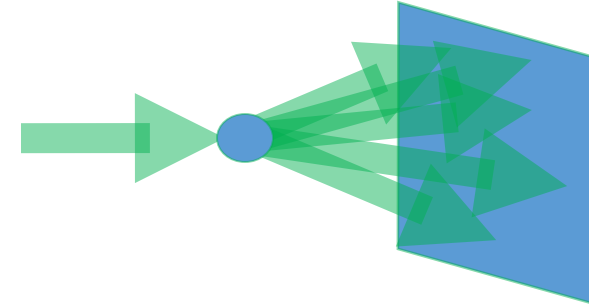
1.2) Calibration of beamline parameters



- Wavelength
- Sample to detector distance
- X,Y detector coordinate system (beam centre)
- Detector tilt

1.2) Calibration of beamline parameters

- Calibration against a powder (single crystal) reference sample with well known lattice parameter
- Operation normally done by beamline staff, but users should know how to do
- Standards: Silicon, LaB₆, CeO₂.....
- Software: FIT2D, Dioptas



1.2) Calibration of beamline parameters

1 of 1

Export Download Print E-mail

[View at Publisher](#)

Fit2D

High Pressure Research
Volume 14, Issue 4-5, 1996, Pages 235-248

Two-dimensional detector software: From real detector to idealised image or two-theta scan (Article)

Hammersley, A.P., Svensson, S.O., Hanfland, M., Fitch, A.N., Häusermann, D. 

Europ. Synchrt. Radiation Facility, BP 220, 38043 Grenoble Cedex, France

Abstract  View references (32)

Detector systems introduce distortions into acquired data. To obtain accurate angle and intensity information, it is necessary to calibrate, and apply corrections. Intensity non-linearity, spatial distortion, and non-uniformity of intensity response, are the primary considerations. It is better to account for the distortions within scientific analysis software, but often it is more practical to correct the distortions to produce 'idealised' data. Calibration methods and software have been developed for single crystal diffraction experiments, using both approaches. For powder diffraction experiments the additional task of converting a two-dimensional image to a one-dimensional spectrum is used to allow Rietveld analysis. This task may be combined with distortion correction to produce intensity information and error estimates. High-pressure experiments can introduce additional complications and place new demands on software. Flexibility is needed to be able to integrate different angular regions separately, and to produce profiles as a function of angle of azimuth. Methods to cope with awkward data are described, and examples of the techniques applied to data from high pressure experiments are presented.

Metrics  View all metrics >

3054  Citations in Scopus
99th Percentile

5.46  Field-Weighted Citation Impact

 PlumX Metrics
Usage, Captures, Mentions, Social Media and Citations beyond Scopus.

Cited by 3054 documents

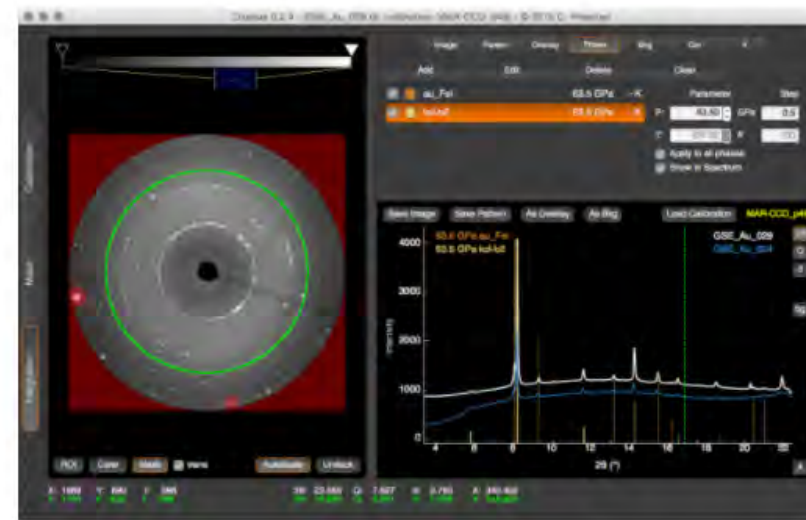
Investigation of the precipitation of Na₂SO₄ in supercritical water
Voisin, T. , Errigible, A. , Philippot, G. (2017) *Chemical Engineering Science*

The critical role of Si doping in enhancing the stability of M₆C carbides

Dioptas

Dioptas is a Python-based program for on-the-fly data processing and exploration of two-dimensional X-ray diffraction area detector data. It is specifically designed for the large amount of data collected at XRD beamlines at synchrotrons. Its fast data reduction algorithm and graphical data exploration capabilities make it ideal for online data processing during XRD experiments and batch post-processing of large numbers of images.

Dioptas is written with interactivity and speed in mind while still being as versatile as possible. It employs an algorithm for calibration of any possible detector geometry, features easy-to-use masking tools, and offers very fast data exploration and phase analysis capabilities. The tunable calibration procedure enables the calibration of even the most complex geometries, including very large detector tilts, the primary beam being outside of the image and very spotty diffraction pattern of the calibrant. The main part of the software is the opportunity to interactively explore the 2d image and integrated pattern at the same time. The very fast integration algorithm (around 0.1s for an 2048px X 2048px image), a reliable tunable automatic background subtraction algorithm and the possibility to display phase lines make it a viable tool for realtime processing online at the beamline. Thus, enabling very fast decision making during the course of the experiment.



Distribution

Dioptas is mainly distributed via an open-source repository at <http://github.com/Dioptas/Dioptas>. However, since some of the required packages can be hard to install on some operating systems by non-expert end-users, we also provide executable packages which can be downloaded by using the link below. Dioptas is cross-platform compatible and has been tested on Windows 7, Windows 8, 10, Mac OS X and Linux Debian systems. Dioptas has a very fast-growing user base and is currently employed for online data processing and post experiment data analysis at CARS(Sectors 13-15, APS), HPCAT (Sector 16, APS), ID27 (ESRF), ID9 (ESRF), ID31 (ESRF) and ECB P02.2 (Petra III). Furthermore, non-high pressure beamlines and in-house laboratories are starting to adapt it.

Publications

A paper about Dioptas has been published in High Pressure Research:

- **Prescher, C., Prakapenka, V.B., 2015. DIOPTAS : a program for reduction of two-dimensional X-ray diffraction data and data exploration.**
High Press. Res. 35:3, 223-230. [link](#)

- Silicon NIST collected at XPRESS beamline (Elettra)
- Pilatus 6M area detector
- Approximate sample to detector distance: 250 mm (from uncalibrated motor position)
- Beam energy: ~ 25 keV (i.e. ~ 0.495)
- Pixel size: 0.172x0.172 mm
 - Using Fit2D and Dioptas to calibrate experimental geometry and integrate powder diffraction from samples

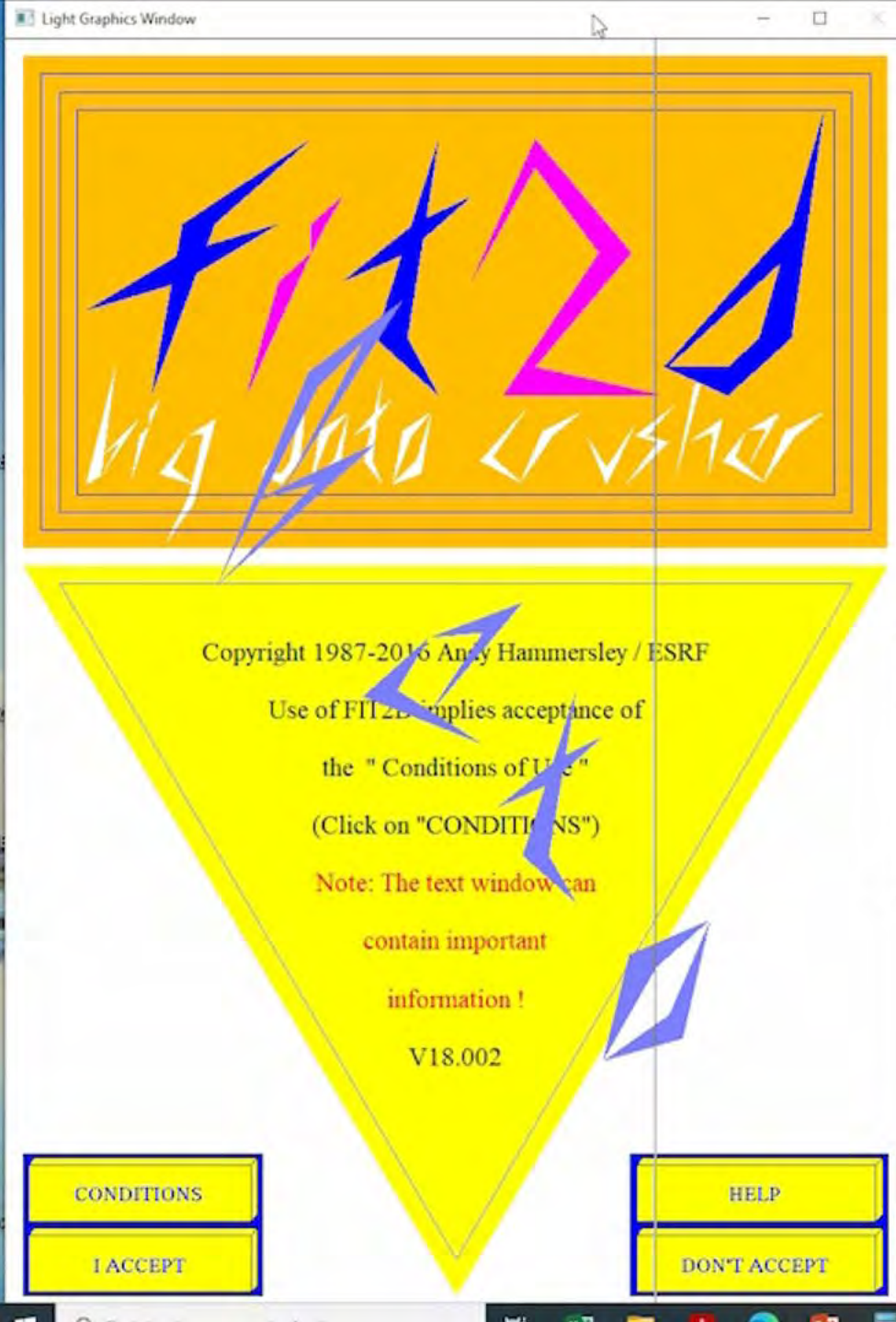


Image Cake Pattern

Load File

Calibration Parameters

Start values

- Distance: 200.000 mm
- Wavelength: 0.334400 Å
- Polarization: 0.990
- Pixel width: 79 µm
- Pixel height: 79 µm

Calibrant: LaB6

Rotate +90 Rotate -90
Flip horizontal Flip vertical
Reset transformations

Peak Selection

Current Ring Number: 1 automatic increase

automatic peak search

single peak search

Search size: 10 Undo Clear All Peaks

Refinement Options

automatic refinement

use mask transparent

Peak Search Algorithm: Massif

Delta 2 θ : 0.1

Intensity Mean Factor: 3.00

Intensity Limit: 55000

Number of rings: 15

Distortion Correction

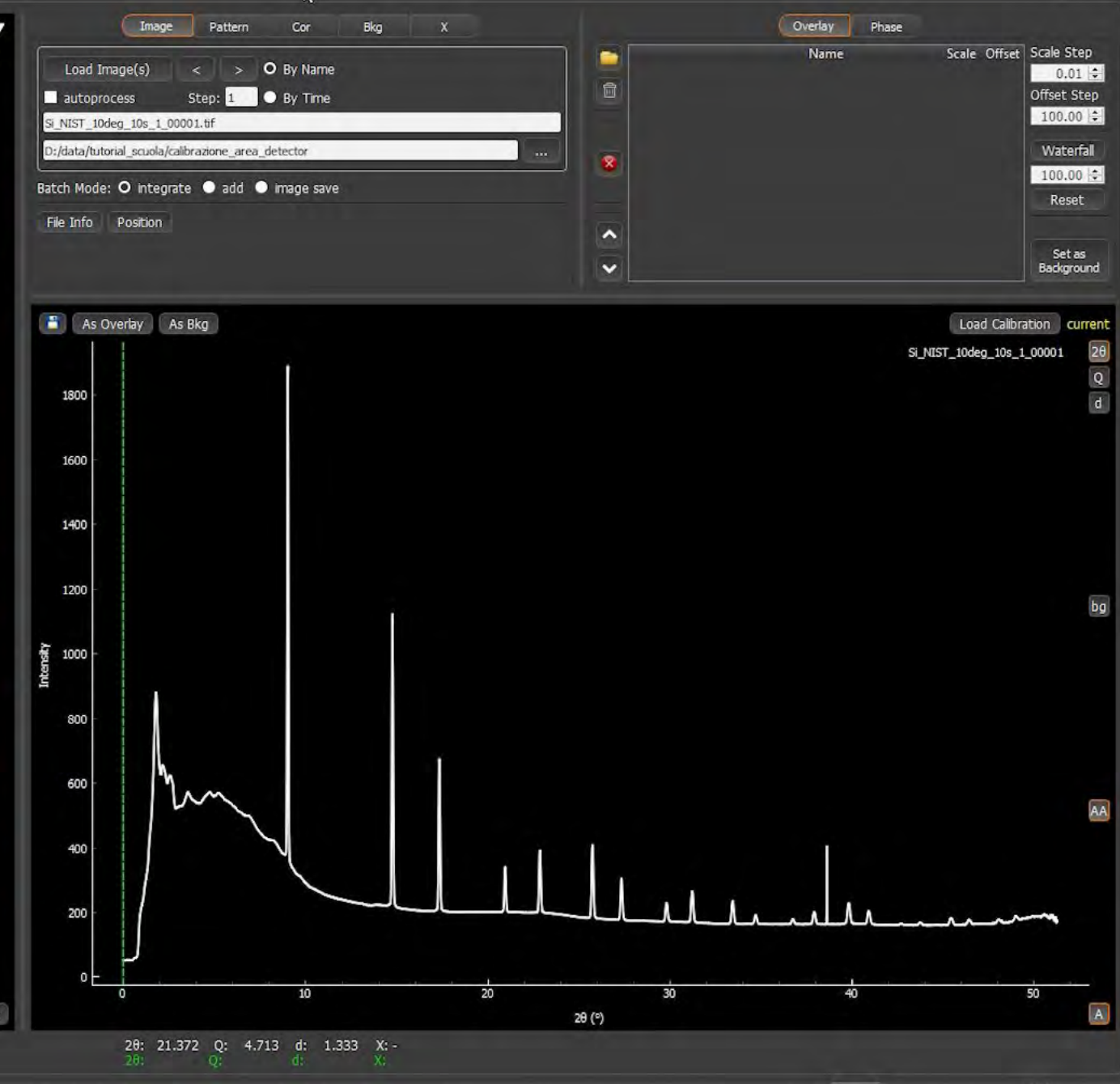
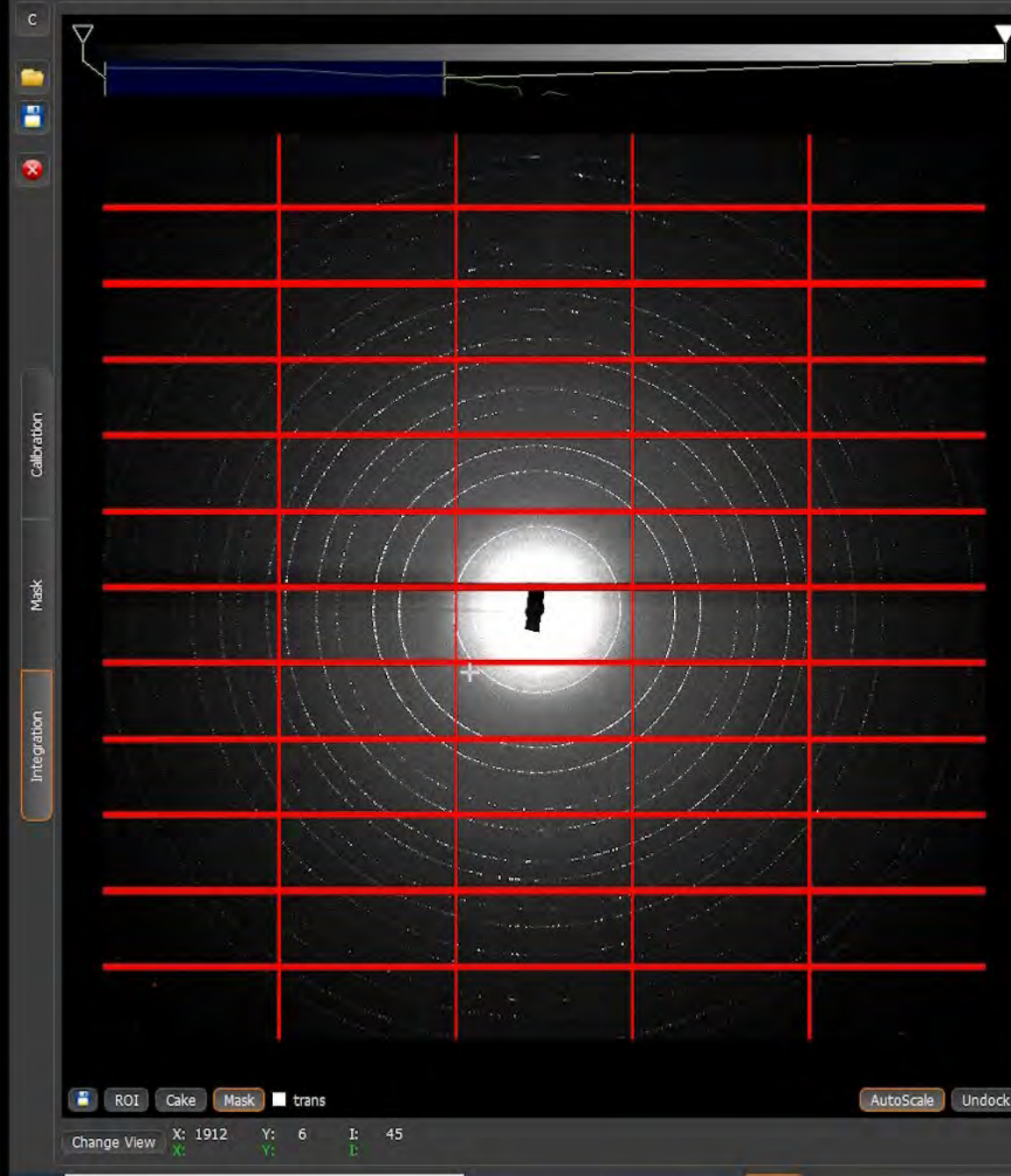
Load Splinefile None

pyFAI Parameters

Fit2d Parameters

Calibrate Refine x: 1976.2 y: 2105.2 Load Calibration Save Calibration

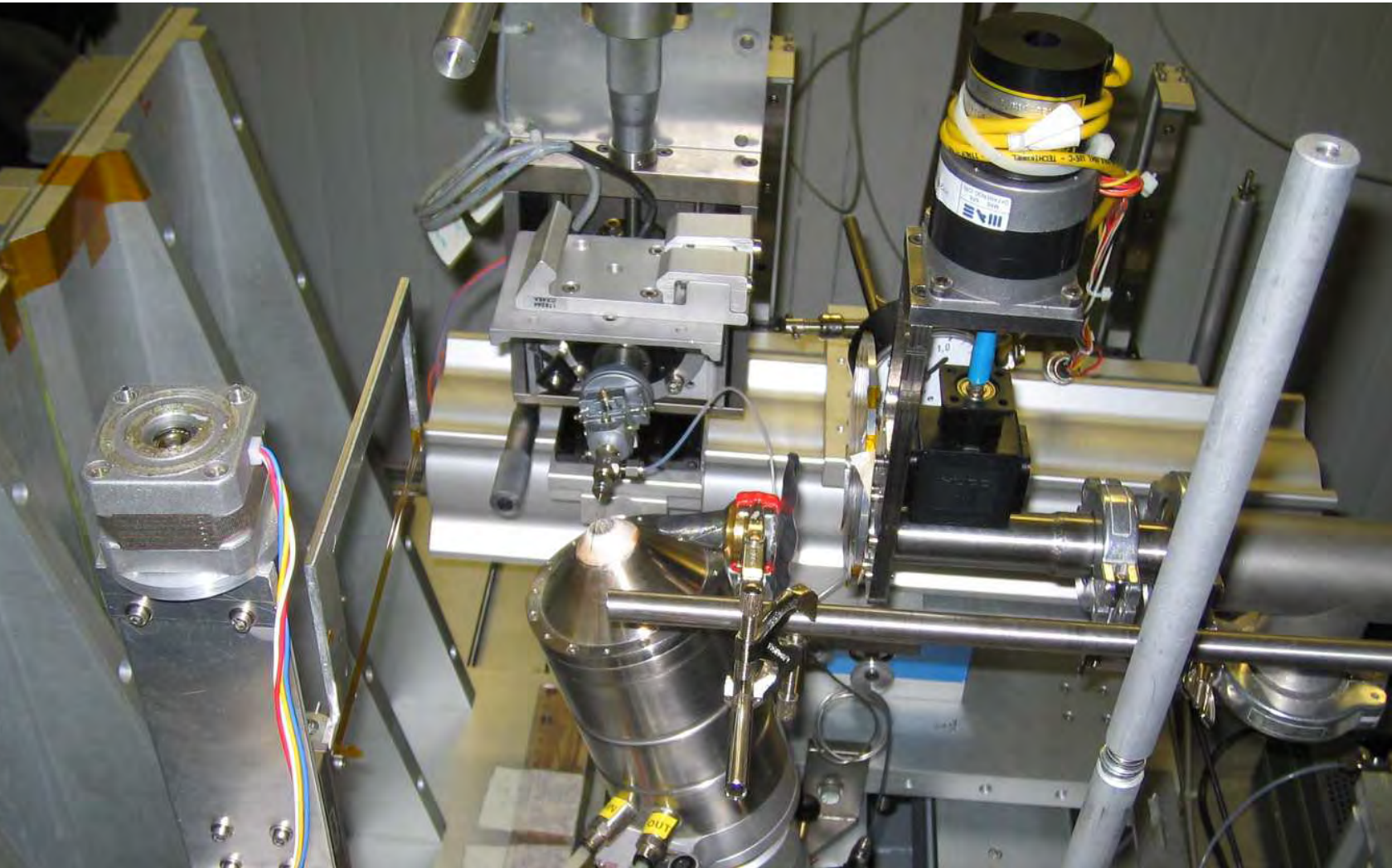
Integration of sample XRPD



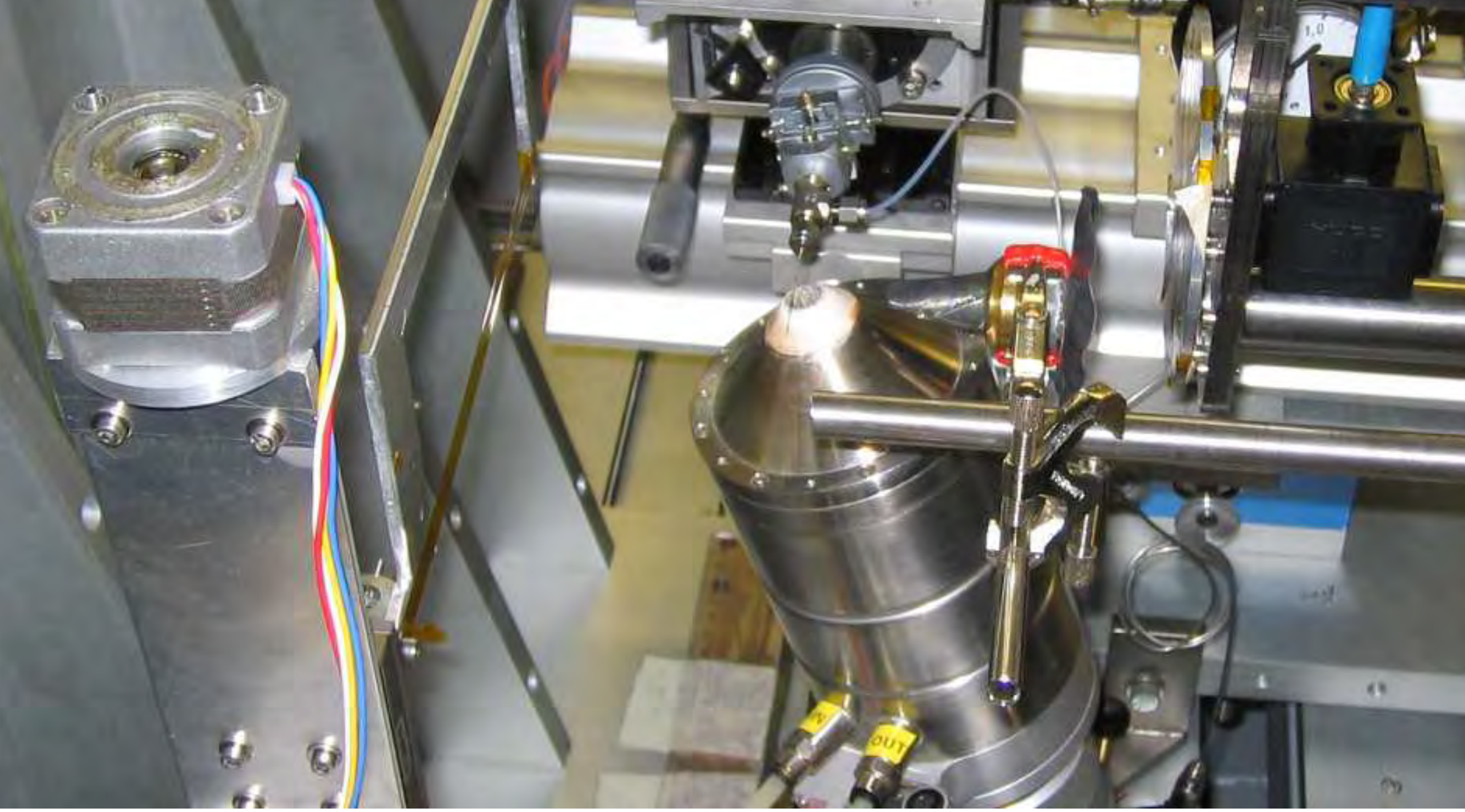
1.3) Use of unit cell volume for determination of bulk properties: thermal expansion

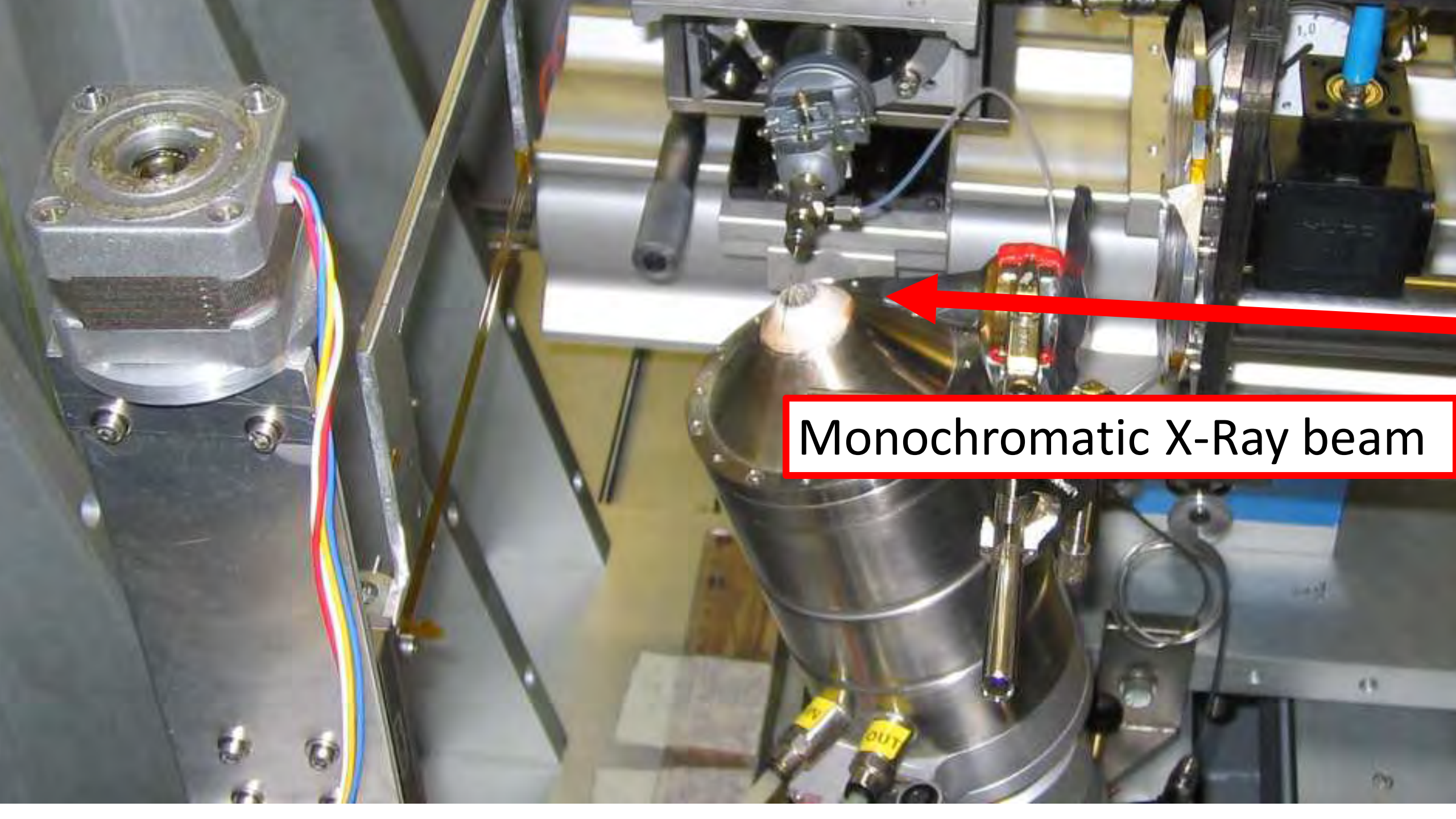
$$\begin{aligned}\text{Thermal expansion: } \alpha &= 1/V (\partial V / \partial T) \\ &= \partial \ln V / \partial T\end{aligned}$$

Determination of unit cell volume at different temperatures



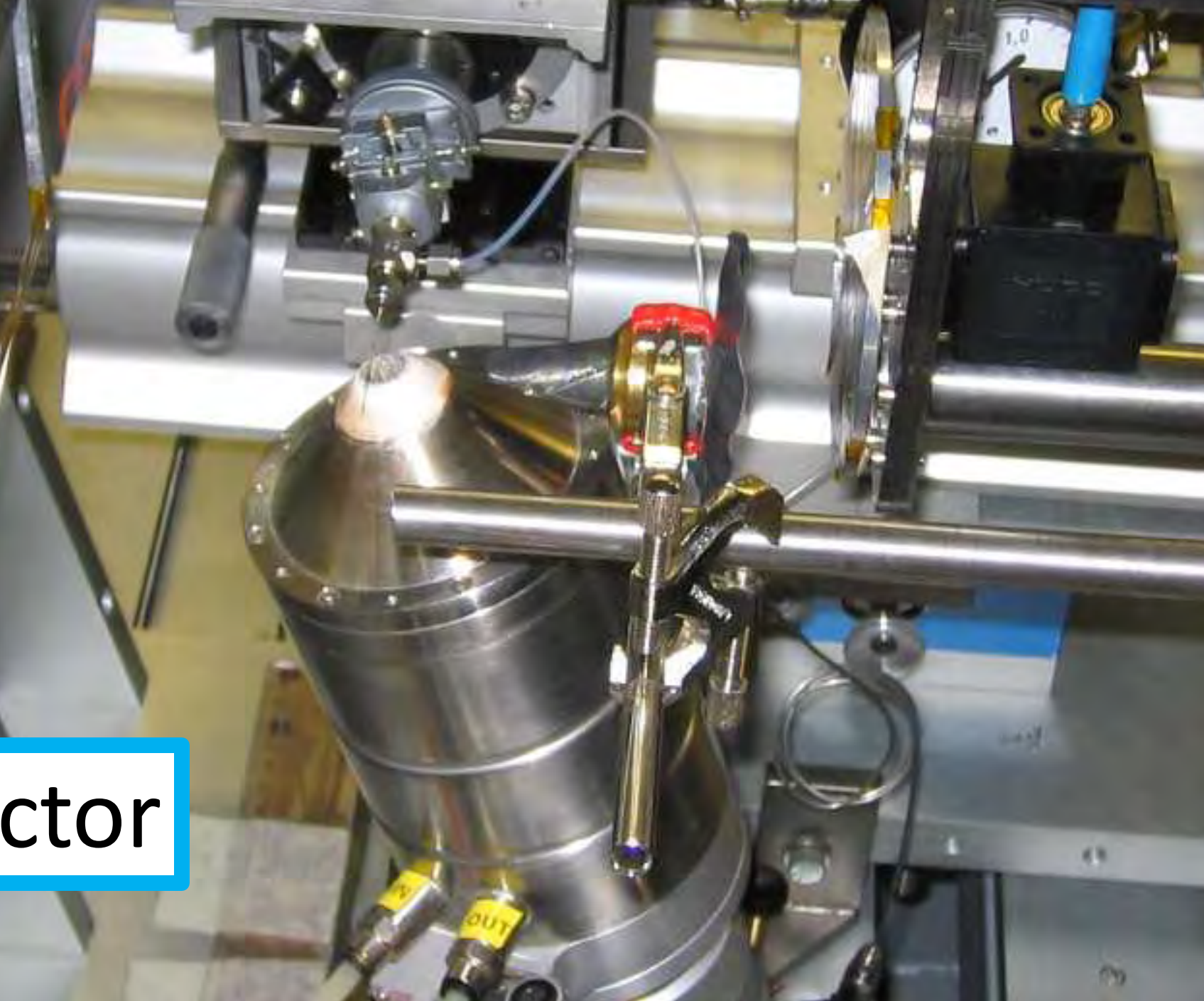
«Hystorical» (2005) beamline setup for HT X-ray powder diffraction @ GILDA beamline (CRG beamline – ESRF, now LISA beamline)

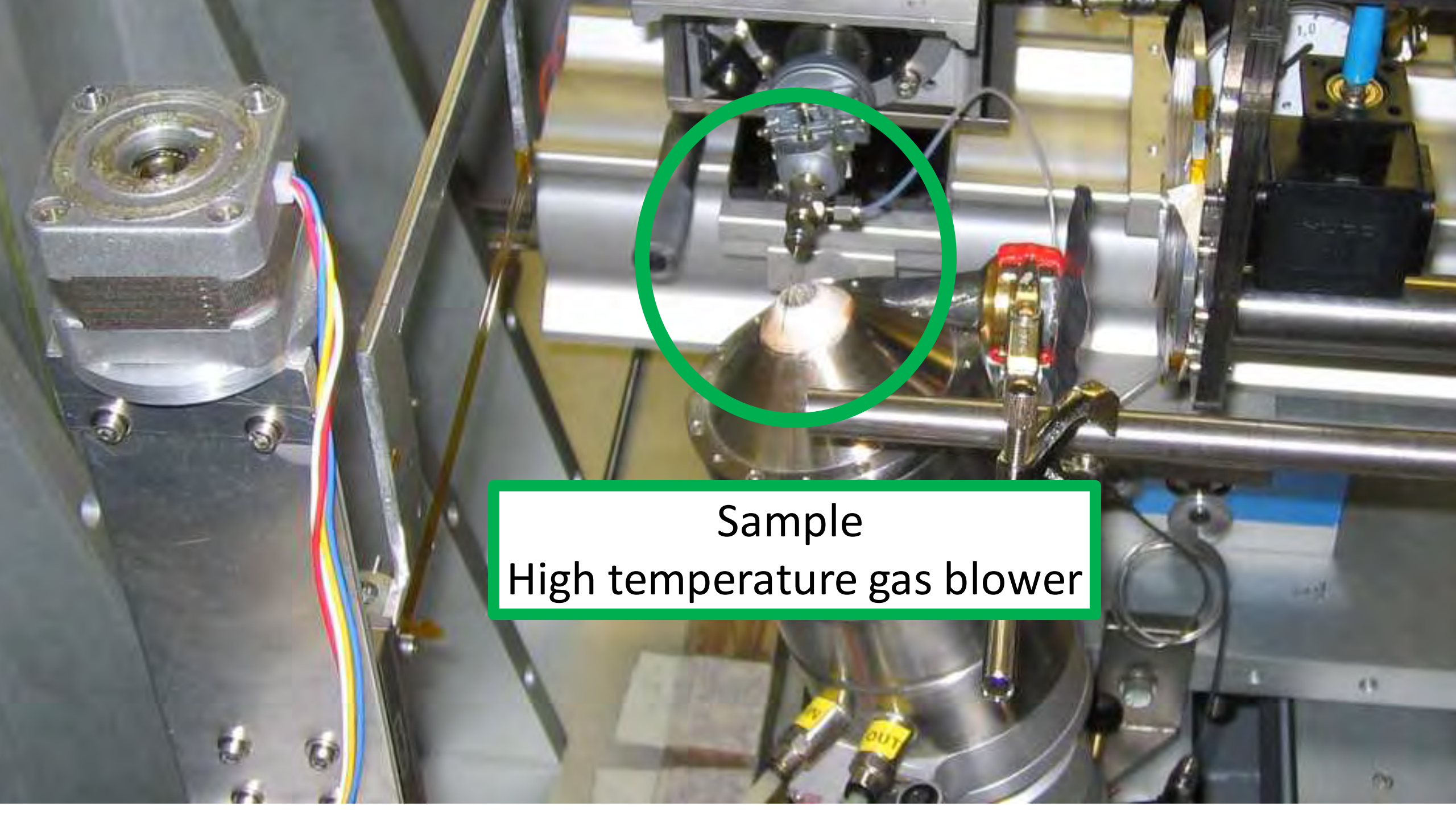




Monochromatic X-Ray beam

Area detector





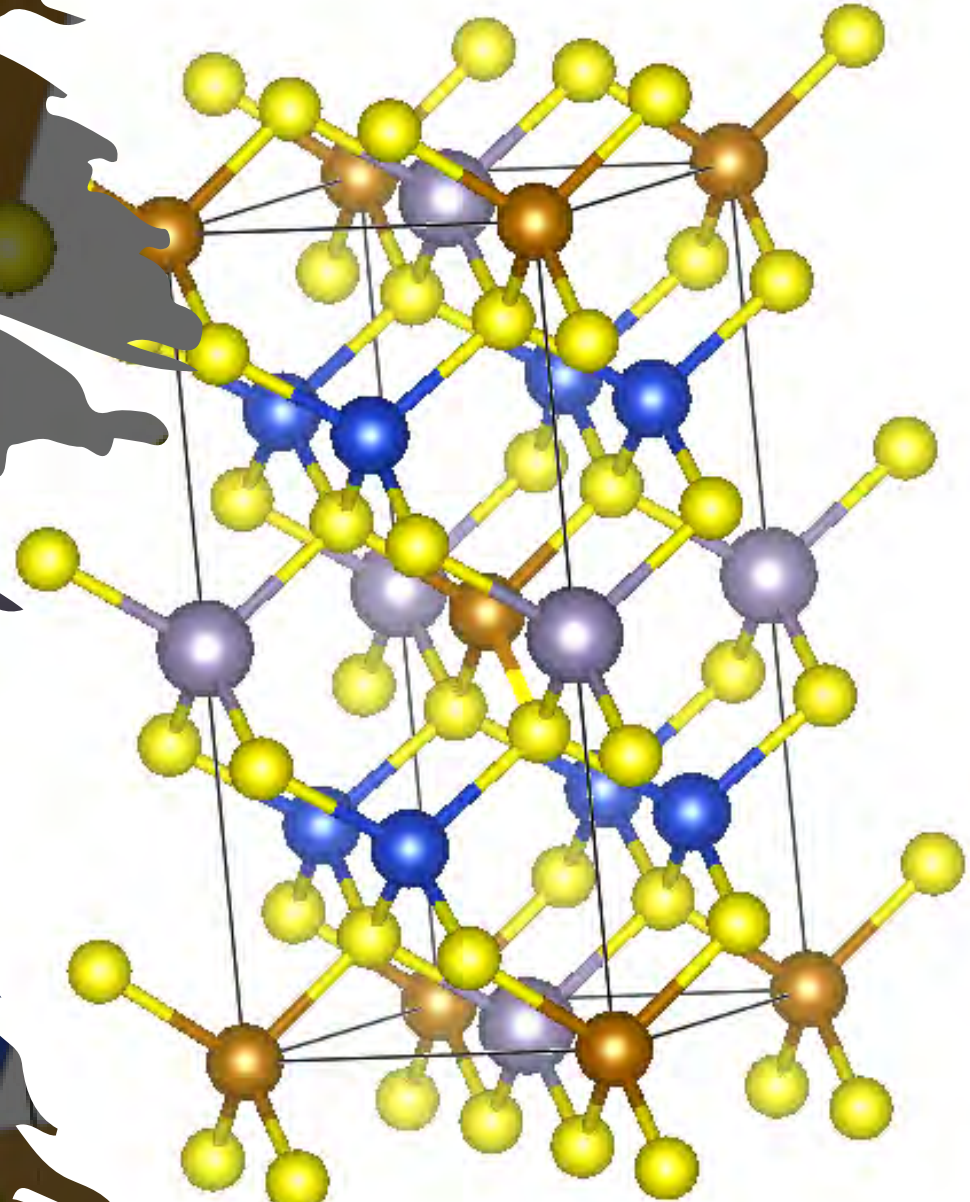
Sample
High temperature gas blower

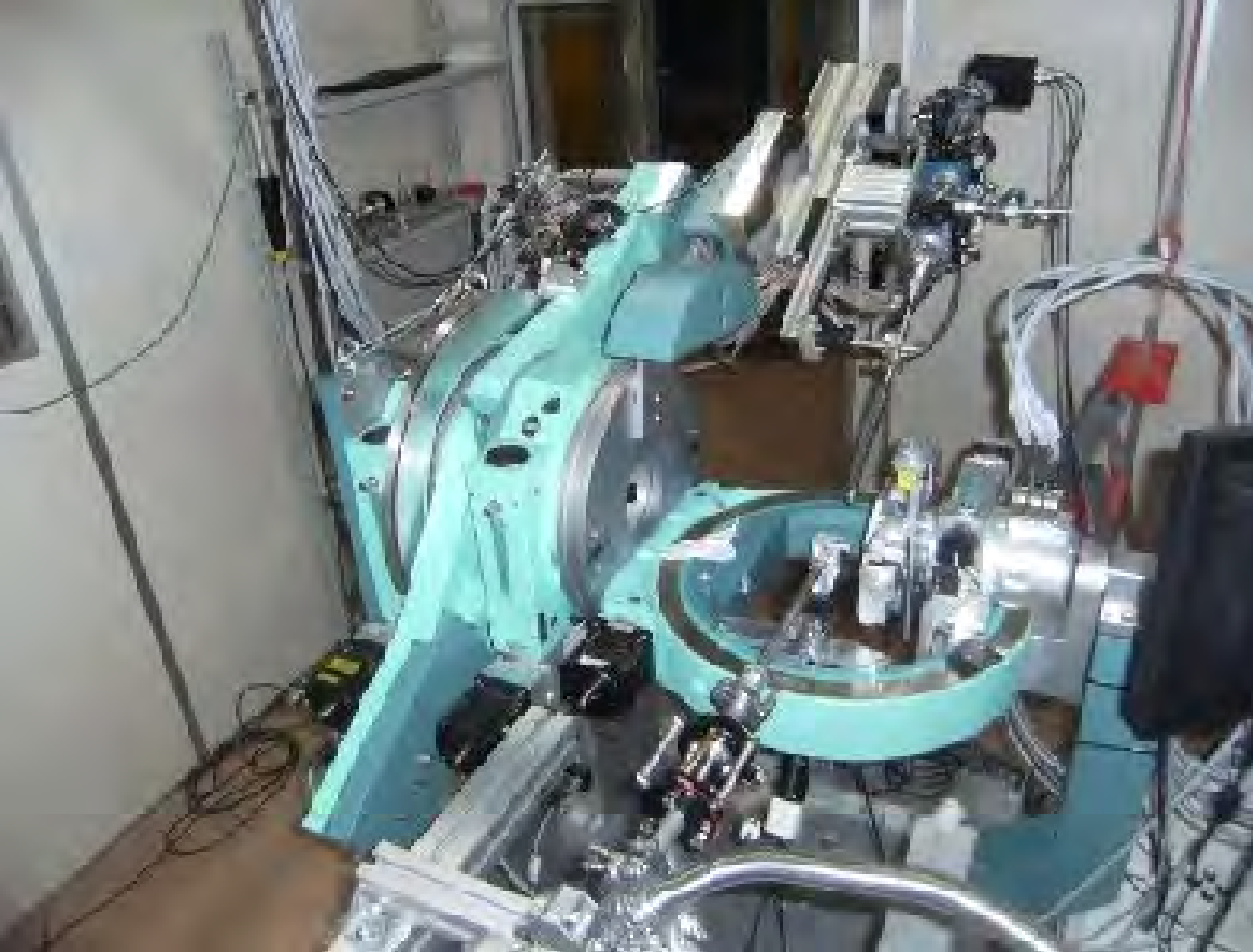
Example: thermal expansion of stannite, $\text{Cu}_2\text{FeSnS}_4$



- Ore mineral for tin, together with cassiterite SnO_2
- Important structure in material science together with kesterite, $\text{Cu}_2\text{ZnSnS}_4$ (for photovoltaic application)
- In the last decade increase of publication on synthesis of these materials. The knowledge of structural behaviour as function of temperature, chemistry, etc... is relevant for stabilization of phases with specific properties

- Example of Rietveld fit of stannite at variable temperatures and determination of thermal expansion
- Use of GSAS and GSAS-II software

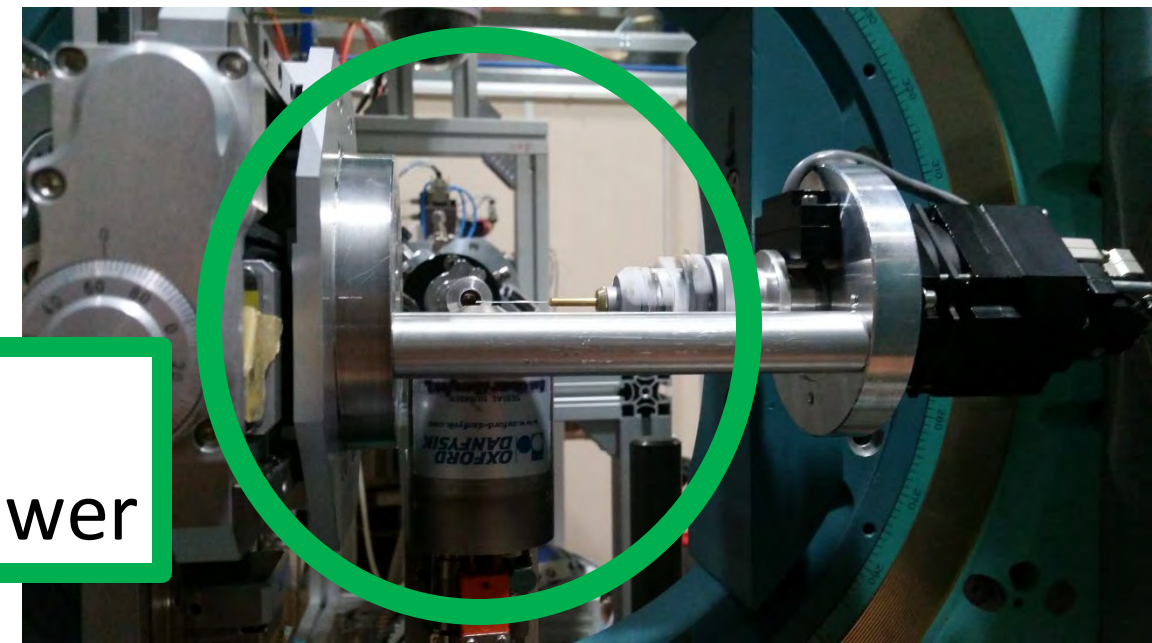




Sample
High temperature gas blower

Data collected @ MCX beamline (Elettra)

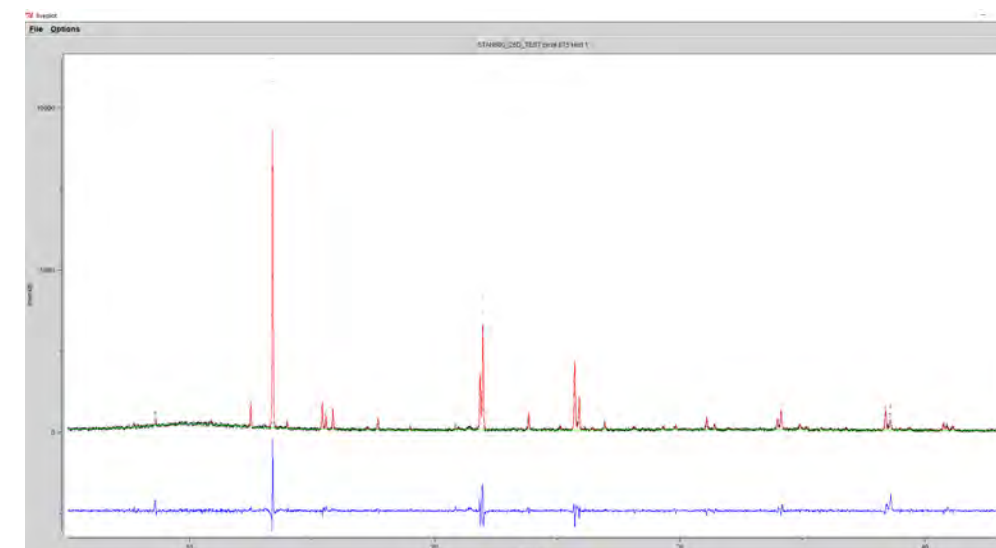
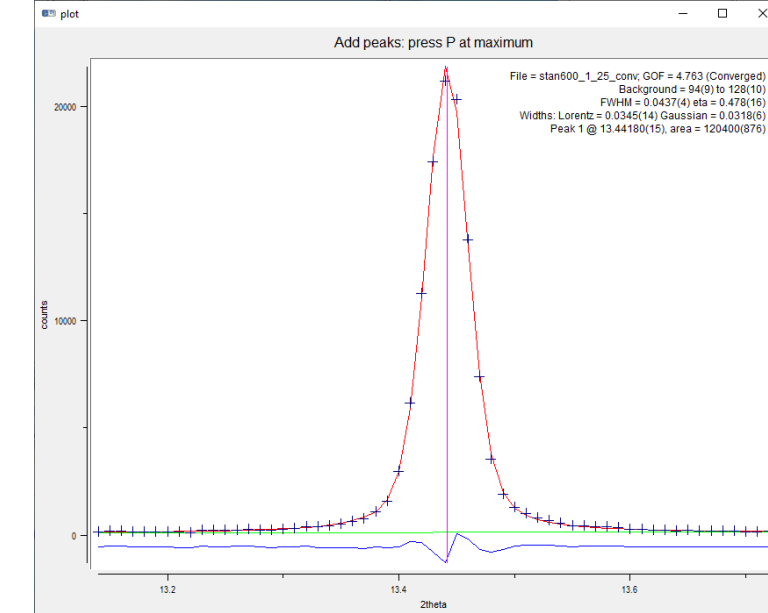
High resolution powder diffraction



Single peak fit: fast, useful for preliminary information on unit cell

Full profile fit: more accurate lattice parameter determination. It allows also structural and microstructural analysis, quantitative analysis...

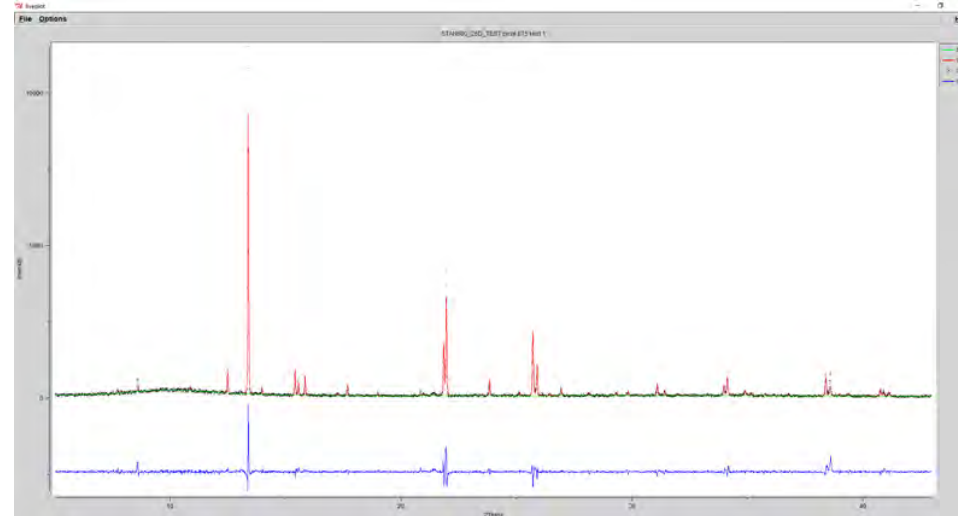
Rietveld fit



Rietveld fit

Simulation of powder pattern

Least square minimization on experimental pattern



Refinable parameters:

Unit cell

Scale factor

Crystal structure

Peak shape

Background

Other parameters (i.e. preferred orientation....)

Information needed:

- 1) Experimental pattern
- 2) Wavelength
- 3) Crystal structure (unit cell, symmetry and atomic coordinates)
(eventually other parameters, i.e. instrumental resolution...)

[Mineralogical Society of America](#), Founded December 30, 1919

The American Mineralogist Crystal Structure Database

The [Crystal Structure Database](#) has been compiled by Bob Downs and Paul Heese of the University of Arizona. It includes every structure published in both the American Mineralogist, The Canadian Mineralogist, the European Journal of Mineralogy and is beginning to include structures from Physics and Chemistry of Minerals.

The database is maintained under the care of the Mineralogical Society of America and the Mineralogical Association of Canada, and financed by the National Science Foundation.

The data is retrieved via a compound query using pop-up windows with the fields "Mineral Name", "Author", "Title", "Year", or "Volume".

A complete description of the American Mineralogist crystal structure database and use with interactive software is available ([pdf, 156 K](#))

Copyright © 1997 - 2021 [Mineralogical Society of America](#). All rights reserved. Email any comments, suggestions or problems with site to webmaster@minsocam.org
or write Mineralogical Society of America, 3635 Concorde Pkwy Ste 500, Chantilly, VA 20151-1110 United States Tel +1 (703) 652-9950 Fax +1 (703) 652-9951

American Mineralogist Crystal Structure Database

This site is an interface to a crystal structure database that includes every structure published in the American Mineralogist, The Canadian Mineralogist, European Journal of Mineralogy and Physics and Chemistry of Minerals, as well as selected datasets from other journals. The database is maintained under the care of the Mineralogical Society of America and the Mineralogical Association of Canada, and financed by the National Science Foundation.

stannite [Mineral](#)

[Author](#)

[Chemistry Search](#)

[Cell Parameters and Symmetry](#)

[Diffraction Search](#)

[General Search](#)
[Search Tips](#)

Logic interface **AND** **OR**

Viewing ([About File Formats](#)) amc long form amc short form cif

Download amc cif diffraction data

[People](#)



[Extra](#)

Number of Files downloaded since Apr 1, 2003: 920296930

Data Last Updated: July 28, 2021

Web Page Last Updated: July 31, 2018

This page has been accessed 3608222 times.

Also see our [complete list of minerals](#) and [complete list of authors](#).

This material is based upon work supported by the National Science Foundation under Grant Nos. EAR-0112782, and EAR-0622371. Any opinions, findings, and conclusions or recommendations expressed in this material are those of the authors and do not necessarily reflect the views of the National Science Foundation.

Should the use of the database require a citation, then please use: Downs, R.T. and Hall-Wallace, M. (2003) The American Mineralogist Crystal Structure Database. American Mineralogist 88, 247-250. ([pdf file](#))

Contact [Robert T Downs](#) for suggestions and corrections.

[Stannite](#) Bonazzi P, Bindi L, Bernardini G P, Menchetti S The Canadian Mineralogist 41 (2003) 639-647

A model for the mechanism of incorporation of Cu, Fe and Zn in the stannite - kesterite series, Cu₂FeSnS₄ - Cu₂ZnSnS₄

Sample: Fe100

_database_code_amcsd 0005838

5.4495 5.4495 10.726 90 90 90 I-42m

Unit cell and spacegroup

| atom | x | y | z | Uiso |
|--------|--------|--------|--------|--------|
| Cu(4d) | 0 | 1/2 | 1/4 | .01924 |
| Fe(2a) | 0 | 0 | 0 | .01219 |
| Sn(2b) | 0 | 0 | 1/2 | .01025 |
| S(8i) | .75581 | .75581 | .87012 | .01134 |

[Download AMC data \(View Text File\)](#)

[Download CIF data \(View Text File\)](#)

[Download diffraction data \(View Text File\)](#)

[View Jmol 3-D Structure \(permalink\)](#)

[Stannite](#) Bonazzi P, Bindi L, Bernardini G P, Menchetti S The Canadian Mineralogist 41 (2003) 639-647

A model for the mechanism of incorporation of Cu, Fe and Zn in the stannite - kesterite series, Cu₂FeSnS₄ - Cu₂ZnSnS₄

Sample: Fe100

_database_code_amcsd 0005838

5.4495 5.4495 10.726 90 90 90 I-42m

| atom | x | y | z | Uiso |
|--------|--------|--------|--------|--------|
| Cu(4d) | 0 | 1/2 | 1/4 | .01924 |
| Fe(2a) | 0 | 0 | 0 | .01219 |
| Sn(2b) | 0 | 0 | 1/2 | .01025 |
| S(8i) | .75581 | .75581 | .87012 | .01134 |

Atomic coordinates

Atomic displacement parameters

[Download AMC data \(View Text File\)](#)

[Download CIF data \(View Text File\)](#)

[Download diffraction data \(View Text File\)](#)

[View Jmol 3-D Structure \(permalink\)](#)

[Stannite](#)

 Bonazzi P, Bindi L, Bernardini G P, Menchetti S

 The Canadian Mineralogist 41 (2003) 639-647

A model for the mechanism of incorporation of Cu, Fe and Zn in the stannite - kesterite series, Cu₂FeSnS₄ - Cu₂ZnSnS₄

Sample: Fe100

_database_code_amcsd 0005838

5.4495 5.4495 10.726 90 90 90 I-42m

| atom | x | y | z | Uiso |
|--------|--------|--------|--------|--------|
| Cu(4d) | 0 | 1/2 | 1/4 | .01924 |
| Fe(2a) | 0 | 0 | 0 | .01219 |
| Sn(2b) | 0 | 0 | 1/2 | .01025 |
| S(8i) | .75581 | .75581 | .87012 | .01134 |

[Download AMC data \(View Text File\)](#)

[Download CIF data \(View Text File\)](#)

[Download diffraction data \(View Text File\)](#)

[View Jmol 3-D Structure \(permalink\)](#)

CIF:
formatted Crystallographic
Information File

Calculation of powder pattern

$$2d_{hkl} \sin\theta = (n)\lambda$$

Bragg's law + structure factor

$$F_{hkl} = \sum_{j=1}^m f_j \exp\left(\frac{2\pi i}{\lambda} \vec{r}_j \cdot \vec{s}\right)$$

Calculation of diffraction angle as function
of hkl (Miller index) + calculation of intensity
of each diffraction

Structure factor

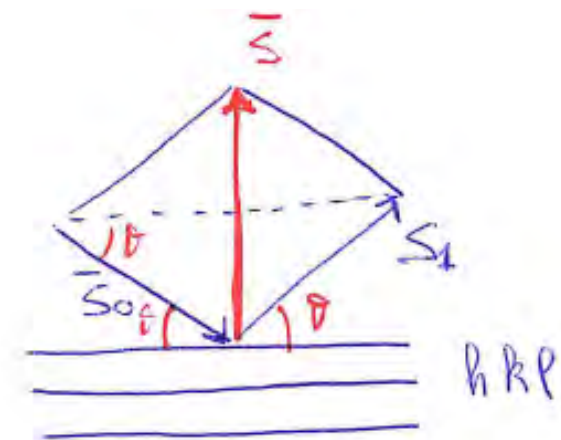
Intensity of diffraction: function of atomic species and structure

$$F_{hkl} = \sum_{j=1}^m f_j \exp\left(\frac{2\pi i}{\lambda} (\vec{r}_j \cdot \vec{s})\right)$$

f_j = atomic scattering factor

r_j = atomic position vector (i.e. atomic coordinates)

\mathbf{S} = scattering vector ($s_1 - s_0$) s_1 : direction of diffracted beam
 s_0 : direction of primary beam



Peak list

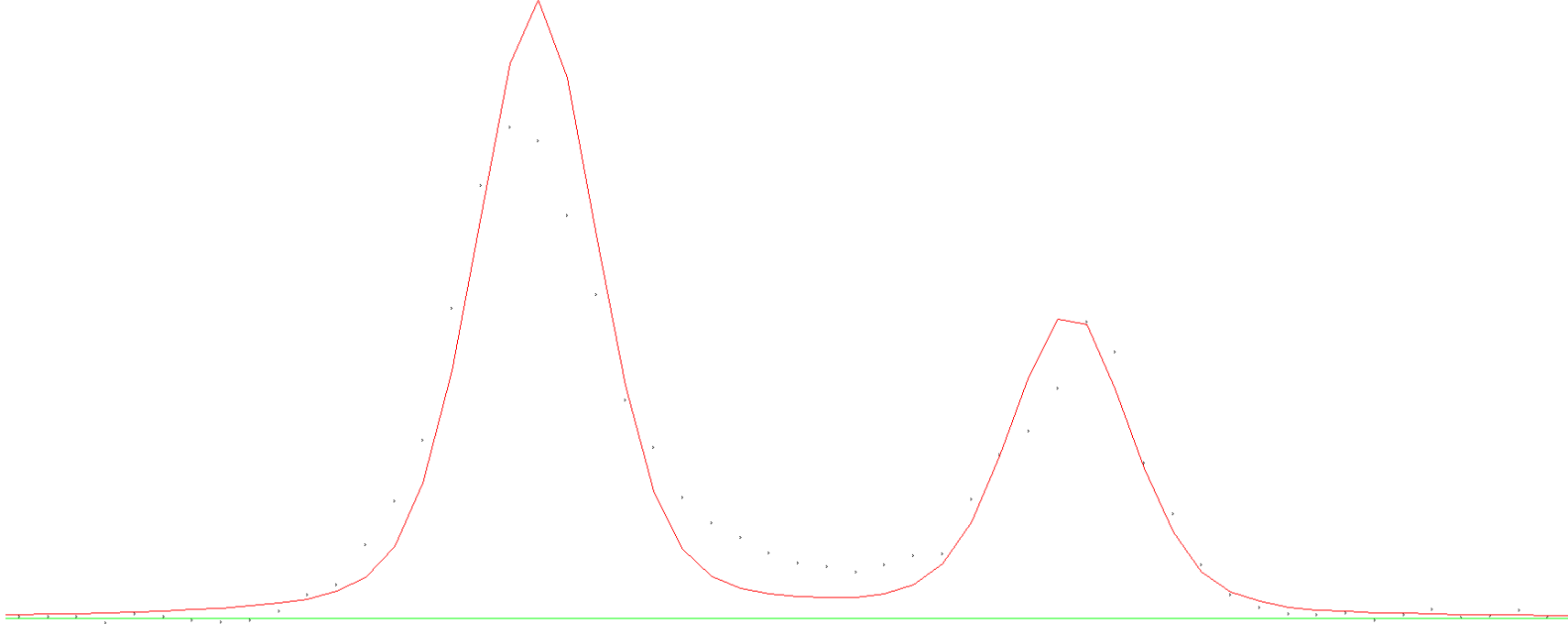
| No. | h | k | l | d [Å] | 2Theta [deg] | I [%] |
|-----|---|---|---|-------|--------------|-------|
| 1 | 0 | 0 | 2 | | | |
| 2 | 1 | 0 | 1 | | | |
| 3 | 1 | 1 | 0 | | | |
| 4 | 1 | 1 | 2 | | | |
| 5 | 1 | 0 | 3 | | | |
| 6 | 2 | 0 | 0 | | | |
| 7 | 0 | 0 | 4 | | | |
| 8 | 2 | 0 | 2 | | | |
| 9 | 2 | 1 | 1 | | | |
| 10 | 1 | 1 | 4 | | | |
| 11 | 2 | 1 | 3 | | | |
| 12 | 1 | 0 | 5 | | | |
| 13 | 2 | 2 | 0 | | | |
| 14 | 2 | 0 | 4 | | | |
| 15 | 2 | 2 | 2 | | | |
| 16 | 3 | 0 | 1 | | | |
| 17 | 3 | 1 | 2 | | | |
| 18 | 1 | 1 | 6 | | | |
| 19 | 2 | 2 | 4 | | | |
| 20 | 3 | 2 | 1 | | | |
| 21 | 3 | 1 | 4 | | | |
| 22 | 4 | 0 | 0 | | | |
| 23 | 0 | 0 | 8 | | | |
| 24 | 2 | 2 | 6 | | | |
| 25 | 3 | 3 | 2 | | | |
| 26 | 3 | 1 | 6 | | | |
| 27 | 4 | 0 | 4 | | | |
| 28 | 2 | 0 | 8 | | | |
| 29 | 4 | 2 | 4 | | | |
| 30 | 2 | 2 | 8 | | | |

Peak list

| No. | h | k | l | d [Å] | 2Theta [deg] | I [%] |
|-----|---|---|---|---------|--------------|-------|
| 1 | 0 | 0 | 2 | 5.36700 | 7.788 | |
| 2 | 1 | 0 | 1 | 4.85700 | 8.608 | |
| 3 | 1 | 1 | 0 | 3.85200 | 10.860 | |
| 4 | 1 | 1 | 2 | 3.12900 | 13.379 | |
| 5 | 1 | 0 | 3 | 2.99000 | 14.004 | |
| 6 | 2 | 0 | 0 | 2.72400 | 15.380 | |
| 7 | 0 | 0 | 4 | 2.68300 | 15.616 | |
| 8 | 2 | 0 | 2 | 2.42900 | 17.261 | |
| 9 | 2 | 1 | 1 | 2.37640 | 17.646 | |
| 10 | 1 | 1 | 4 | 2.20220 | 19.054 | |
| 11 | 2 | 1 | 3 | 2.01380 | 20.856 | |
| 12 | 1 | 0 | 5 | 1.99800 | 21.023 | |
| 13 | 2 | 2 | 0 | 1.92580 | 21.821 | |
| 14 | 2 | 0 | 4 | 1.91240 | 21.975 | |
| 15 | 2 | 2 | 2 | 1.81360 | 23.189 | |
| 16 | 3 | 0 | 1 | 1.79130 | 23.481 | |
| 17 | 3 | 1 | 2 | 1.64090 | 25.669 | |
| 18 | 1 | 1 | 6 | 1.62320 | 25.954 | |
| 19 | 2 | 2 | 4 | 1.56520 | 26.933 | |
| 20 | 3 | 2 | 1 | 1.49620 | 28.200 | |
| 21 | 3 | 1 | 4 | 1.45030 | 29.112 | |
| 22 | 4 | 0 | 0 | 1.36250 | 31.034 | |
| 23 | 0 | 0 | 8 | 1.34220 | 31.515 | |
| 24 | 2 | 2 | 6 | 1.31140 | 32.275 | |
| 25 | 3 | 3 | 2 | 1.24930 | 33.927 | |
| 26 | 3 | 1 | 6 | 1.24150 | 34.147 | |
| 27 | 4 | 0 | 4 | 1.21500 | 34.915 | |
| 28 | 2 | 0 | 8 | 1.20440 | 35.233 | |
| 29 | 4 | 2 | 4 | 1.10990 | 38.344 | |
| 30 | 2 | 2 | 8 | 1.10170 | 38.641 | |

Peak list

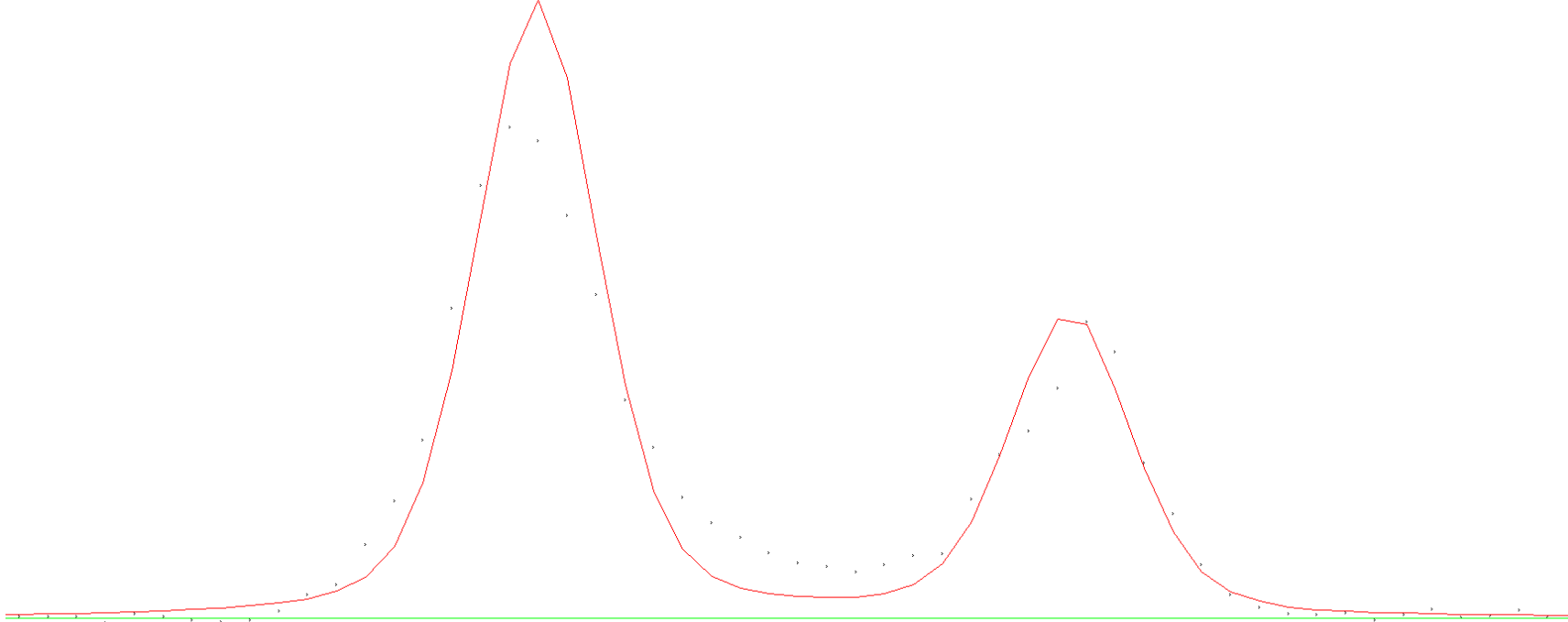
| No. | h | k | l | d [Å] | 2Theta [deg] | I [%] |
|-----|---|---|---|---------|--------------|-------|
| 1 | 0 | 0 | 2 | 5.36700 | 7.788 | 2.0 |
| 2 | 1 | 0 | 1 | 4.85700 | 8.608 | 3.0 |
| 3 | 1 | 1 | 0 | 3.85200 | 10.860 | 2.0 |
| 4 | 1 | 1 | 2 | 3.12900 | 13.379 | 100.0 |
| 5 | 1 | 0 | 3 | 2.99000 | 14.004 | 1.0 |
| 6 | 2 | 0 | 0 | 2.72400 | 15.380 | 6.0 |
| 7 | 0 | 0 | 4 | 2.68300 | 15.616 | 4.0 |
| 8 | 2 | 0 | 2 | 2.42900 | 17.261 | 2.0 |
| 9 | 2 | 1 | 1 | 2.37640 | 17.646 | 2.0 |
| 10 | 1 | 1 | 4 | 2.20220 | 19.054 | 1.0 |
| 11 | 2 | 1 | 3 | 2.01380 | 20.856 | 1.0 |
| 12 | 1 | 0 | 5 | 1.99800 | 21.023 | 1.0 |
| 13 | 2 | 2 | 0 | 1.92580 | 21.821 | 15.0 |
| 14 | 2 | 0 | 4 | 1.91240 | 21.975 | 27.0 |
| 15 | 2 | 2 | 2 | 1.81360 | 23.189 | 1.0 |
| 16 | 3 | 0 | 1 | 1.79130 | 23.481 | 1.0 |
| 17 | 3 | 1 | 2 | 1.64090 | 25.669 | 13.0 |
| 18 | 1 | 1 | 6 | 1.62320 | 25.954 | 7.0 |
| 19 | 2 | 2 | 4 | 1.56520 | 26.933 | 2.0 |
| 20 | 3 | 2 | 1 | 1.49620 | 28.200 | 1.0 |
| 21 | 3 | 1 | 4 | 1.45030 | 29.112 | 1.0 |
| 22 | 4 | 0 | 0 | 1.36250 | 31.034 | 2.0 |
| 23 | 0 | 0 | 8 | 1.34220 | 31.515 | 1.0 |
| 24 | 2 | 2 | 6 | 1.31140 | 32.275 | 1.0 |
| 25 | 3 | 3 | 2 | 1.24930 | 33.927 | 2.0 |
| 26 | 3 | 1 | 6 | 1.24150 | 34.147 | 3.0 |
| 27 | 4 | 0 | 4 | 1.21500 | 34.915 | 1.0 |
| 28 | 2 | 0 | 8 | 1.20440 | 35.233 | 1.0 |
| 29 | 4 | 2 | 4 | 1.10990 | 38.344 | 3.0 |
| 30 | 2 | 2 | 8 | 1.10170 | 38.641 | 2.0 |



Simulation of diffraction:

Sum of simulated peaks

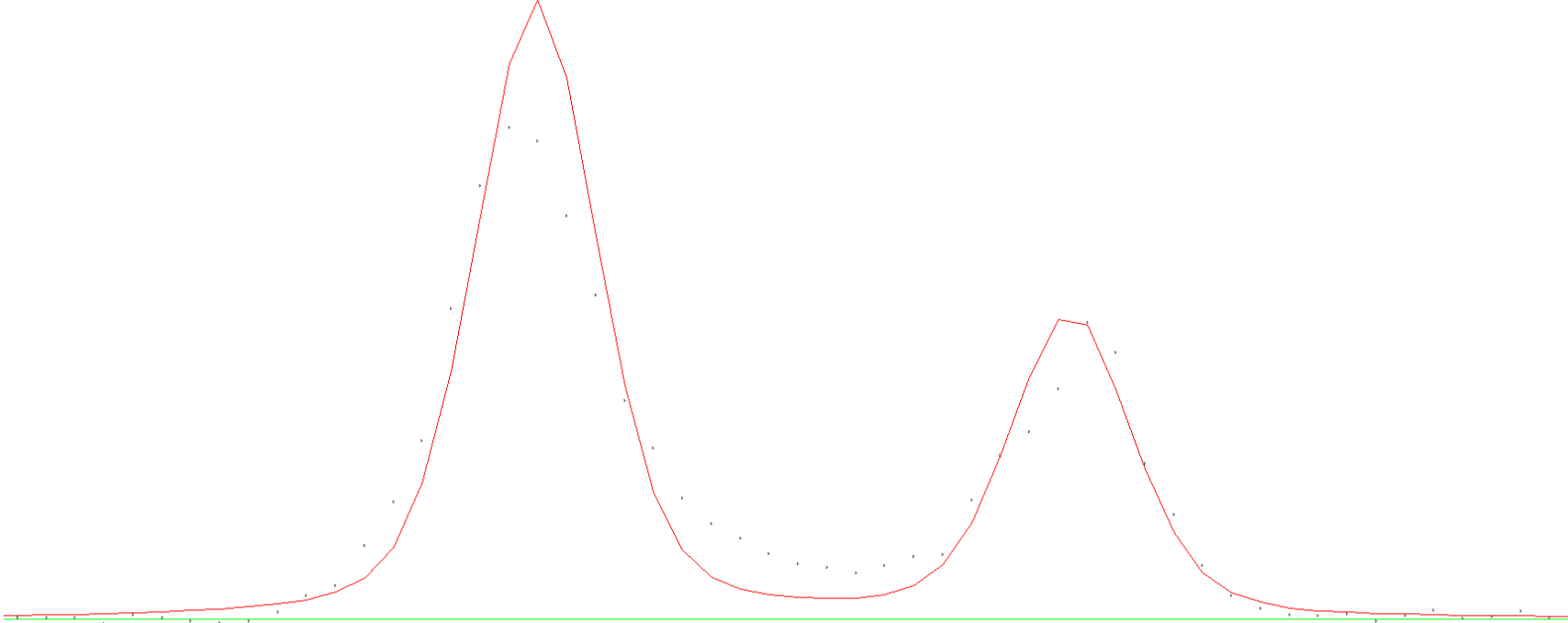
Peak position (bragg's law) + peak scale factor (Structure factor) + peak shape



$h_1 k_1 l_1$

$h_2 k_2 l_2$

Peak position: bragg's law



Scale factor (proportional to squared structure factor)

h1 k1 l1

*

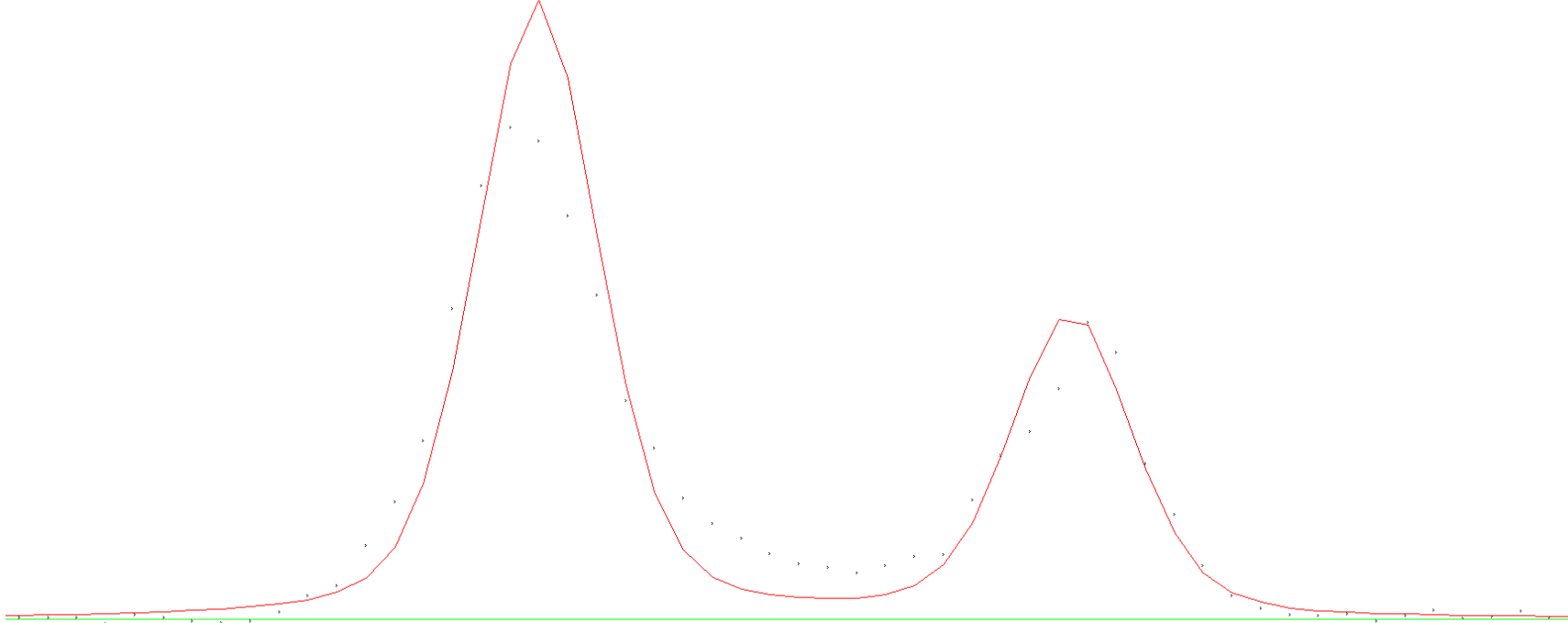


h2 k2 l2

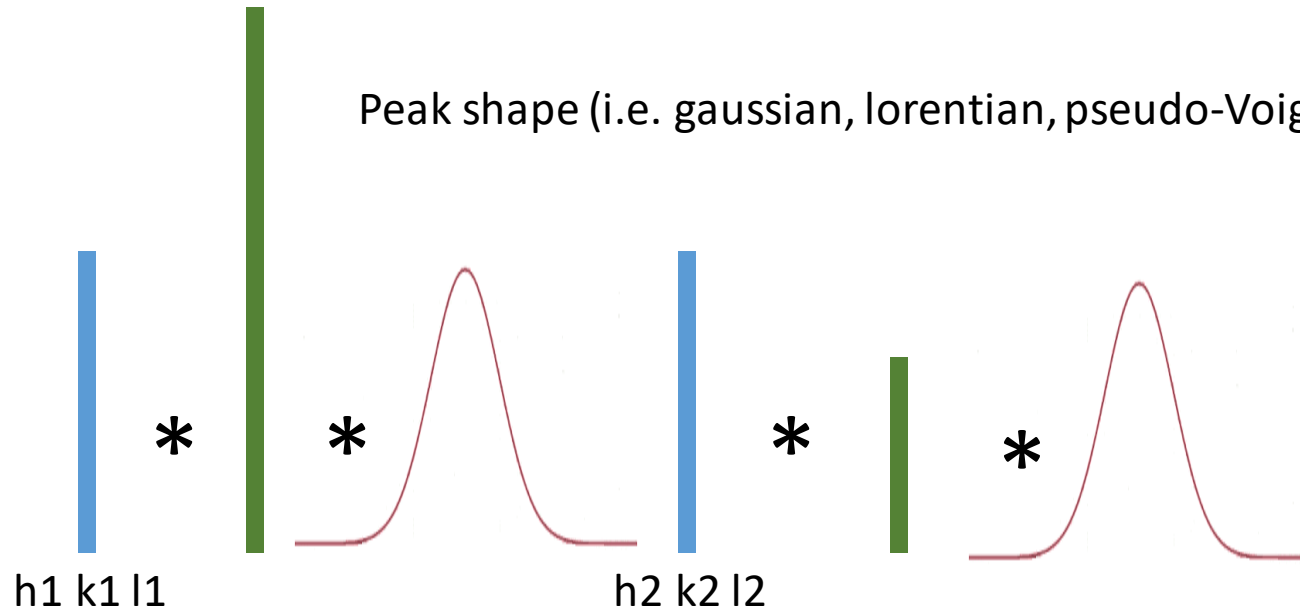
*

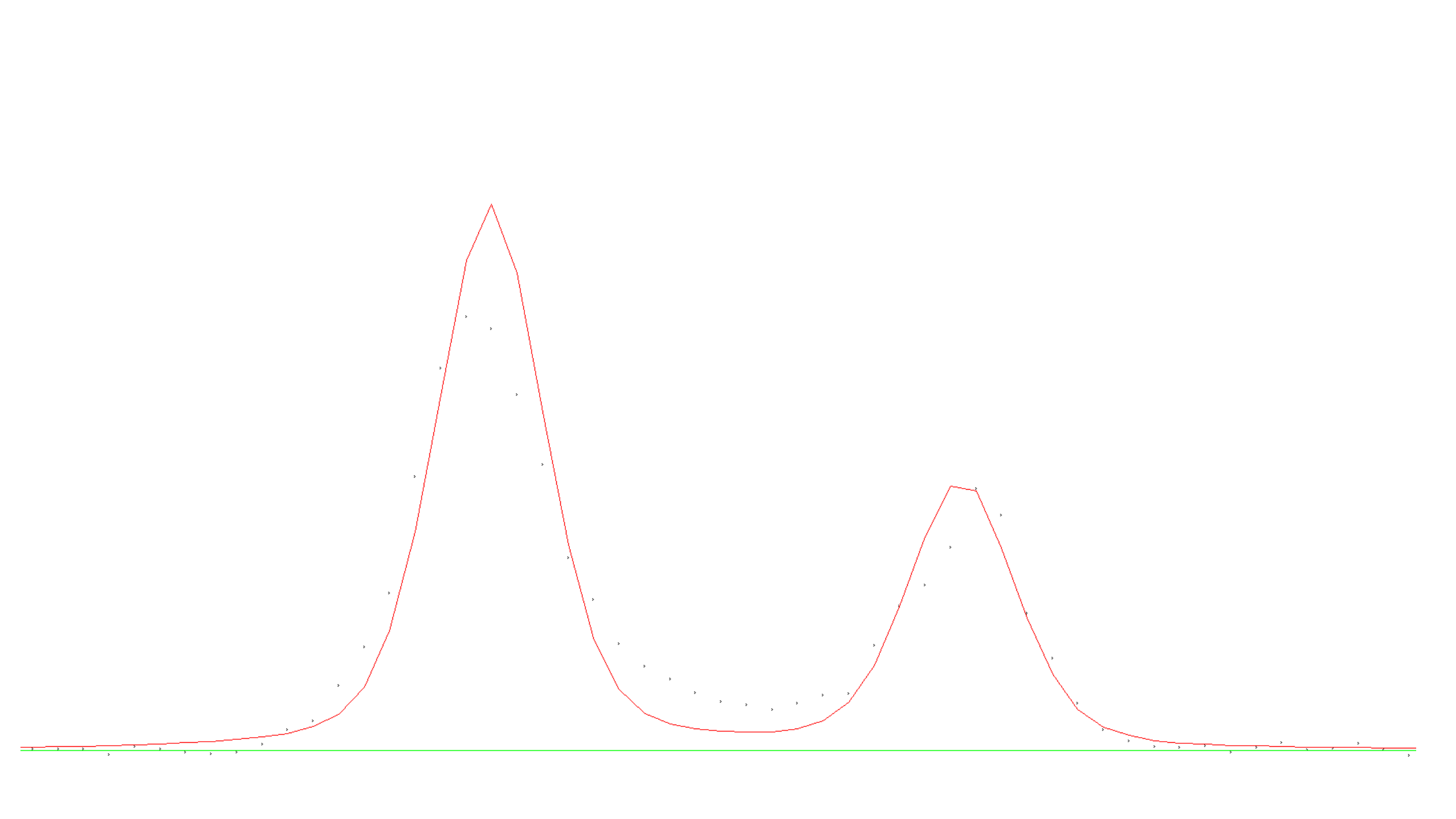


Peak position: bragg's law



Peak shape (i.e. gaussian, lorentian, pseudo-Voigt, etc...)





thermal_expansion

File Home Condividi Visualizza

Aggiungi ad Accesso rapido Copia Incolla Taglia Copia percorso Incolla collegamento Sposta in Copia in Elimina Rinomina Nuova cartella Nuovo elemento Apri Accesso facilitato Proprietà Nuovo Cronologia Selezione tutto Deseleziona tutto Inverti selezione

Appunti Organizza Nuovo Apri Selezione

Questo PC > Questo PC > DATA (D:) > data > tutorial_scuola > thermal_expansion

Cerca in thermal_expansion

| | Nome | Ultima modifica | Tipo | Dimensione |
|----------------------------|---------------------|------------------|---------------------|------------|
| Accesso rapido | elettra.prm | 05/08/2016 18:22 | Adobe Premiere P... | 2 KB |
| Desktop | STAN_001.cif | 11/09/2021 23:02 | File CIF | 10 KB |
| Download | STAN_001.EXP | 11/09/2021 23:02 | File EXP | 19 KB |
| Documenti | STAN_001_phase1.cif | 11/09/2021 23:02 | File CIF | 2 KB |
| Immagini | STAN_001_publ.cif | 11/09/2021 23:02 | File CIF | 5 KB |
| calibrazione_area_detector | stannite_025C.gsa | 08/08/2016 10:29 | File GSA | 46 KB |
| gsas | stannite_050C.gsa | 08/08/2016 10:29 | File GSA | 46 KB |
| thermal_expansion | stannite_100C.gsa | 08/08/2016 10:29 | File GSA | 46 KB |
| tutorial_scuola | stannite_150C.gsa | 08/08/2016 10:29 | File GSA | 46 KB |
| Creative Cloud Files | stannite_200C.gsa | 08/08/2016 10:29 | File GSA | 46 KB |
| OneDrive | stannite_250C.gsa | 08/08/2016 10:29 | File GSA | 46 KB |
| Questo PC | stannite_300C.gsa | 08/08/2016 10:29 | File GSA | 46 KB |
| Desktop | stannite_350C.gsa | 08/08/2016 10:29 | File GSA | 46 KB |
| Documenti | stannite_400C.gsa | 08/08/2016 10:29 | File GSA | 46 KB |

Selezionare il file di cui visualizzare l'anteprima.

Rete

14 elementi

thermal_expansion

File Home Condividi Visualizza

Aggiungi ad Accesso rapido Copia Incolla Taglia Copia percorso Incolla collegamento Sposta in Copia in Elimina Rinomina Nuova cartella Nuovo elemento Apri Accesso facilitato Proprietà Nuovo Cronologia Selezione tutto Deseleziona tutto Inverti selezione

Appunti Organizza Nuovo Apri Selezione

Questo PC > Questo PC > DATA (D:) > data > tutorial_scuola > thermal_expansion

Cerca in thermal_expansion

| | Nome | Ultima modifica | Tipo | Dimensione |
|----------------------------|---------------------|------------------|---------------------|------------|
| Accesso rapido | elettra.prm | 05/08/2016 18:22 | Adobe Premiere P... | 2 KB |
| Desktop | STAN_001.cif | 11/09/2021 23:02 | File CIF | 10 KB |
| Download | STAN_001.EXP | 11/09/2021 23:02 | File EXP | 19 KB |
| Documenti | STAN_001_phase1.cif | 11/09/2021 23:02 | File CIF | 2 KB |
| Immagini | STAN_001_publ.cif | 11/09/2021 23:02 | File CIF | 5 KB |
| calibrazione_area_detector | stannite_025C.gsa | 08/08/2016 10:29 | File GSA | 46 KB |
| gsas | stannite_050C.gsa | 08/08/2016 10:29 | File GSA | 46 KB |
| thermal_expansion | stannite_100C.gsa | 08/08/2016 10:29 | File GSA | 46 KB |
| tutorial_scuola | stannite_150C.gsa | 08/08/2016 10:29 | File GSA | 46 KB |
| Creative Cloud Files | stannite_200C.gsa | 08/08/2016 10:29 | File GSA | 46 KB |
| OneDrive | stannite_250C.gsa | 08/08/2016 10:29 | File GSA | 46 KB |
| Questo PC | stannite_300C.gsa | 08/08/2016 10:29 | File GSA | 46 KB |
| Desktop | stannite_350C.gsa | 08/08/2016 10:29 | File GSA | 46 KB |
| Documenti | stannite_400C.gsa | 08/08/2016 10:29 | File GSA | 46 KB |

Selezionare il file di cui visualizzare l'anteprima.

Rete

14 elementi

thermal_expansion

File Home Condividi Visualizza

Aggiungi ad Copia Incolla Taglia Copia percorso Sposta in Copia in Elimina Rinomina Nuova cartella Nuovo element... Accesso facilitato Proprietà Apri Selezione tutto Cronologia Deseleziona tutto Inverti selezione

Appunti Organizza Nuovo

Questo PC > DATA (D:) > data > tutorial_scuola > thermal_expansion

Cerca in thermal_expansion

| | A | B | C | D |
|----|---|---|---|---|
| 1 | | | | |
| 2 | | | | |
| 3 | | | | |
| 4 | | | | |
| 5 | | | | |
| 6 | | | | |
| 7 | | | | |
| 8 | | | | |
| 9 | | | | |
| 10 | | | | |
| 11 | | | | |
| 12 | | | | |
| 13 | | | | |
| 14 | | | | |
| 15 | | | | |
| 16 | | | | |
| 17 | | | | |
| 18 | | | | |
| 19 | | | | |
| 20 | | | | |
| 21 | | | | |
| 22 | | | | |
| 23 | | | | |
| 24 | | | | |
| 25 | | | | |
| 26 | | | | |
| 27 | | | | |
| 28 | | | | |
| 29 | | | | |
| 30 | | | | |
| 31 | | | | |
| 32 | | | | |
| 33 | | | | |
| 34 | | | | |
| 35 | | | | |
| 36 | | | | |
| 37 | | | | |

Nome Ultima modifica Tipo Dimensione

elettra.prm 05/08/2016 18:22 Adobe Premiere P... 2 KB

STAN_001.cif 11/09/2021 23:02 File CIF 10 KB

STAN_001.EXP 11/09/2021 23:02 File EXP 19 KB

STAN_001_phase1.cif 11/09/2021 23:02 File CIF 2 KB

STAN_001_publ.cif 11/09/2021 23:02 File CIF 5 KB

STAN025.CMT 11/09/2021 23:24 File CMT 3 KB

STAN025.EXP 11/09/2021 23:24 File EXP 13 KB

STAN025.LST 11/09/2021 23:24 File LST 633 KB

STAN025.00A 11/09/2021 23:23 File 00A 12 KB

STAN025.00B 11/09/2021 23:23 File 00B 12 KB

STAN025.00C 11/09/2021 23:23 File 00C 12 KB

STAN025.001 11/09/2021 23:21 File 001 1 KB

STAN025.002 11/09/2021 23:21 File 002 2 KB

STAN025.003 11/09/2021 23:21 File 003 5 KB

STAN025.004 11/09/2021 23:22 File 004 9 KB

STAN025.005 11/09/2021 23:22 File 005 9 KB

STAN025.006 11/09/2021 23:22 File 006 12 KB

STAN025.007 11/09/2021 23:23 File 007 12 KB

STAN025.008 11/09/2021 23:23 File 008 12 KB

STAN025.009 11/09/2021 23:23 File 009 12 KB

STAN025.P01 11/09/2021 23:24 File P01 200 KB

STAN025.R01 11/09/2021 23:24 File R01 7 KB

stannite.xlsx 11/09/2021 23:28 Foglio di lavoro di... 7 KB

stannite_025C.gsa 08/08/2016 10:29 File GSA 46 KB

stannite_050C.gsa 08/08/2016 10:29 File GSA 46 KB

stannite_100C.gsa 08/08/2016 10:29 File GSA 46 KB

stannite_150C.gsa 08/08/2016 10:29 File GSA 46 KB

stannite_200C.gsa 08/08/2016 10:29 File GSA 46 KB

stannite_250C.gsa 08/08/2016 10:29 File GSA 46 KB

stannite_300C.gsa 08/08/2016 10:29 File GSA 46 KB

stannite_350C.gsa 08/08/2016 10:29 File GSA 46 KB

stannite_400C.gsa 08/08/2016 10:29 File GSA 46 KB

32 elementi 1 elemento selezionato 6.04 KB

thermal_expansion

File Home Condividi Visualizza

Aggiungi ad Accesso rapido Copia Incolla Taglia Copia percorso Incolla collegamento Sposta in Copia in Elimina Rinomina Nuova cartella Nuovo element... Nuova Apri Selezione tutto Proprietà Accesso facilitato Cronologia Inverti selezione

Appunti Organizza Nuovo Apri Selezione

Questo PC > DATA (D:) > data > tutorial_scuola > thermal_expansion

Cerca in thermal_expansion

| | A | B | C | D |
|----|---|---|---|---|
| 1 | | | | |
| 2 | | | | |
| 3 | | | | |
| 4 | | | | |
| 5 | | | | |
| 6 | | | | |
| 7 | | | | |
| 8 | | | | |
| 9 | | | | |
| 10 | | | | |
| 11 | | | | |
| 12 | | | | |
| 13 | | | | |
| 14 | | | | |
| 15 | | | | |
| 16 | | | | |
| 17 | | | | |
| 18 | | | | |
| 19 | | | | |
| 20 | | | | |
| 21 | | | | |
| 22 | | | | |
| 23 | | | | |
| 24 | | | | |
| 25 | | | | |
| 26 | | | | |
| 27 | | | | |
| 28 | | | | |
| 29 | | | | |
| 30 | | | | |
| 31 | | | | |
| 32 | | | | |
| 33 | | | | |
| 34 | | | | |
| 35 | | | | |
| 36 | | | | |
| 37 | | | | |

Nome Ultima modifica Tipo Dimensione

elettra.prm 05/08/2016 18:22 Adobe Premiere P... 2 KB

STAN_001.cif 11/09/2021 23:02 File CIF 10 KB

STAN_001.EXP 11/09/2021 23:02 File EXP 19 KB

STAN_001_phase1.cif 11/09/2021 23:02 File CIF 2 KB

STAN_001_publ.cif 11/09/2021 23:02 File CIF 5 KB

STAN025.CMT 11/09/2021 23:24 File CMT 3 KB

STAN025.EXP 11/09/2021 23:24 File EXP 13 KB

STAN025.LST 11/09/2021 23:24 File LST 633 KB

STAN025.00A 11/09/2021 23:23 File 00A 12 KB

STAN025.00B 11/09/2021 23:23 File 00B 12 KB

STAN025.00C 11/09/2021 23:23 File 00C 12 KB

STAN025.001 11/09/2021 23:21 File 001 1 KB

STAN025.002 11/09/2021 23:21 File 002 2 KB

STAN025.003 11/09/2021 23:21 File 003 5 KB

STAN025.004 11/09/2021 23:22 File 004 9 KB

STAN025.005 11/09/2021 23:22 File 005 9 KB

STAN025.006 11/09/2021 23:22 File 006 12 KB

STAN025.007 11/09/2021 23:23 File 007 12 KB

STAN025.008 11/09/2021 23:23 File 008 12 KB

STAN025.009 11/09/2021 23:23 File 009 12 KB

STAN025.P01 11/09/2021 23:24 File P01 200 KB

STAN025.R01 11/09/2021 23:24 File R01 7 KB

stannite.xlsx 11/09/2021 23:28 Foglio di lavoro di... 7 KB

stannite_025C.gsa 08/08/2016 10:29 File GSA 46 KB

stannite_050C.gsa 08/08/2016 10:29 File GSA 46 KB

stannite_100C.gsa 08/08/2016 10:29 File GSA 46 KB

stannite_150C.gsa 08/08/2016 10:29 File GSA 46 KB

stannite_200C.gsa 08/08/2016 10:29 File GSA 46 KB

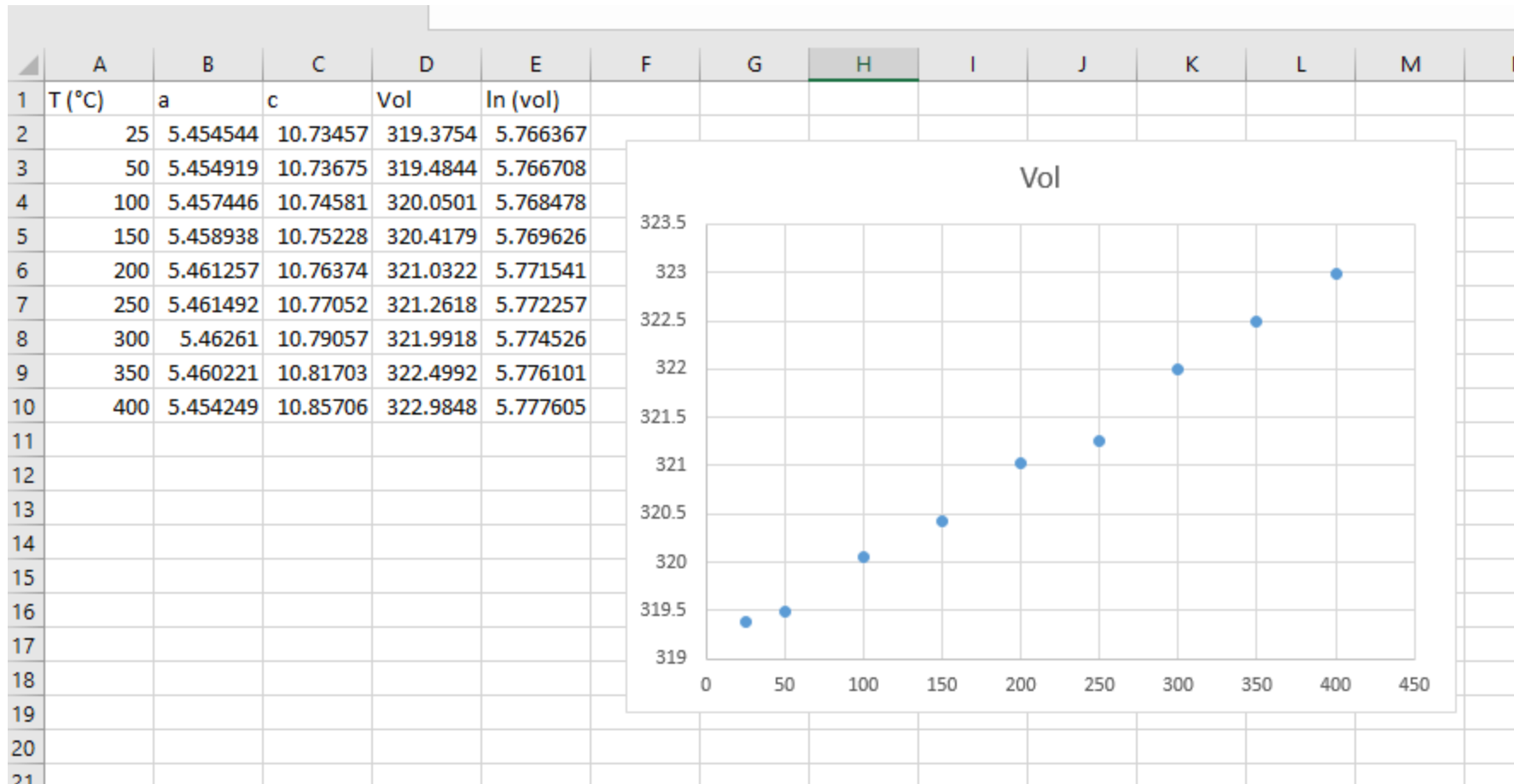
stannite_250C.gsa 08/08/2016 10:29 File GSA 46 KB

stannite_300C.gsa 08/08/2016 10:29 File GSA 46 KB

stannite_350C.gsa 08/08/2016 10:29 File GSA 46 KB

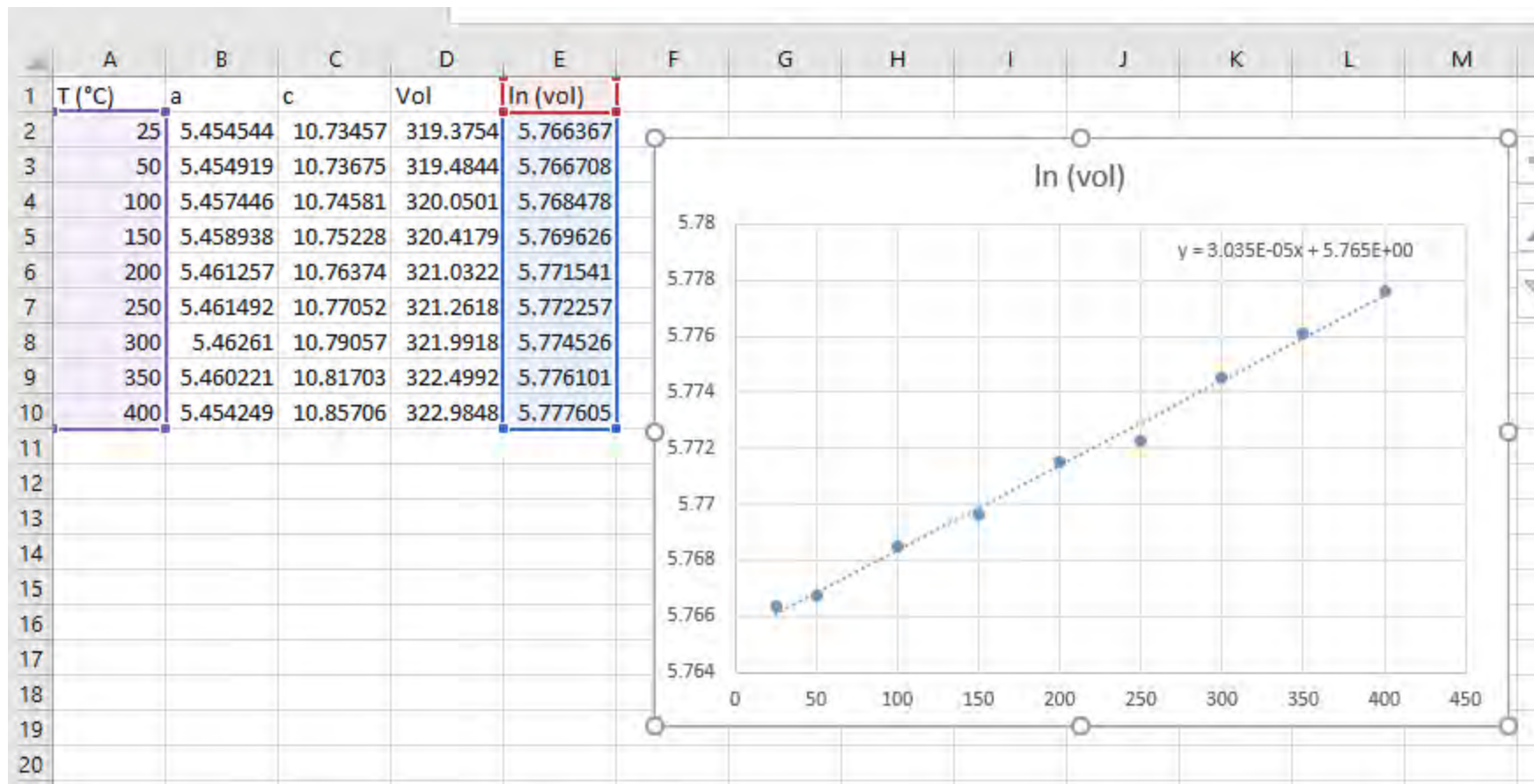
stannite_400C.gsa 08/08/2016 10:29 File GSA 46 KB

32 elementi 1 elemento selezionato 6.04 KB



$$\alpha = 1/V (\partial V / \partial T) = \partial \ln V / \partial T$$

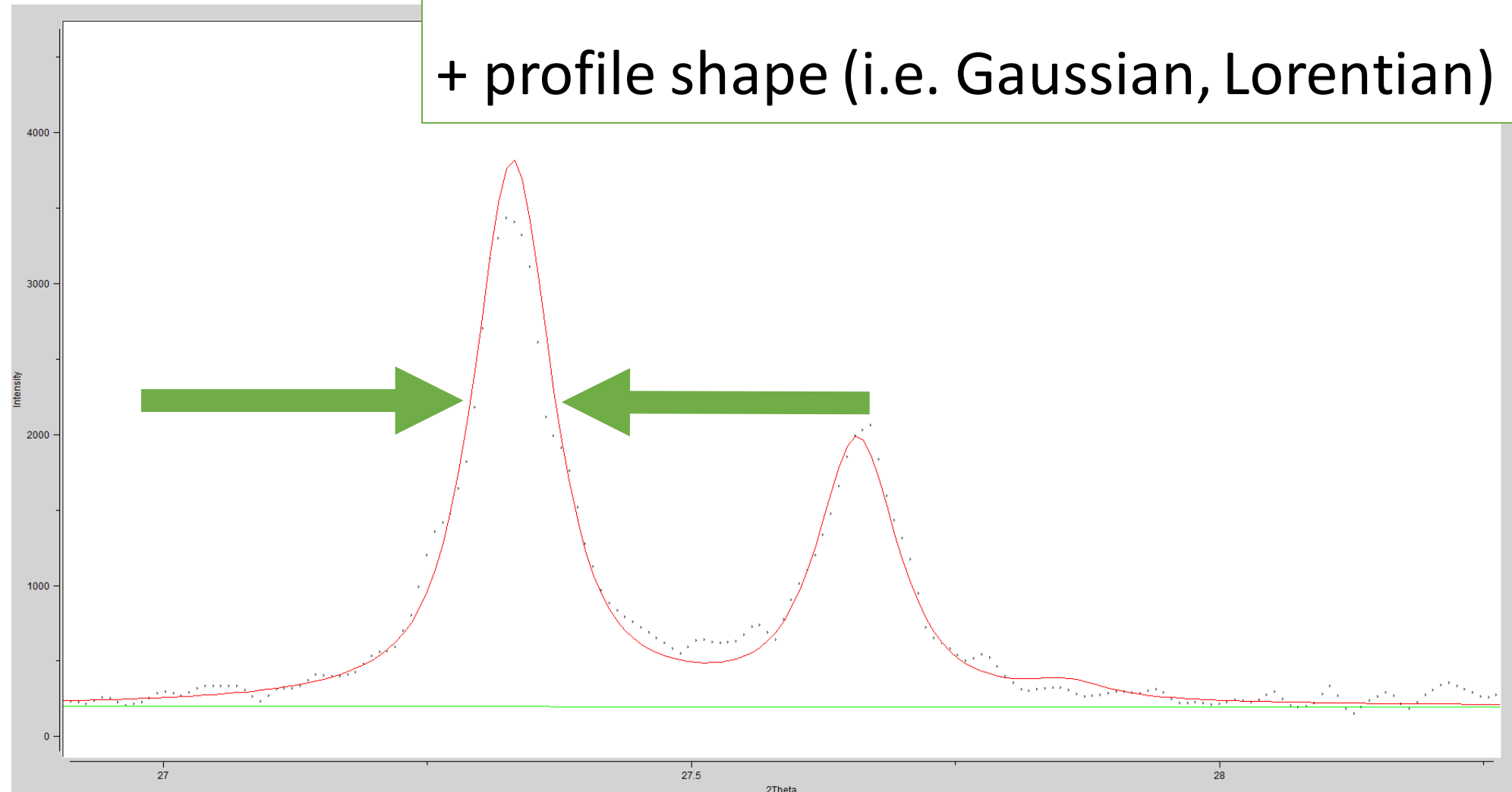
Linear thermal expansion: $\alpha = 30.4 \times 10^{-6} \text{ (K}^{-1}\text{)}$



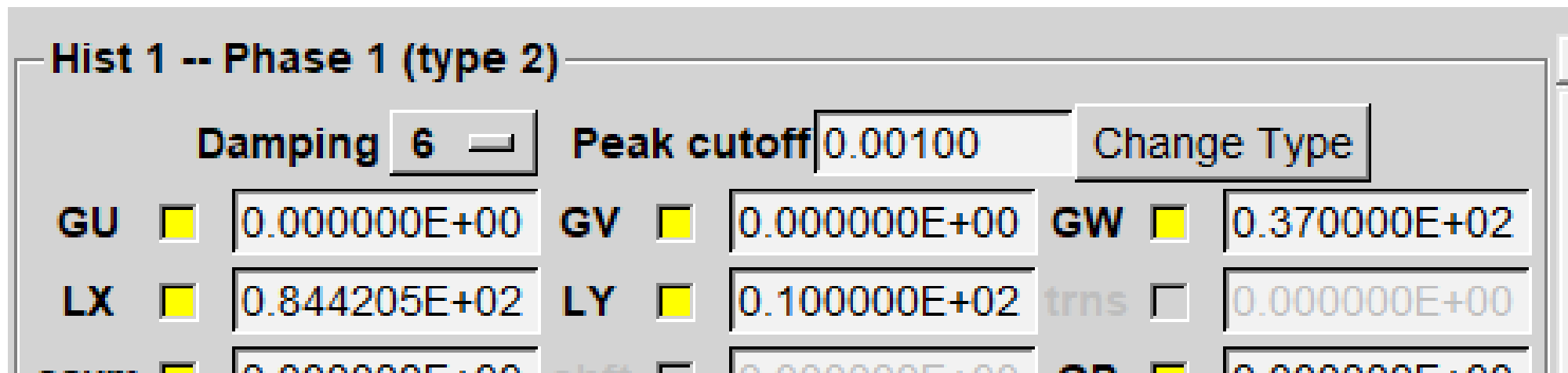
Peak profile

FWHM (Full width at Half Maximum)

+ profile shape (i.e. Gaussian, Lorentzian)

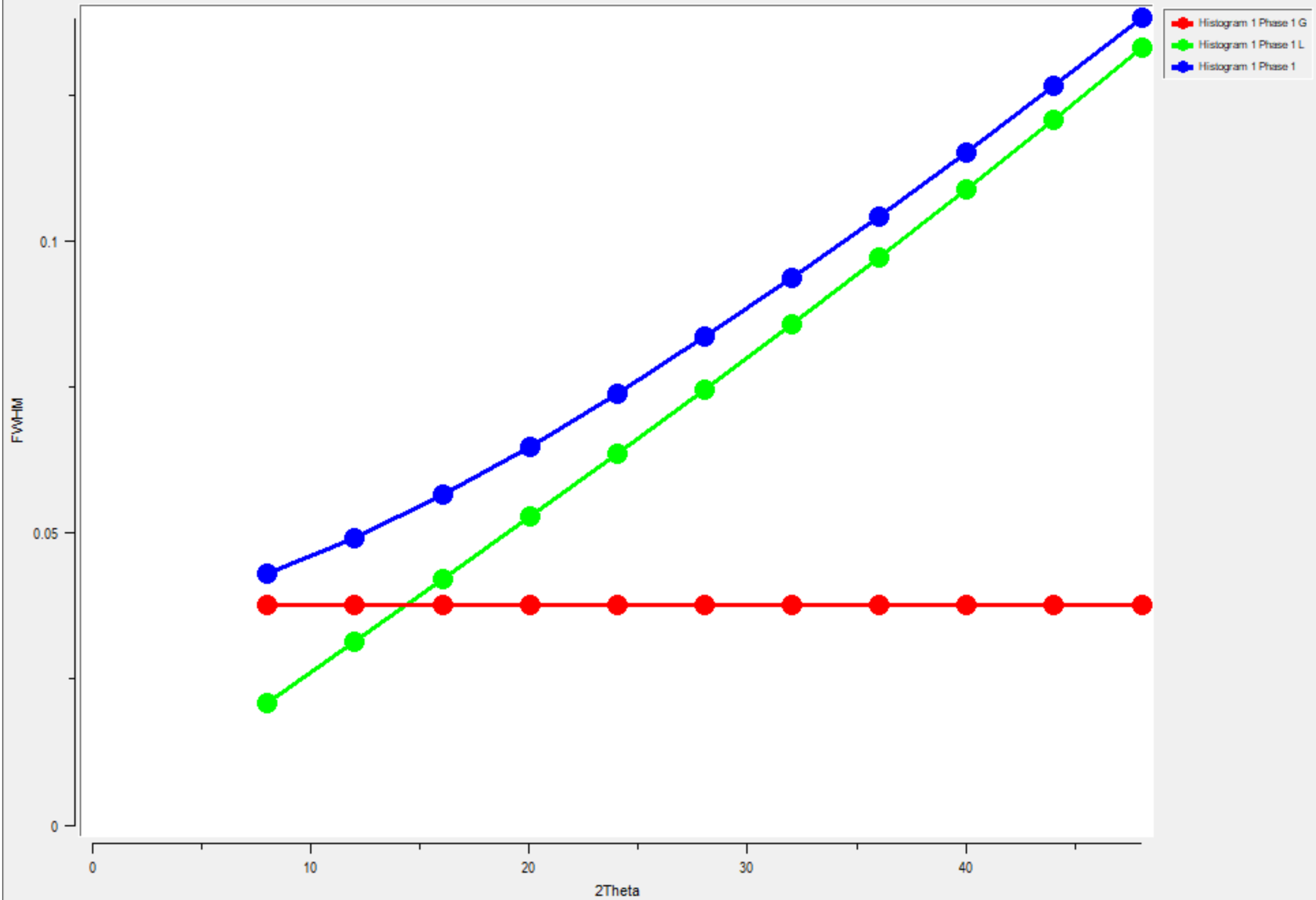


Pseudo-Voigt: Gaussian (G) +Lorentian (L)



GU, GV, GW and LX, LY describe the variation of FWHM of a Gaussian and a Lorentian as function of 2theta angle

76 widplt

[File](#) [Plot Contents](#) [Options](#)[Help](#)

Hist 1 -- Phase 1 (type 2)

Damping

Peak cutoff

Change Type

GU

GV

GW

LX

LY

trns

From GSAS manual

The variance of the peak, σ_2 , varies with 2Θ as

$$\sigma^2 = U \tan^2 \Theta + V \tan \Theta + W + \frac{P}{\cos^2 \Theta}$$

where U, V and W are the coefficients described by Cagliotti, Pauletti and Ricci in 1958 (Nucl. Instrum., 3, 223) and P is the Scherrer coefficient for Gaussian broadening. The Lorentzian coefficient, γ , varies as

$$\gamma = \frac{X + X_e \cos \phi}{\cos \Theta} + (Y + Y_e \cos \phi + \gamma_L d^2) \tan \Theta$$

The first term is the Lorentzian Scherrer broadening and includes an anisotropy coefficient, X_e . The second term describes strain broadening and also includes an anisotropy coefficient. If a sublattice is defined by use of “stacking fault vectors”, then

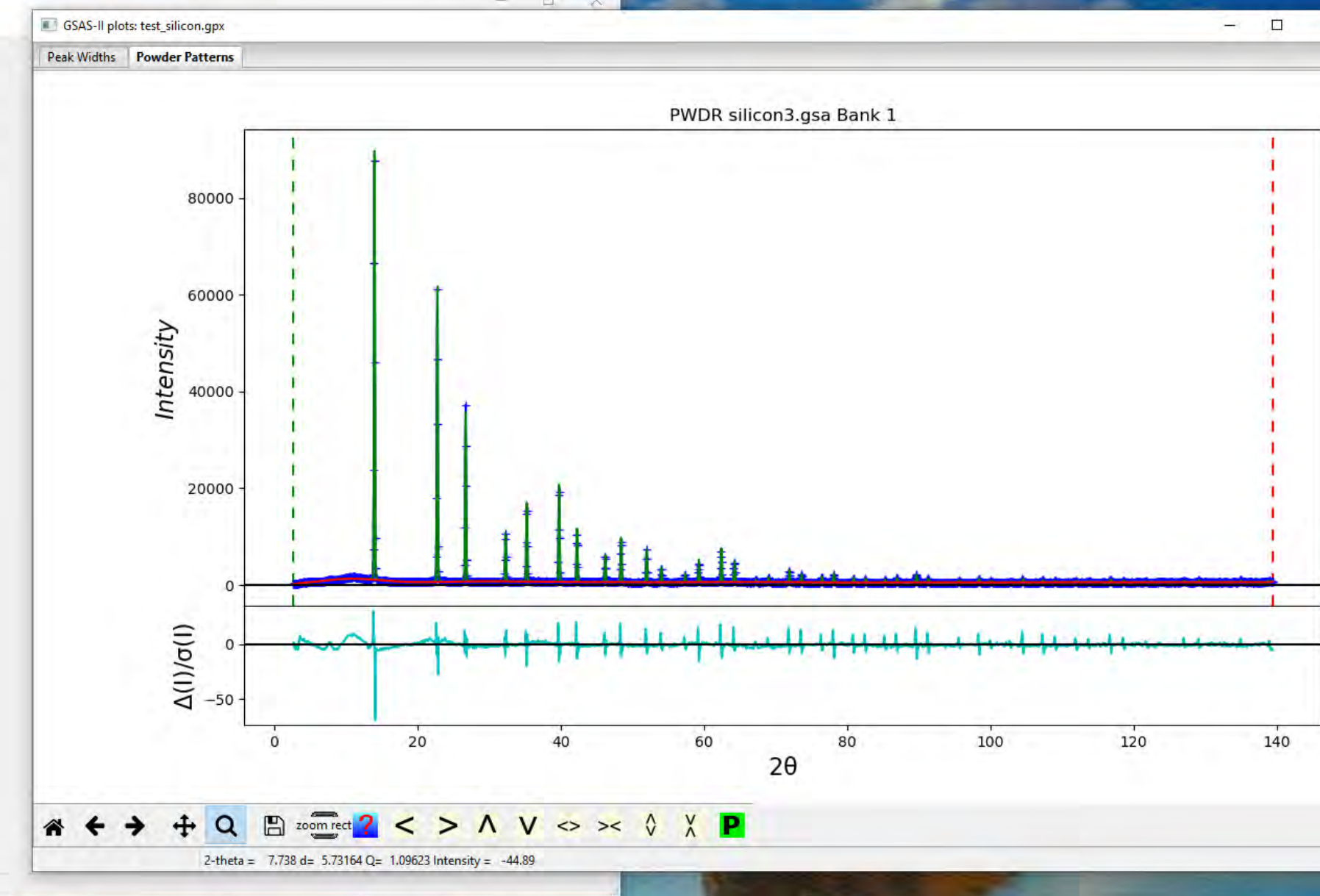
Example: estimation of crystallite size in cubic ZrO₂ (nominally 5 nm by TEM)

- Determination of experimental broadening using a standard (i.e. LaB₆, Silicon)
- Profile fitting of ZrO₂ (using GSAS-II software, which has implemented the deconvolution of sample broadening from instrumental broadening)

File Data Calculate Import Export | Operations | Help

Project: D:\data\tutorial_scuola
 Notebook
 Controls
 Covariance
 Constraints
 Restraints
 Rigid bodies
 Phases
 Silicon
 PWDR silicon3.gsa Bank 1
 Comments
 Limits
 Background
 Instrument Parameters
 Sample Parameters
 Peak List
 Index Peak List
 Unit Cells List
 Reflection Lists

Histogram Type: PXC Bank 1
Name (default) Value Refine?
Azimuth: 0.00
Lam (Å): (0.729320) 0.747631
Zero (0.000): 0.259
Polariz. (0.9600): 0.96
U (0.000): 0.0
V (0.000): 0.0
W (5.402): 33.843
X (0.000): 0.0
Y (0.000): 0.0
Z (0.000): 0.0
SH/L (0.00200): 0.002



Mouse RB drag/drop to reorder

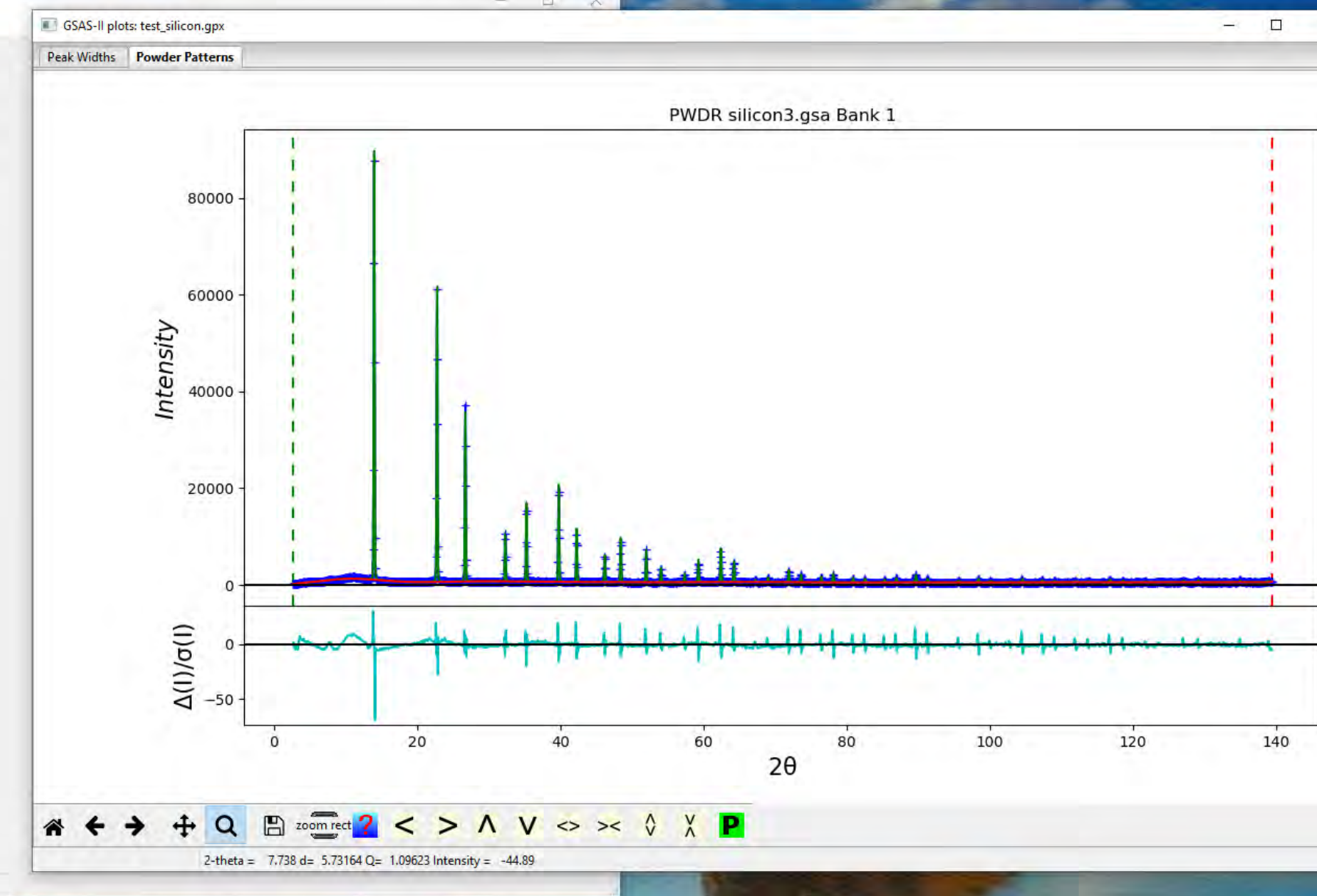
NB: Azimuth is used for polarization only

File Data Calculate Import Export | Operations | Help

- Project: D:\data\tutorial_scuola
- ... Notebook
- ... Controls
- ... Covariance
- ... Constraints
- ... Restraints
- ... Rigid bodies
- ... Phases
 - ... Silicon
- ... PWDR silicon3.gsa Bank 1
 - Comments
 - Limits
 - Background
 - Instrument Parameters
 - Sample Parameters
 - Peak List
 - Index Peak List
 - Unit Cells List
 - Reflection Lists

Histogram Type: PXC Bank 1

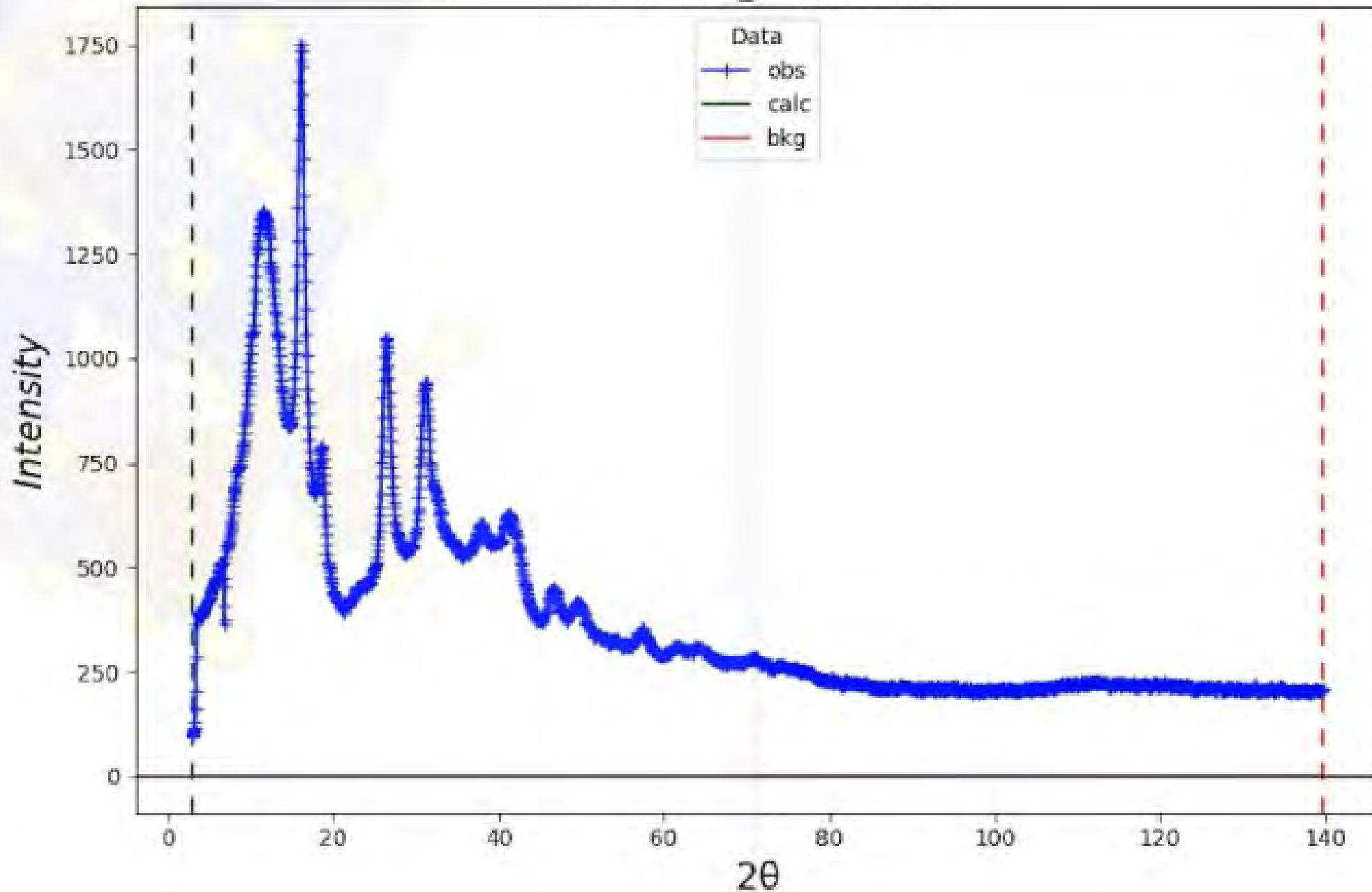
| Name (default) | Value | Refine? |
|--------------------|----------------------|-------------------------------------|
| Azimuth: | 0.00 | |
| Lam (Å): | (0.729320) 0.747631 | <input checked="" type="checkbox"/> |
| Zero (0.000): | 0.259 | <input checked="" type="checkbox"/> |
| Polariz. (0.9600): | 0.96 | <input type="checkbox"/> |
| U (0.000): | 0.0 | <input type="checkbox"/> |
| V (0.000): | 0.0 | <input type="checkbox"/> |
| W (5.402): | 33.843 | <input checked="" type="checkbox"/> |
| X (0.000): | 0.0 | <input type="checkbox"/> |
| Y (0.000): | 0.0 | <input type="checkbox"/> |
| Z (0.000): | 0.0 | <input type="checkbox"/> |
| SH/L (0.00200): | 0.002 | <input type="checkbox"/> |

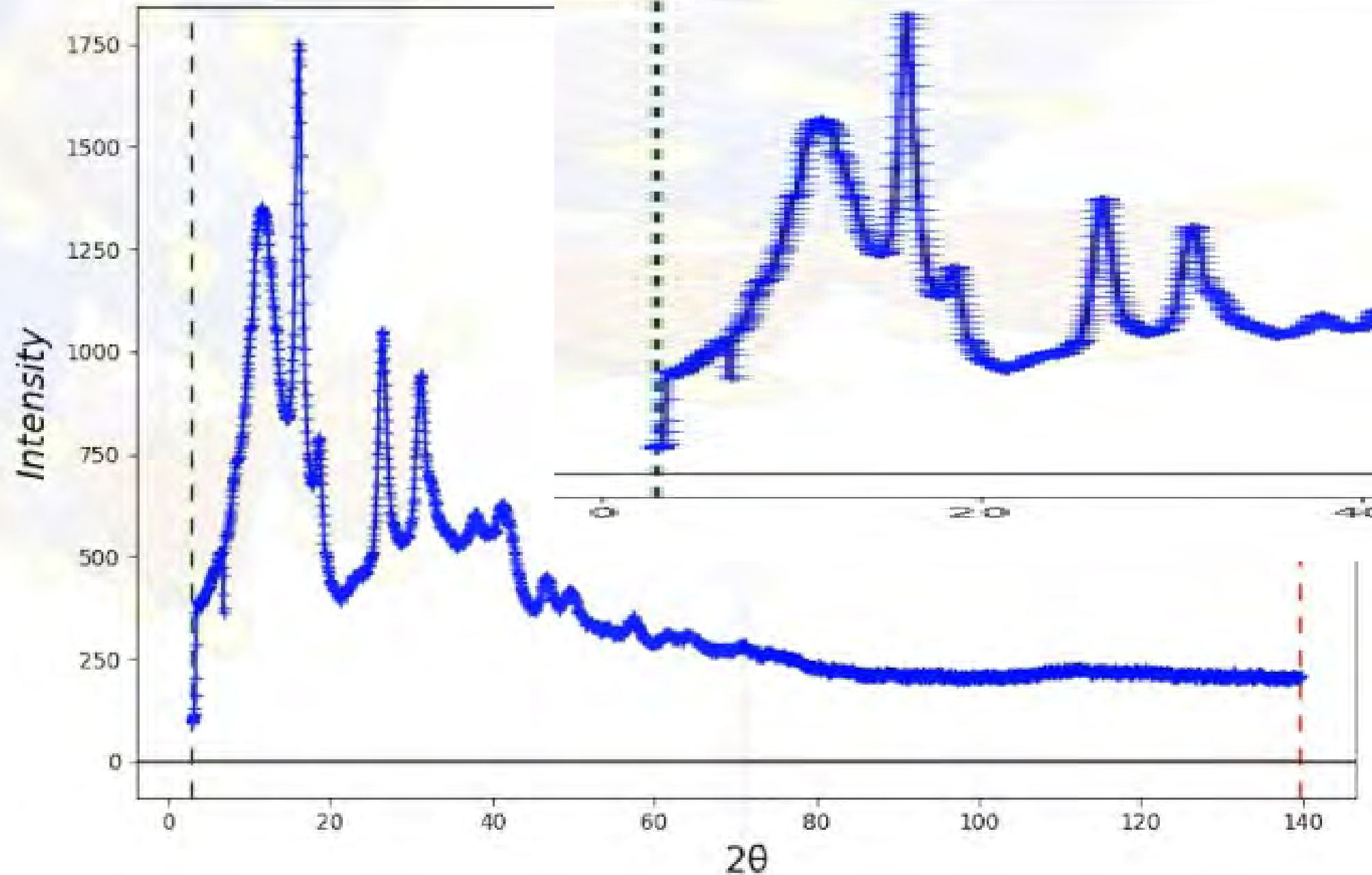


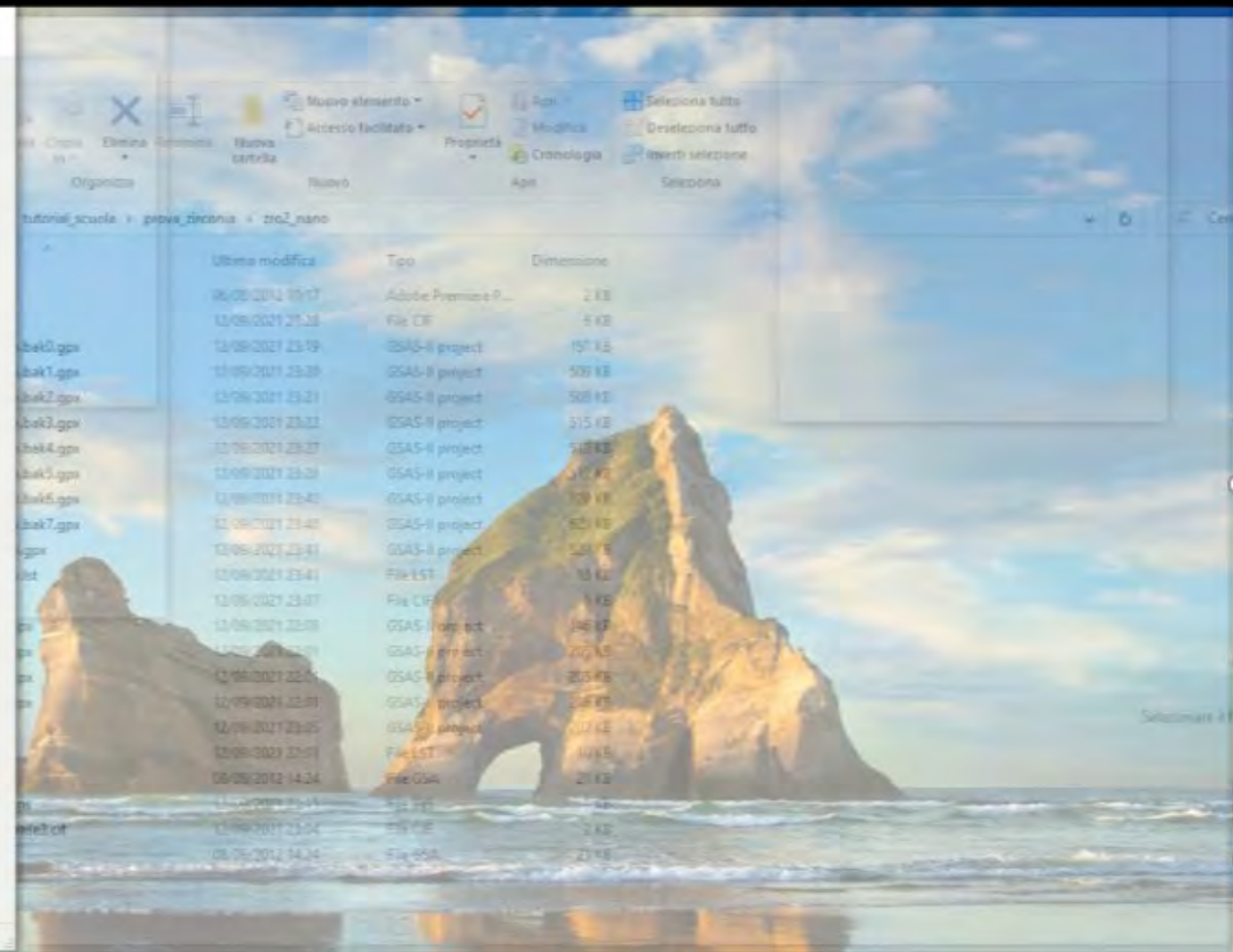
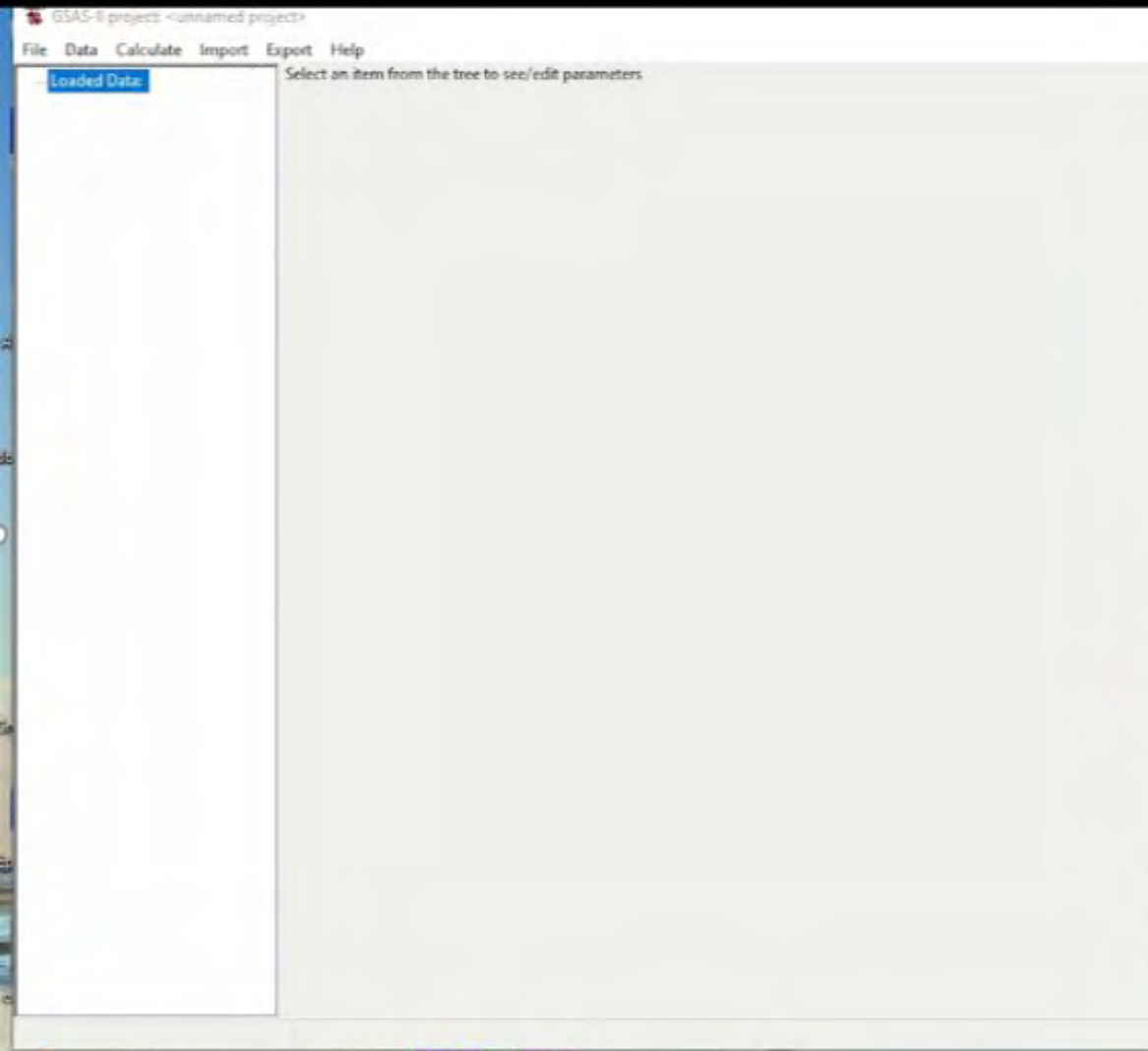
Mouse RB drag/drop to reorder

NB: Azimuth is used for polarization only

PWDR zrrml_01.gsa Bank 1





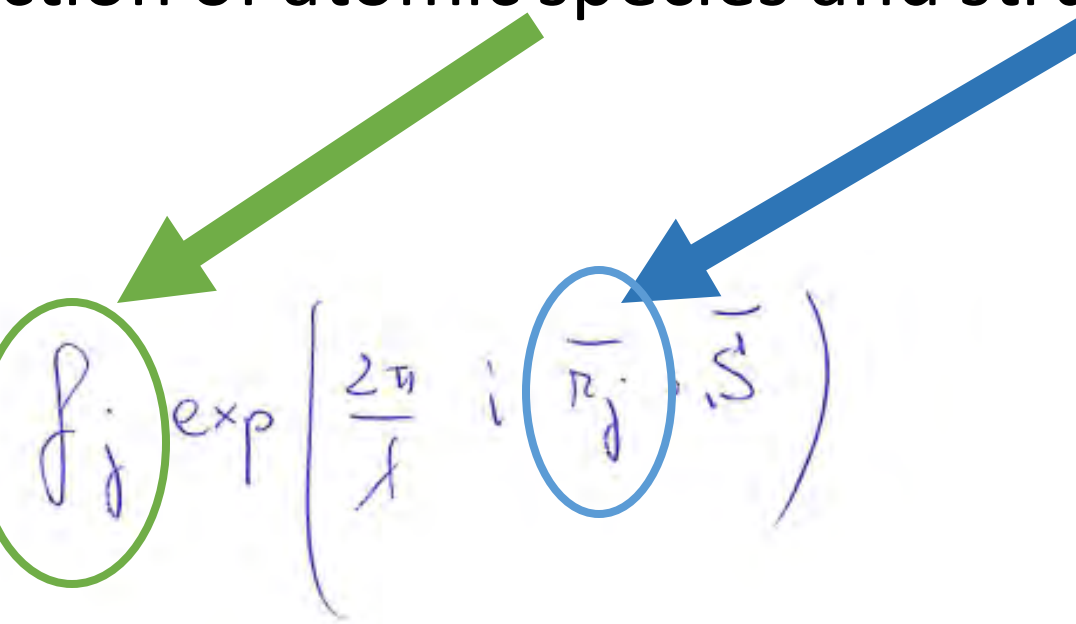


2) Intensity of diffraction: function of atomic species and structure

$$F_{hkl} = \sum_{j=1}^n f_j \exp\left(\frac{2\pi}{\lambda} i \vec{r}_j \cdot \vec{s}\right)$$

Structure factor

Intensity of diffraction: function of atomic species and structure

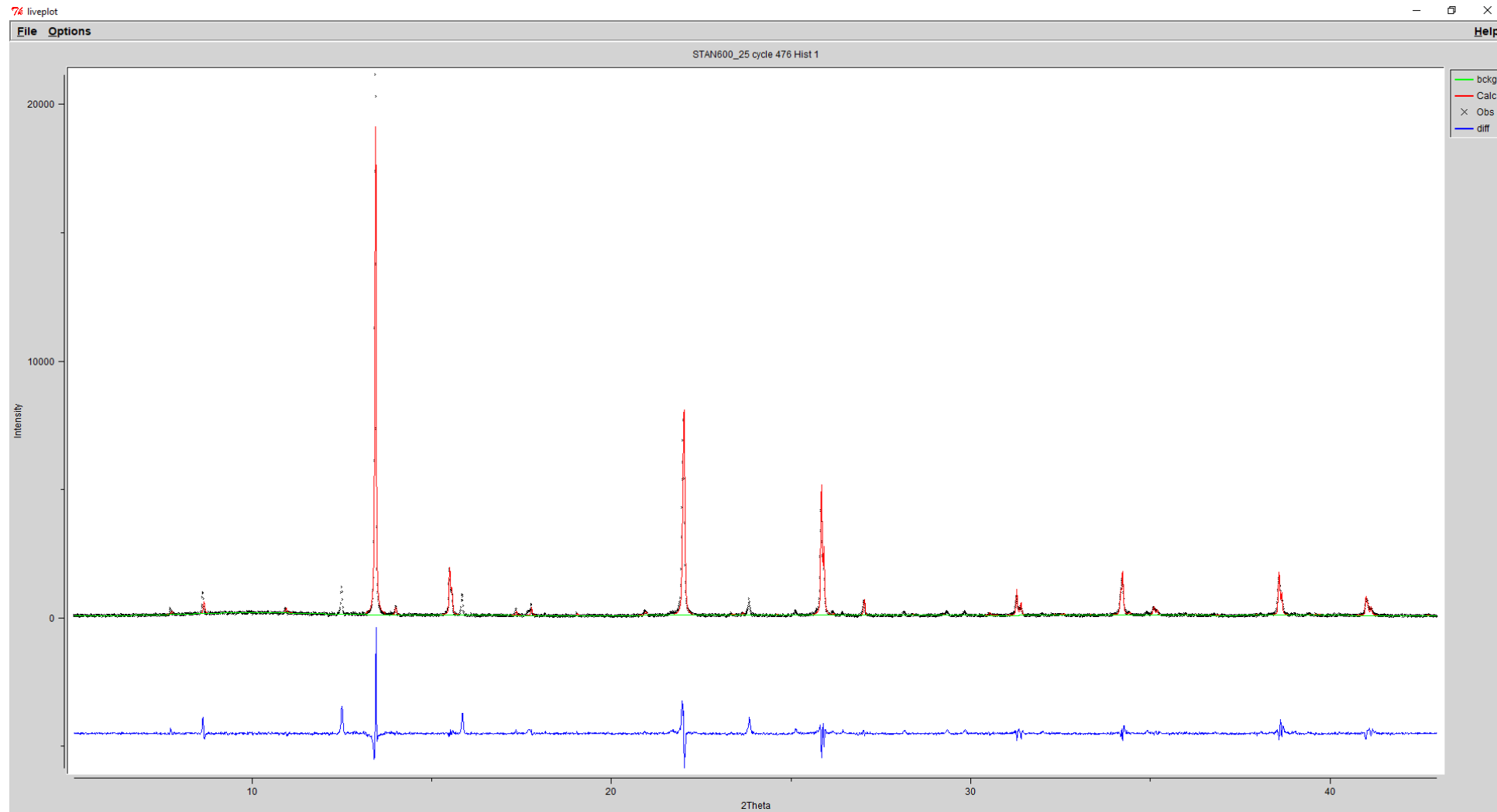
$$F_{hkl} = \sum_{j=1}^m f_j \exp\left(\frac{2\pi}{\lambda} i (\vec{r}_j \cdot \vec{s})\right)$$


Structure factor

- Use of intensity for quantitative analysis and for structure determination

Quantitative analysis:

Stannite Cu₂FeSnS₄ – Rietveld fit – few peaks not fitted

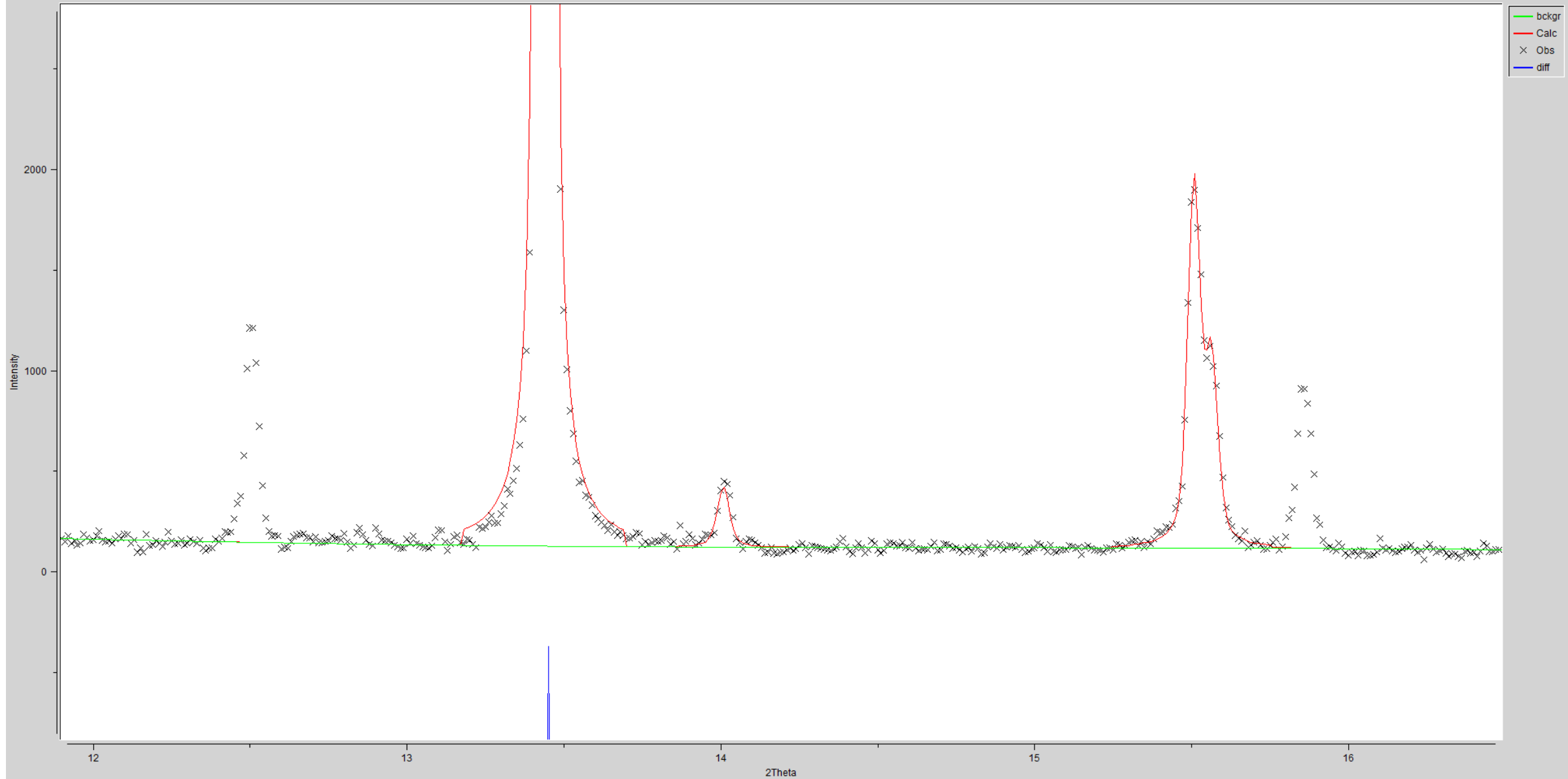


liveplot

- □ ×

File Options Help

STAN600_25 cycle 476 Hist 1

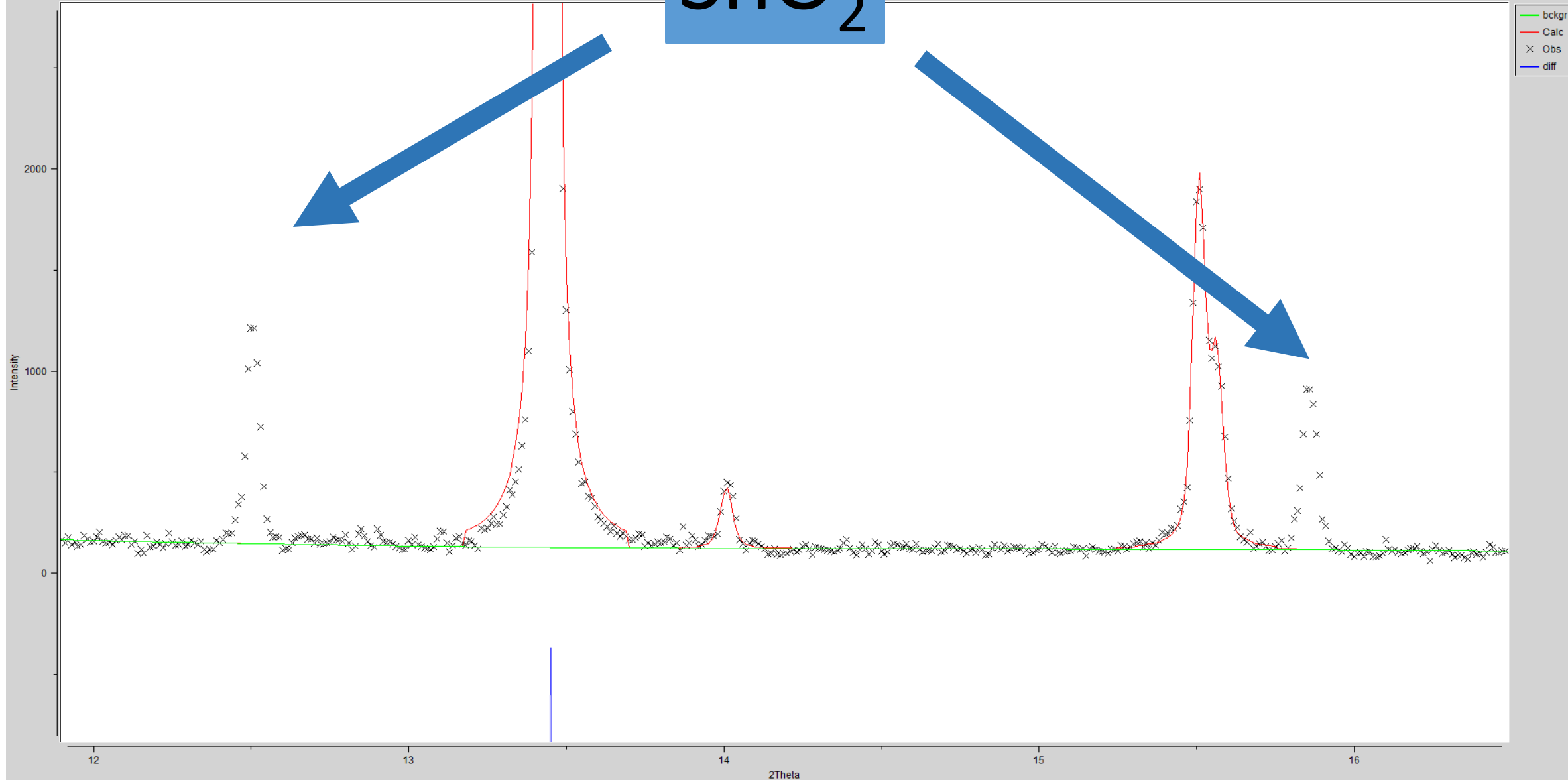


liveplot

File Options

Help

SnO₂



File Options Powder Xtal Graphs Results Calc Macro Import/Export Help

expnam expedt genles powpref powplot lstview liveplot

LS Controls Phase Histogram Scaling Profile Constraints MD Pref Orient SH Pref Orient

Phase: 1 2 Replace

title: sno2

Add
Phase

a 4.741430

b 4.741430

c 3.188082

Edit
Cell

Refine Cell



α 90.0000

β 90.0000

γ 90.0000

Cell damping



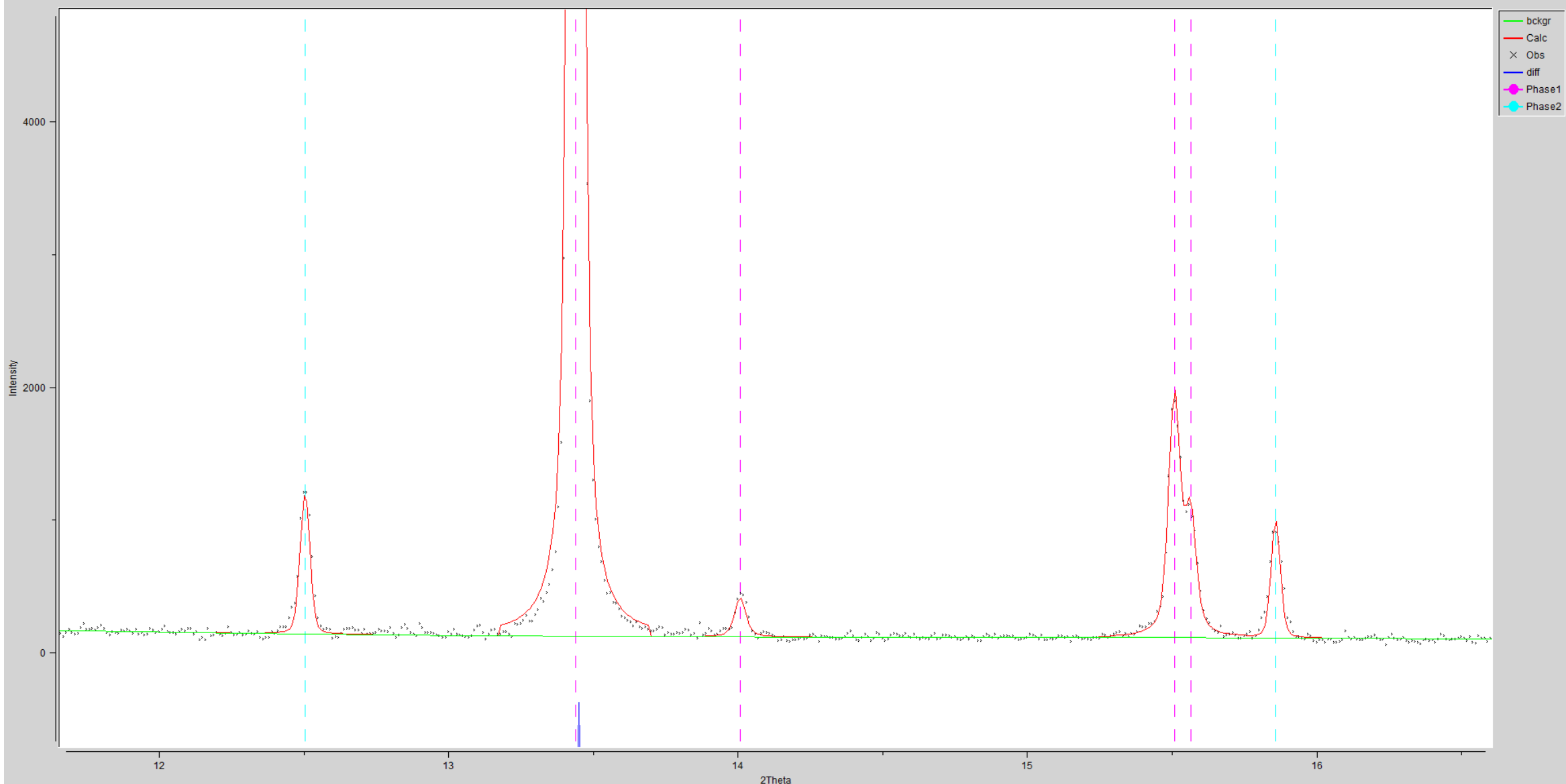
| * | name | type | ref/damp | fractional coordinates | | | Mult | Occupancy | Uiso |
|---|------|------|----------|------------------------|----------|----------|------|-----------|---------|
| 1 | SN1 | SN | 0 0 0 | 0.000000 | 0.000000 | 0.000000 | 2 | 1.0000 | 0.01000 |
| 2 | O2 | O | 0 0 0 | 0.307000 | 0.307000 | 0.000000 | 4 | 1.0000 | 0.01000 |

Add New Atoms

 X U F

Xform Atoms

STAN600_25 cycle 510 Hist 1



76 View STAN600_25.LST

File Edit Go To Options Font: Courier ▾

Help

Calculated unit cell formula weight: 301.376, density: 6.982gm/cm**3

Phase/element fractions for phase no. 1

Hist Elem: 1 1 PXC
Fraction : 2.26796
Sigmas : 0.775638E-01
Shift/esd: 0.00
Wt. Frac.: 0.96004
Sigmas : 0.131197E-02

96 % Stannite

Phase/element fractions for phase no. 2

Hist Elem: 1 1 PXC
Fraction : 0.267887
Sigmas : 0.666184E-02
Shift/esd: 0.00
Wt. Frac.: 0.39959E-01
Sigmas : 0.953988E-03

4 % SnO₂

Phase/element fraction sum(shift/error)**2 : 0.00

Lattice parameters for powder data:

Phase 1

Cycle 510 Chi**2 8.123 Shift/SU 0.01

Structure determination / refinement

76 EXPGUI interface to GSAS: d:/data/elettra_analysis/MCX/stannite/stannite_2021/gsas/STAN600_25.EXP

File Options Powder Xtal Graphs Results Calc Macro Import/Export Help

expnam expedt genles powpref powplot lstdview liveplot

LS Controls Phase Histogram Scaling Profile Constraints MD Pref Orient SH Pref Orient

Phase: 1 2 Replace title: from D:/data/elettra_analysis/MCX/stannite/agosto_2016/

Add Phase a 5.410244 b 5.410244 c 10.781814 Edit Cell Refine Cell Cell damping 5

α 90.0000 β 90.0000 γ 90.0000

| * | name | type | ref/damp | fractional coordinates | | | Mult | Occupancy | Uiso |
|---|------|------|----------|------------------------|----------|----------|------|-----------|---------|
| 1 | CU1 | CU | 0 U9 F9 | 0.000000 | 0.500000 | 0.250000 | 4 | 1.0005 | 0.02234 |
| 2 | FE2 | FE | 0 U9 F9 | 0.000000 | 0.000000 | 0.000000 | 2 | 1.1676 | 0.02852 |
| 3 | SN3 | SN | 0 U9 F9 | 0.000000 | 0.000000 | 0.500000 | 2 | 0.9018 | 0.02130 |
| 4 | S4 | S | X9 U9 0 | 0.759331 | 0.759331 | 0.869389 | 8 | 1.0000 | 0.01838 |

File Options Powder Xtal Graphs Results Calc Macro Import/Export Help

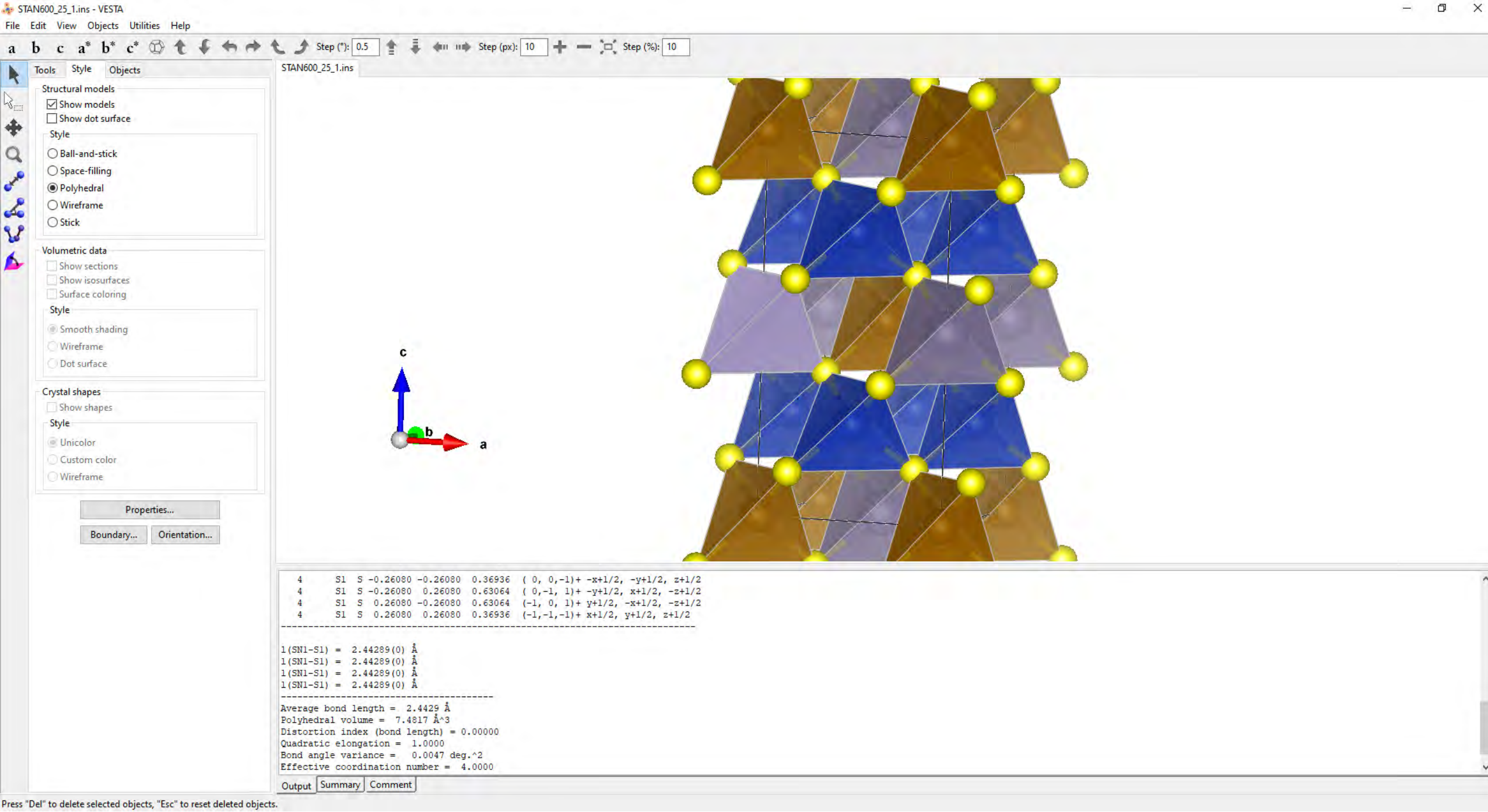
expnam expedt genles powpref powplot lstview liveplot

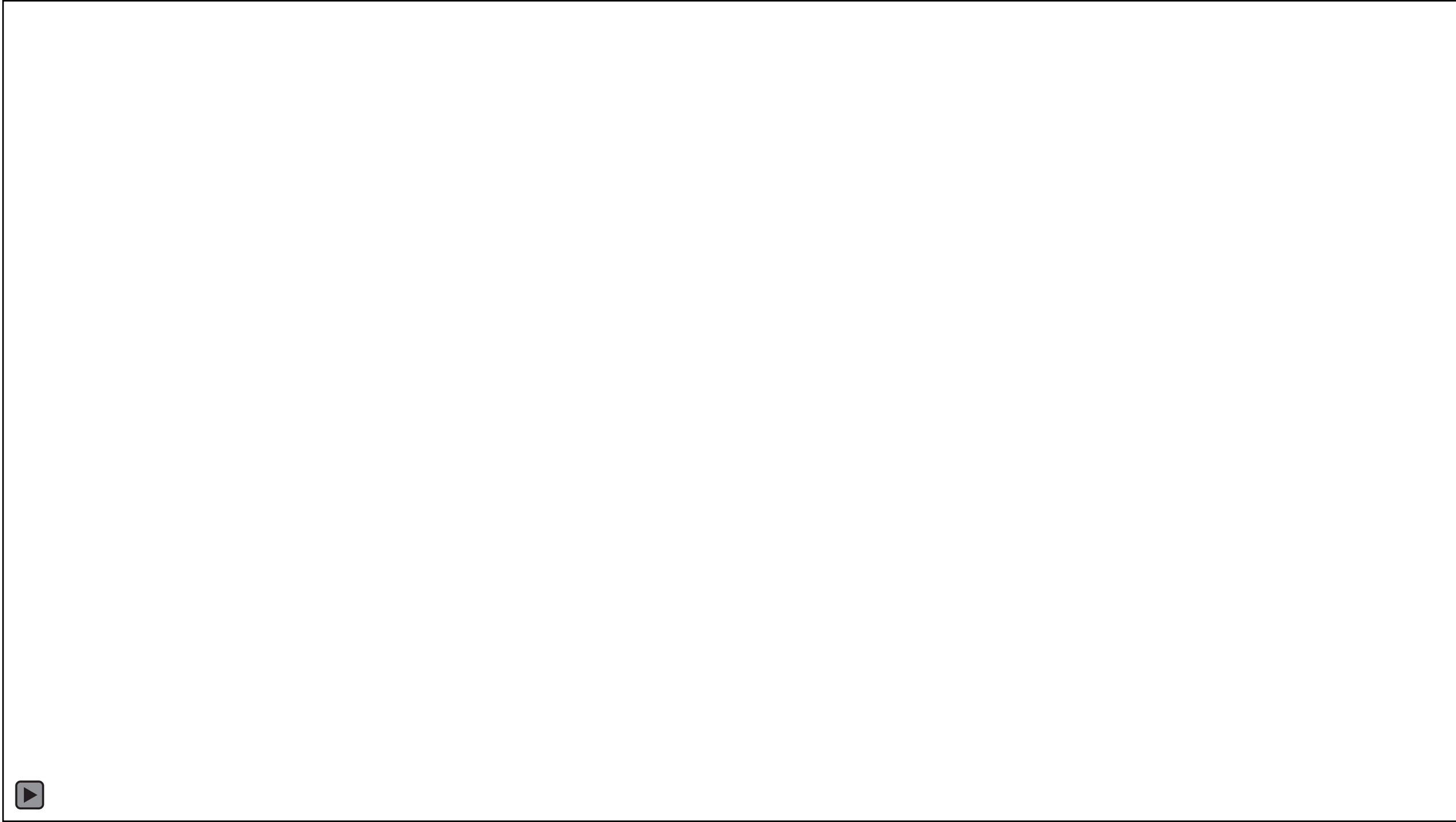
LS Controls Phase Histogram Scaling Profile Constraints MD Pref Orient SH Pref Orient

Phase: 1 2 Replace **title:** from D:/data/elettra_analysis/MCX/stannite/agosto_2016

| | | | | | | |
|-----------|------------------|-----------------|------------------|-----------|--------------|-------------------------------------|
| Add Phase | a 5.410243 | b 5.410243 | c 10.781816 | Edit Cell | Refine Cell | <input checked="" type="checkbox"/> |
| | α 90.0000 | β 90.0000 | γ 90.0000 | Cell | Cell damping | 5 |

| * | name | type | ref/damp | fractional coordinates | | | Mult | Occupancy | Uiso |
|---|------|------|----------|------------------------|----------|----------|------|-----------|---------|
| 1 | CU1 | CU | 0 U9 F9 | 0.000000 | 0.500000 | 0.250000 | 4 | 1.0000 | 0.02229 |
| 2 | FE2 | FE | 0 U9 F9 | 0.000000 | 0.000000 | 0.000000 | 2 | 0.8224 | 0.03087 |
| 3 | SN3 | SN | 0 U9 F9 | 0.000000 | 0.000000 | 0.500000 | 2 | 0.7984 | 0.02048 |
| 4 | S4 | S | X9 U9 O | 0.759427 | 0.759427 | 0.869377 | 8 | 1.0000 | 0.01837 |
| 5 | Sn2 | SN | 0 U9 F9 | 0.000000 | 0.000000 | 0.000000 | 2 | 0.1776 | 0.03087 |
| 6 | Fe3 | FE | 0 U9 F9 | 0.000000 | 0.000000 | 0.500000 | 2 | 0.2016 | 0.02048 |



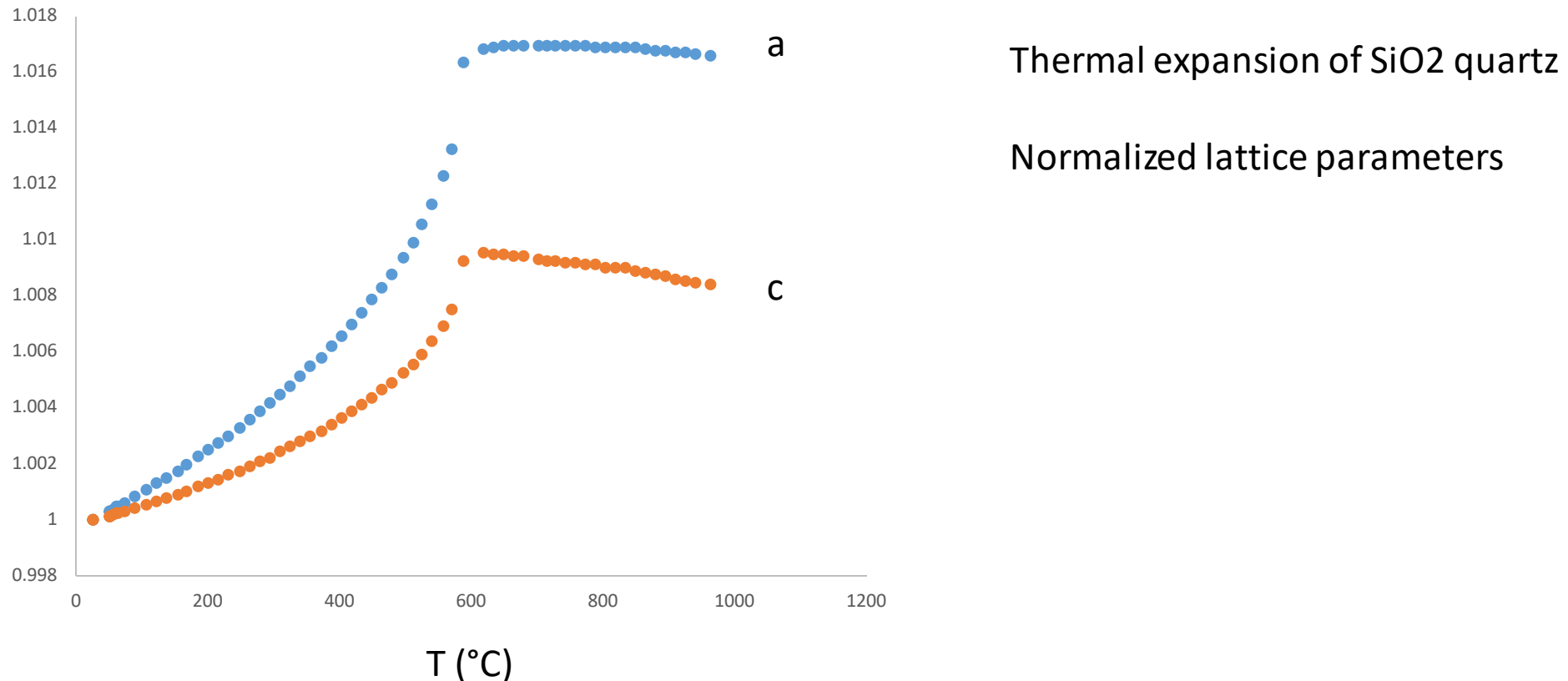


Summary

- Accuracy (and precision) in geometrical parameters (i.e. peak position, lattice parameter) is function of calibration
- Synchrotron experiments (especially in Bragg-Brentano – transmission -geometry) can result in improved accuracy compared to laboratory sources

Summary

- Accuracy (and precision) in geometrical parameters (i.e. peak position, lattice parameter) is function of calibration
- Synchrotron experiments (especially in Bragg-Brentano – transmission -geometry) can result in improved accuracy compared to laboratory sources



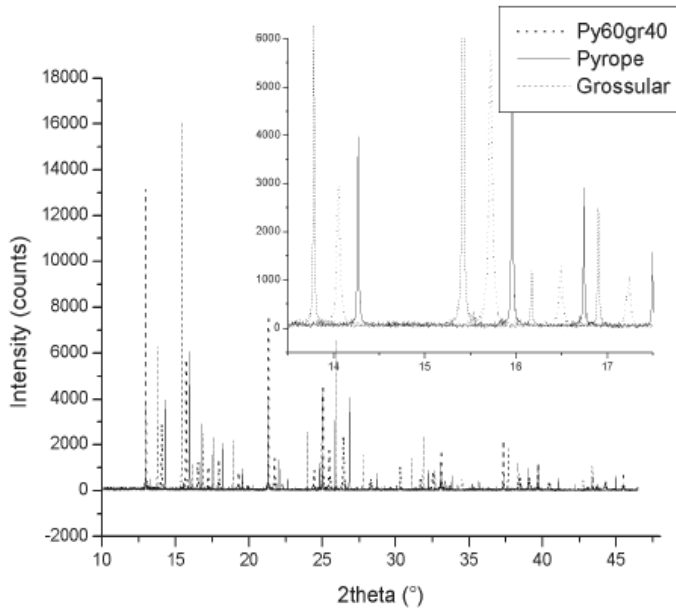
Summary

- Synchrotron high resolution beamlines: improved angular resolution compared to laboratory sources
- Accurate determination of microstructural parameters (i.e. crystallite size, microstrain)

Summary

- Synchrotron high resolution beamlines: improved angular resolution compared to laboratory sources
- Accurate determination of microstructural parameters (i.e. crystallite size, microstrain)

American Mineralogist, Volume 90, pages 506–509, 2005



LETTER
Microscopic strain in synthetic pyrope-grossular solid solutions determined by synchrotron X-ray powder diffraction at 5 K: The relationship to enthalpy of mixing behavior

MONICA DAPIAGGI,^{1,*} CHARLES A. GEIGER,² AND GILBERTO ARTIOLI¹

¹Dipartimento di Scienze della Terra "A. Desio", Università degli Studi di Milano, I-20133 Milano, Italy
²Institut für Geowissenschaften, Christian-Albrechts-Universität, D-24098 Kiel, Germany

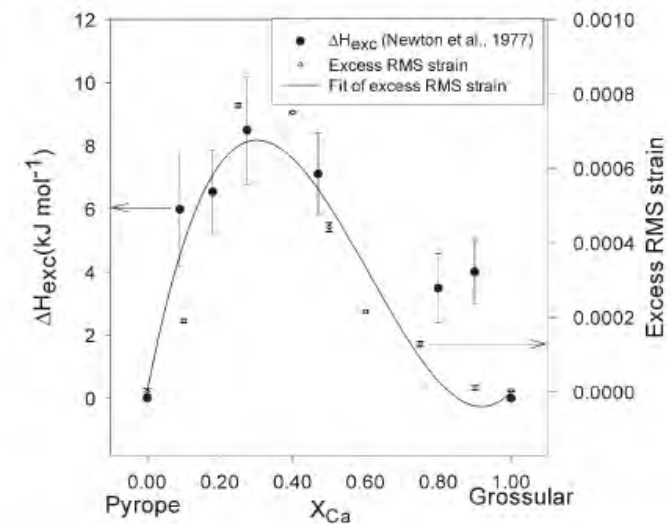
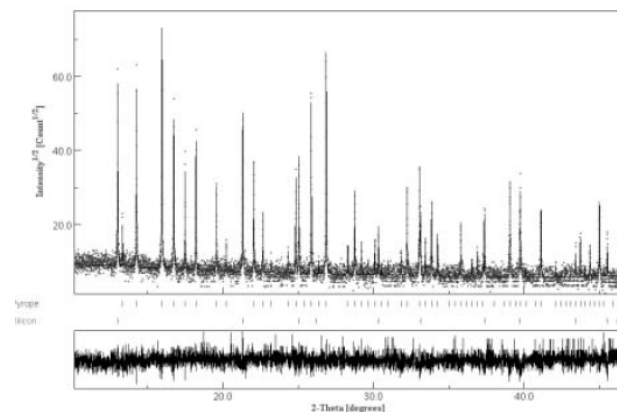


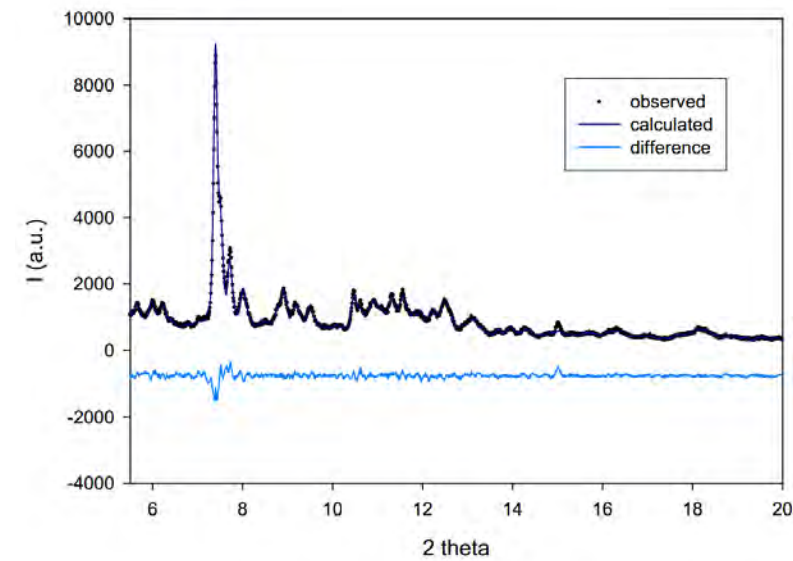
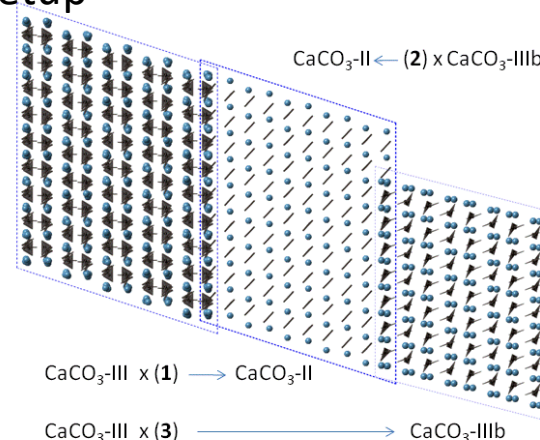
FIGURE 3. Experimental values of the excess enthalpies of mixing (open squares from Newton et al., 1977) and the excess RMS strain (black circles). The error bars represent 2σ variations in the determinations. The solid line is a two parameter asymmetric fit (Eq. 4) to the excess RMS strain data.

Summary

- Synchrotron diffraction with tunable energy – high energy can result in minimization of absorption effects.
Useful for structure determination of sample with atomic species with significant different atomic numbers
- Diffraction in complex environments
- Large experimental space for ad-hoc experimental setup

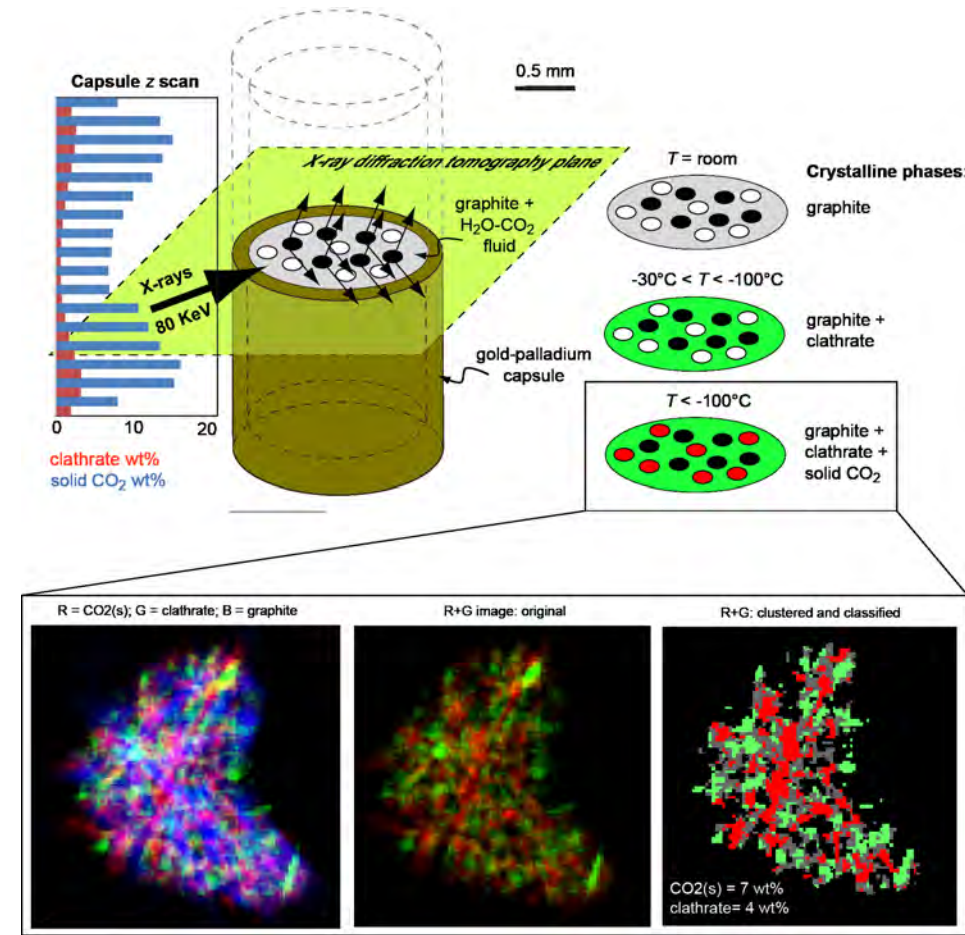
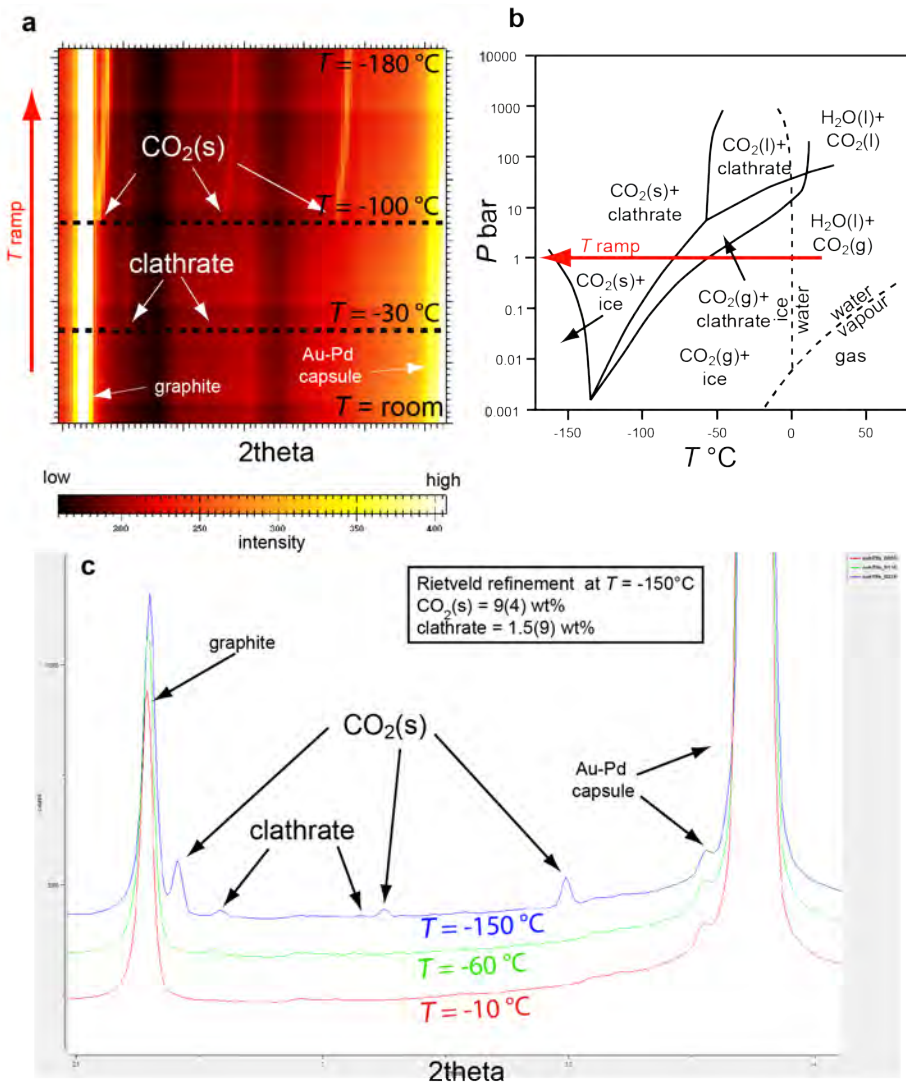
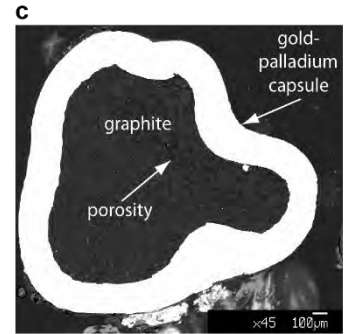
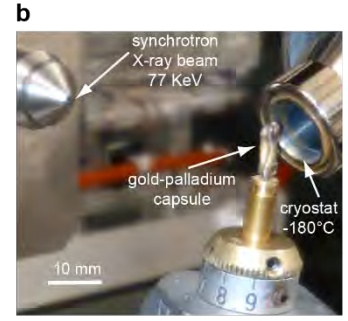
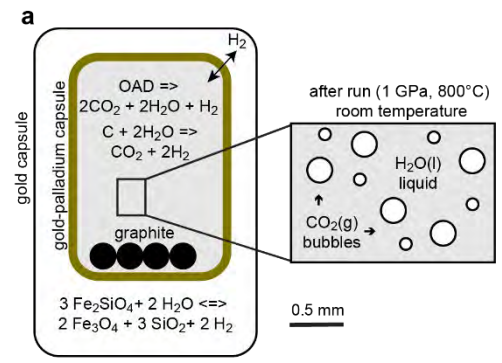
Summary

- Synchrotron diffraction with tunable energy – high energy can result in minimization of absorption effects.
Useful for structure determination of sample with atomic species with significant different atomic numbers
- Diffraction in complex environments
- Large experimental space for ad-hoc experimental setup



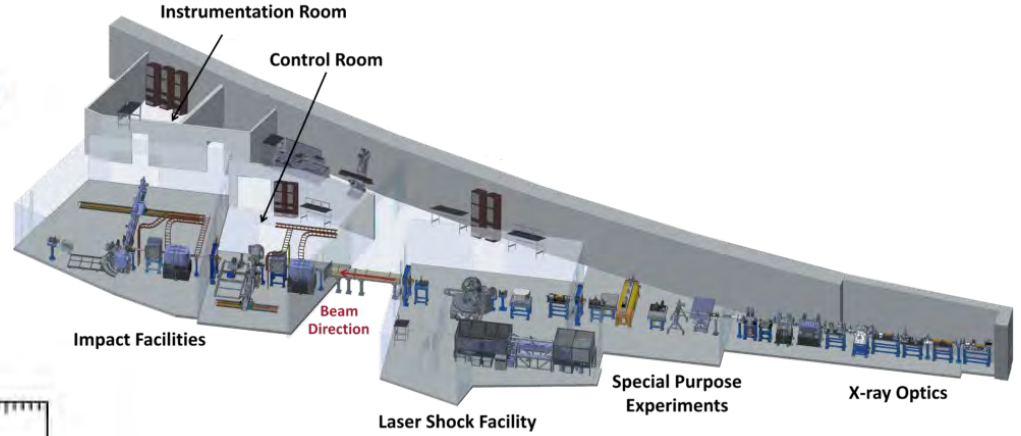
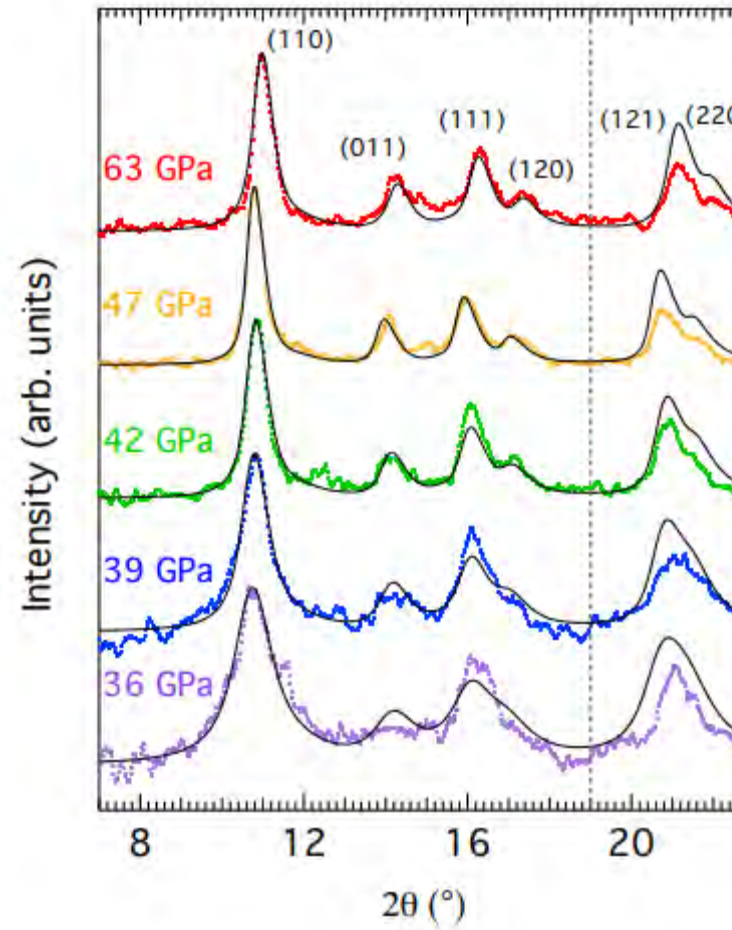
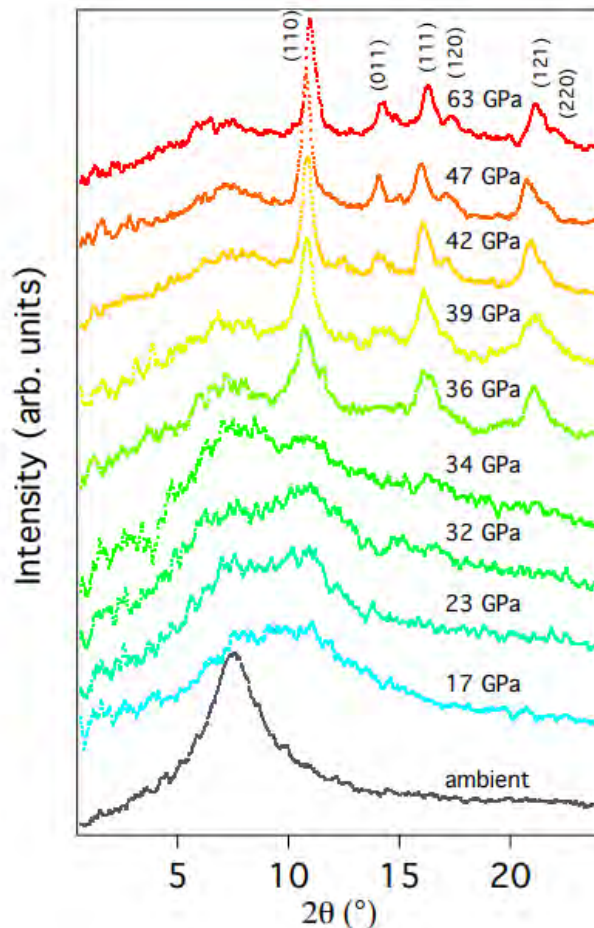
Rietveld fit of complex structural intergrow of different domain in high pressure phase

LVP – Large Volume Press @ ESRF ID06 beamline



In situ X-Ray Diffraction of Shock-Compressed Fused Silica

Sally June Tracy, Stefan J. Turneaure, and Thomas S. Duffy
Phys. Rev. Lett. **120**, 135702 – Published 29 March 2018



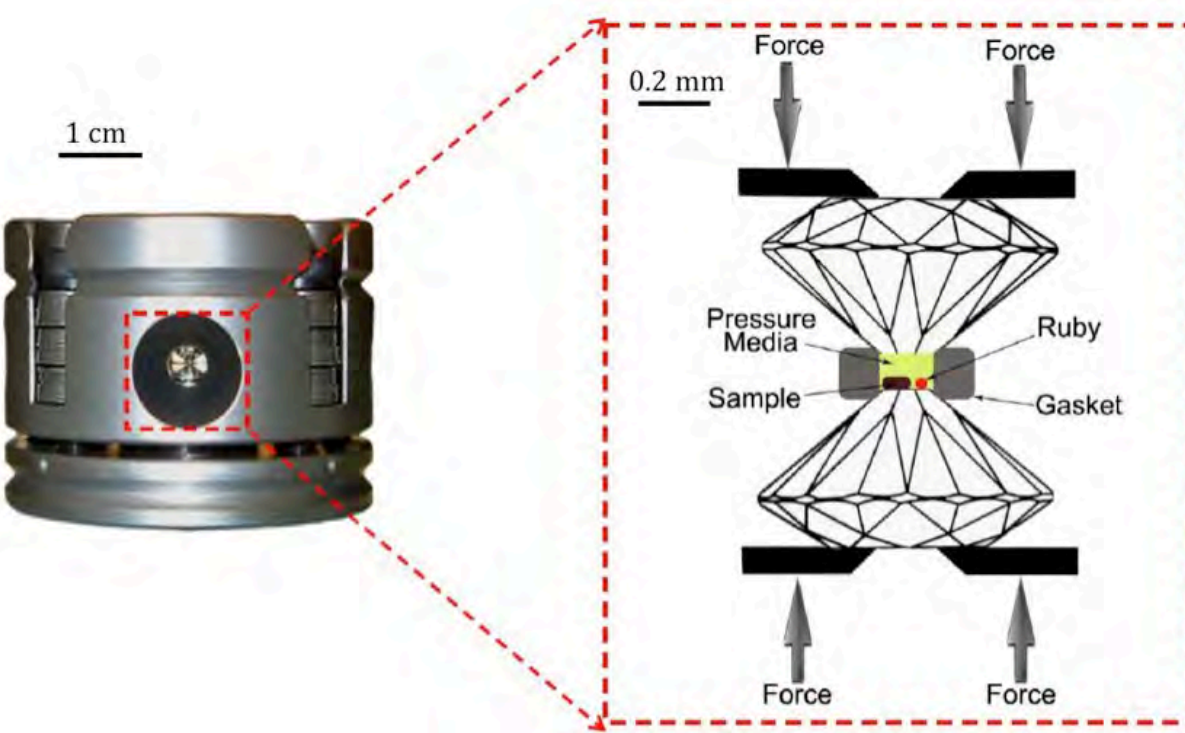
The diffraction data are combined with continuum-level measurements to reveal a complete picture of the material response from the atomic length scale to the continuum level, allowing for the unambiguous determination of the phase(s) formed at \sim 100 ns timescales from 12 to 63 GPa.

Plate impact experiments were carried out at the Dynamic Compression Sector of the Advanced Photon Source (APS). Planar shock waves in fused silica were generated using LiF impactors accelerated in a polycarbonate projectile to a velocity of 1.8–5.6 km/s using either a single-stage propellant gun or a two-stage light gas gun. A schematic of the impact

3) EXAMPLE of crystal structure determination from single crystals at «extreme conditions»

High-pressure and high-temperature

Diamond anvil cell



Diamond culet diameter

1 mm
0.6 mm
0.3 mm
0.125 mm

max pressure

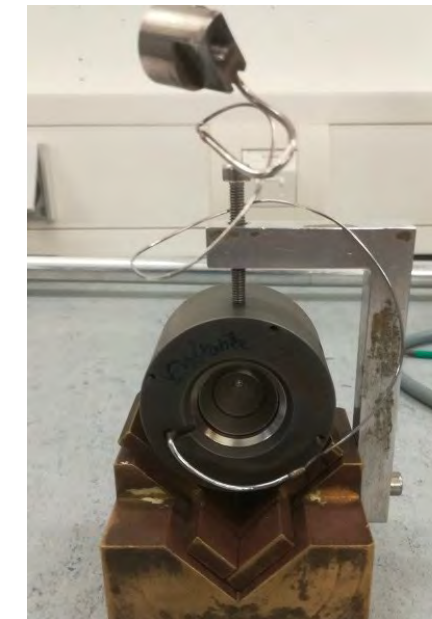
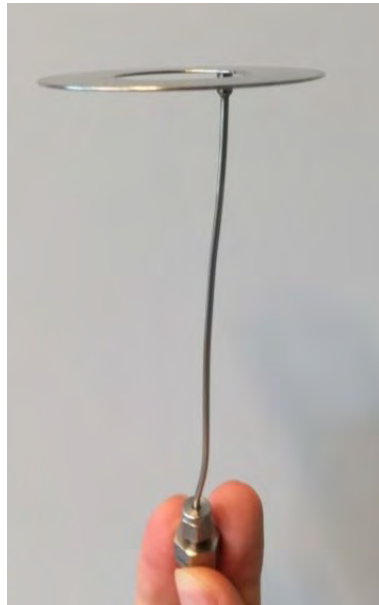
2 GPa
20 GPa
60 GPa
> 100 GPa

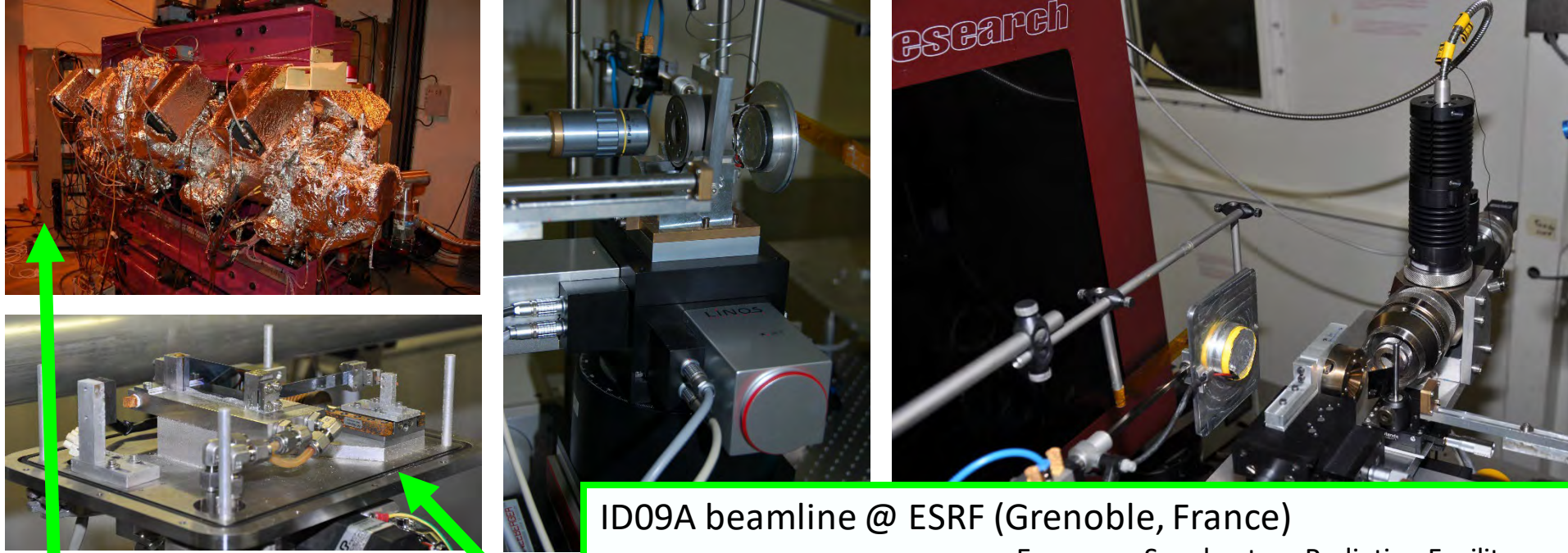
Force:

screws

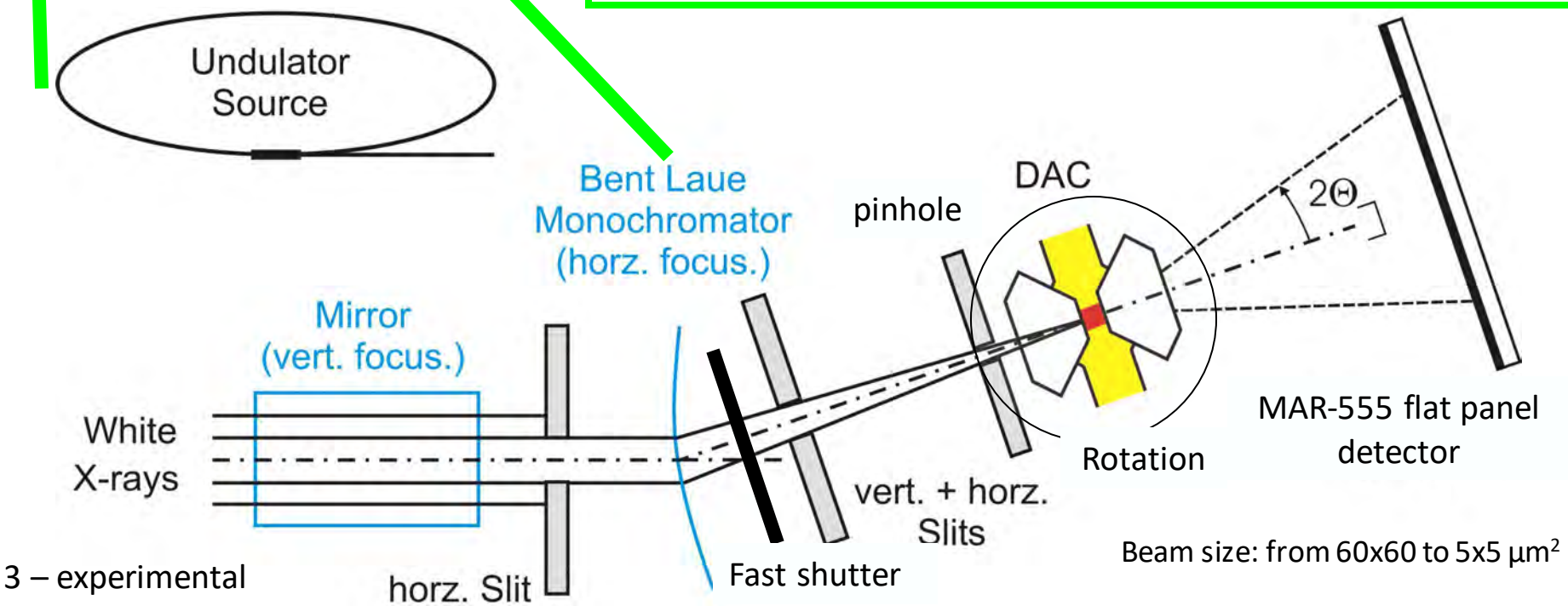


Gas under pressure
(0-200 bar)
and expanding
metallic membrane





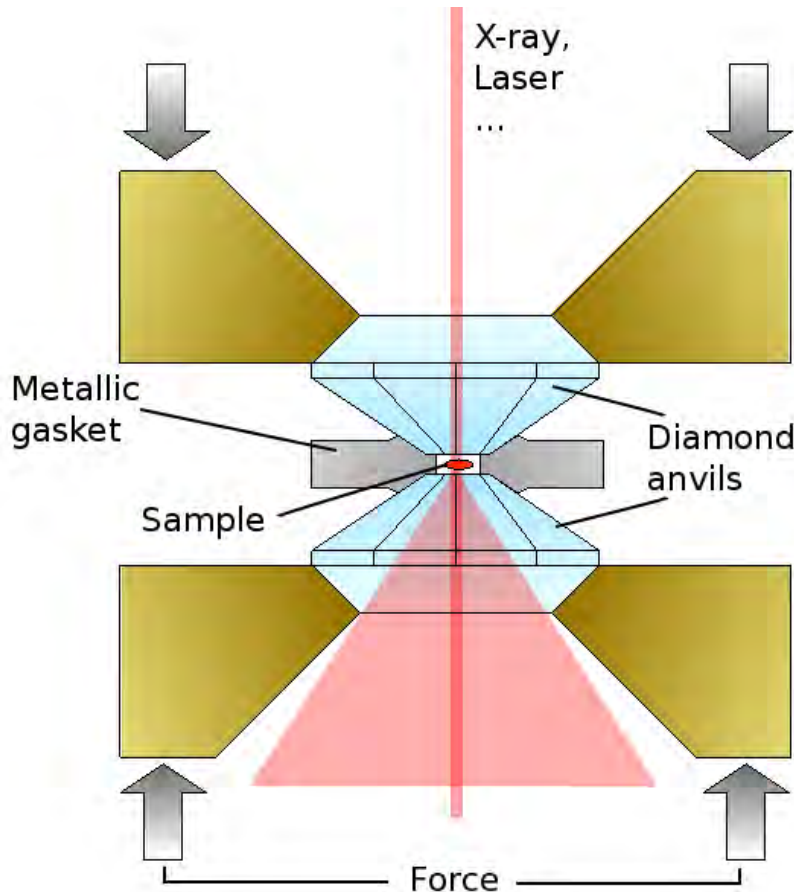
ID09A beamline @ ESRF (Grenoble, France)
European Synchrotron Radiation Facility



Diamond Anvil Cell (DAC) +/- resistive heating +/- laser heating

P max: «routine» 1.5 Mbar – possible experiments up to 6 Mbar

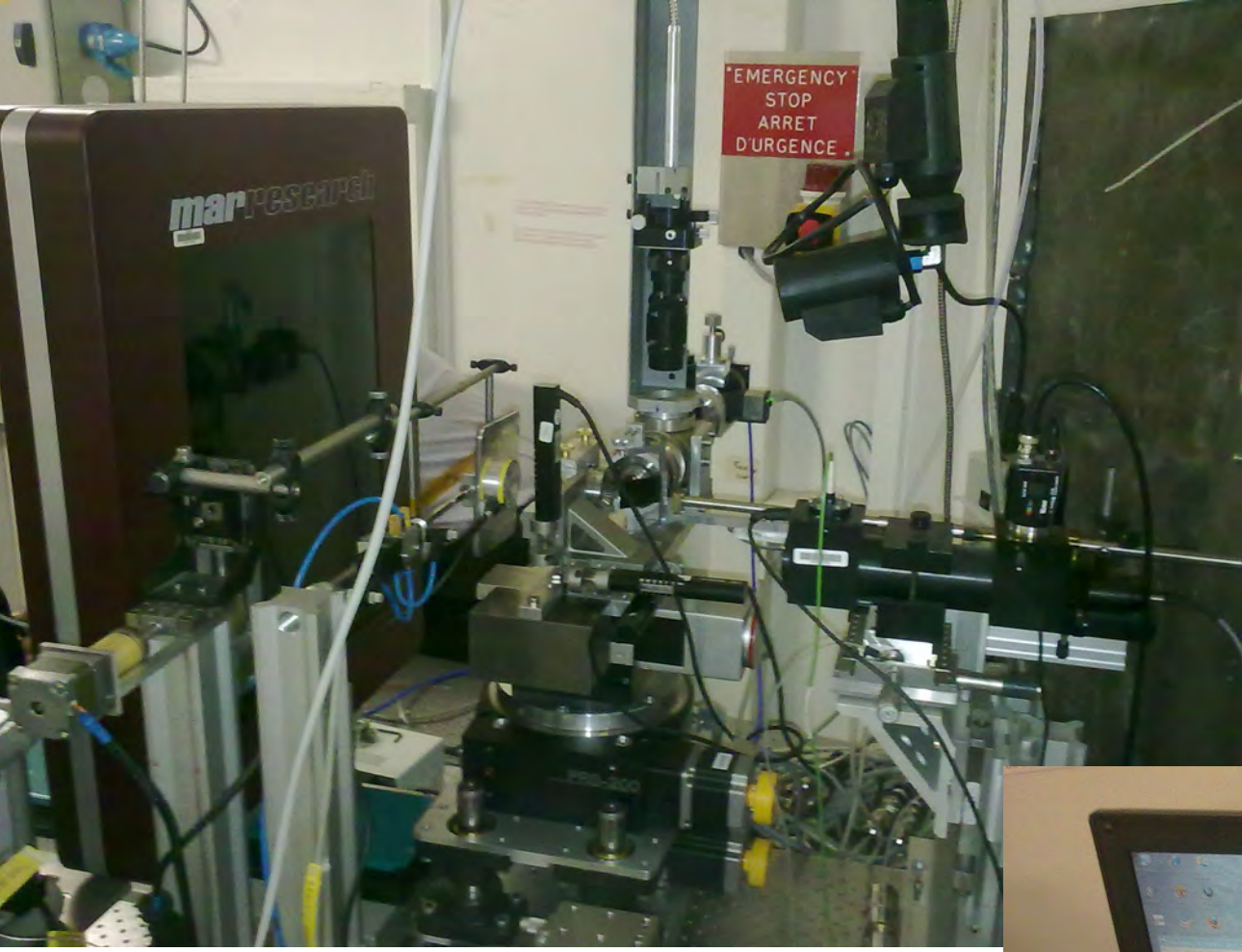
T max: cryostat + resistive: 5-1000 K; laser heating: up to 6000 K



X-ray diffraction
(powder, single crystal)

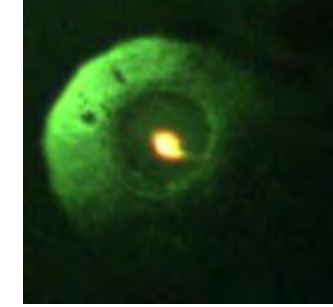
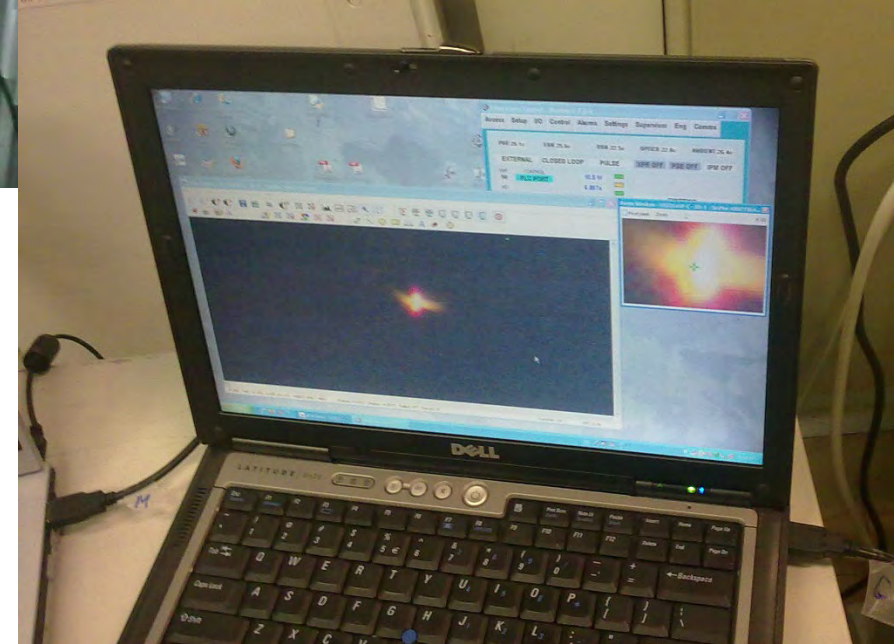
X-ray scattering

X-ray spectroscopy

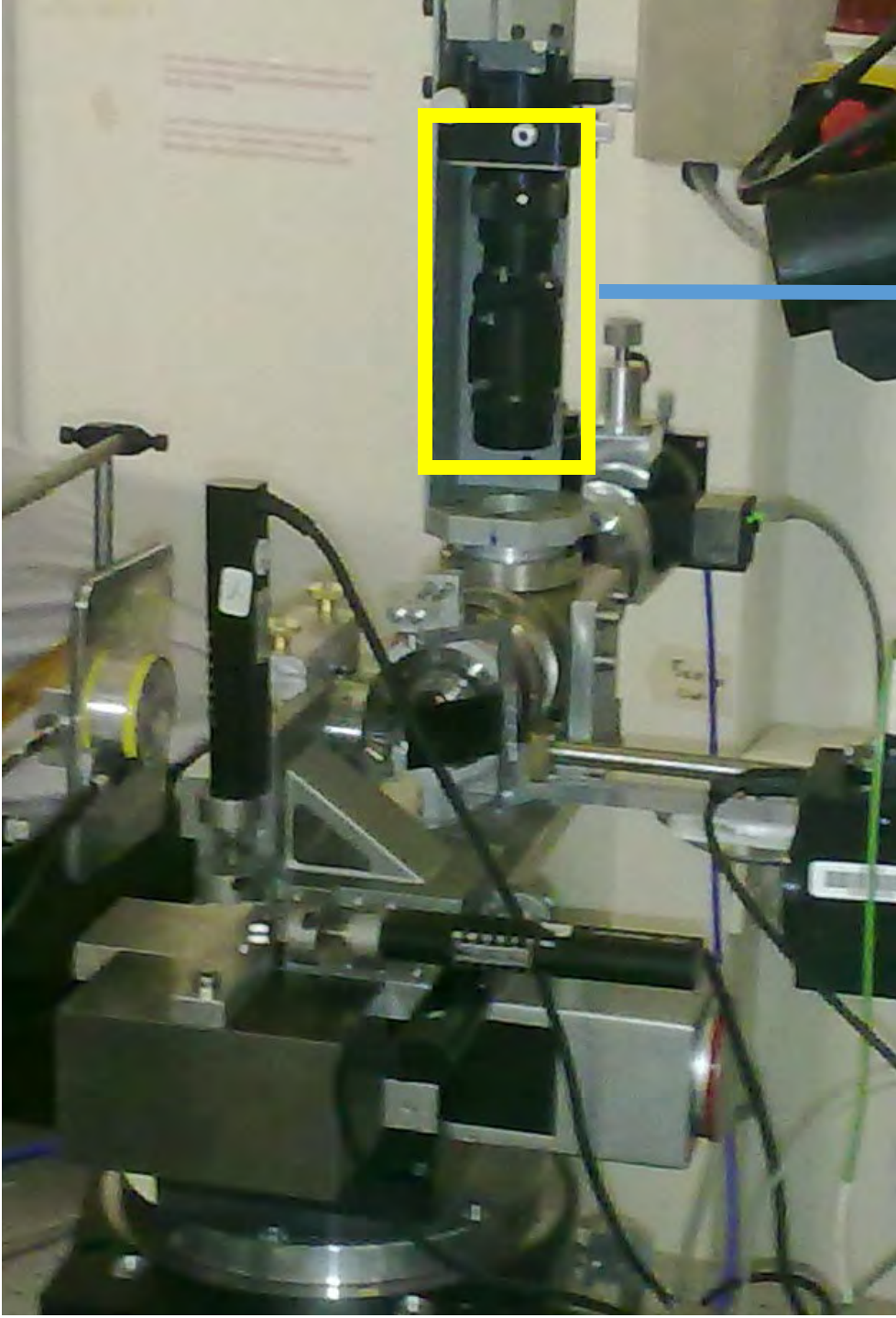


Portable laser heating system for single crystal diffraction

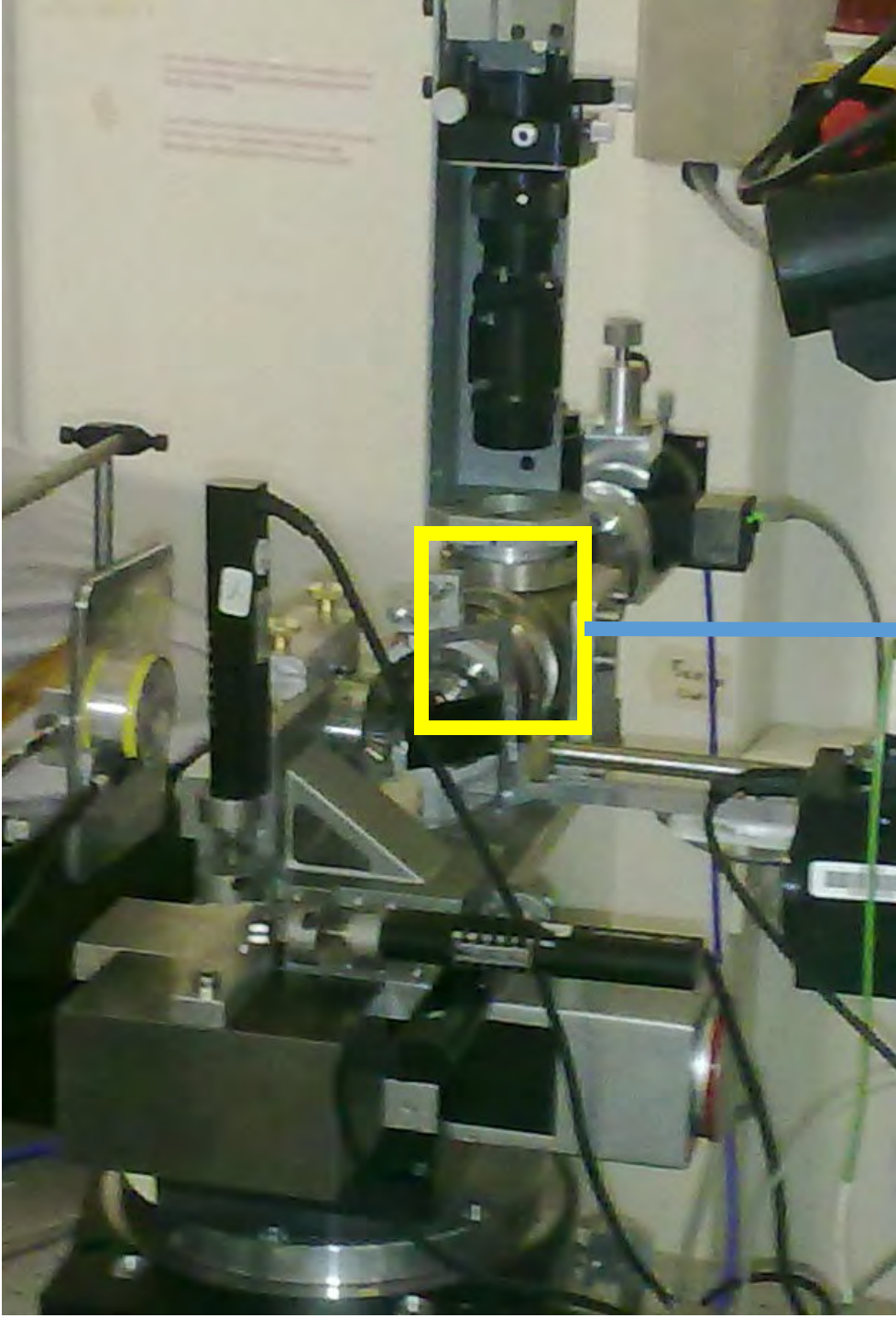
Dubrovinsky et al., HPR 2010



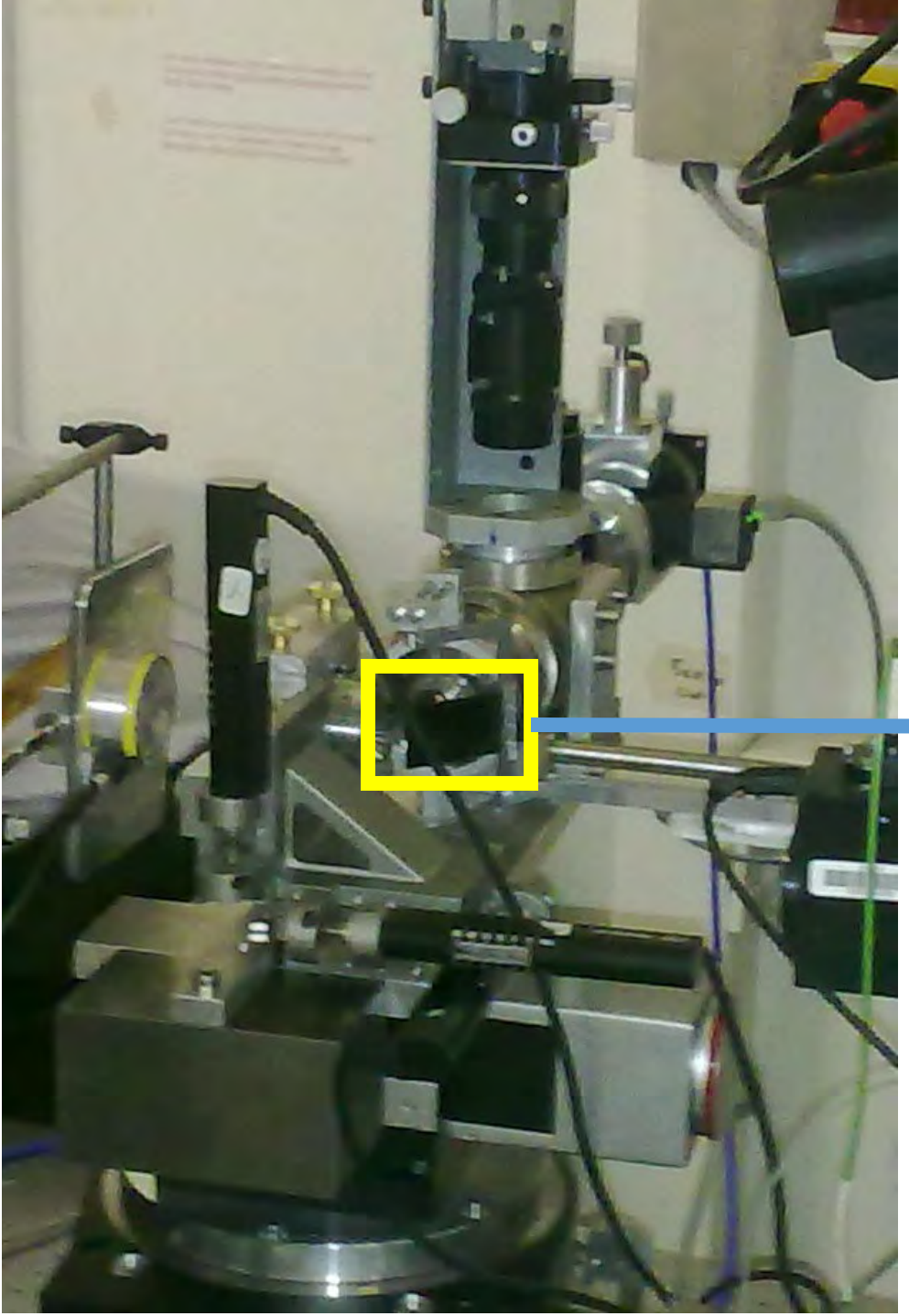




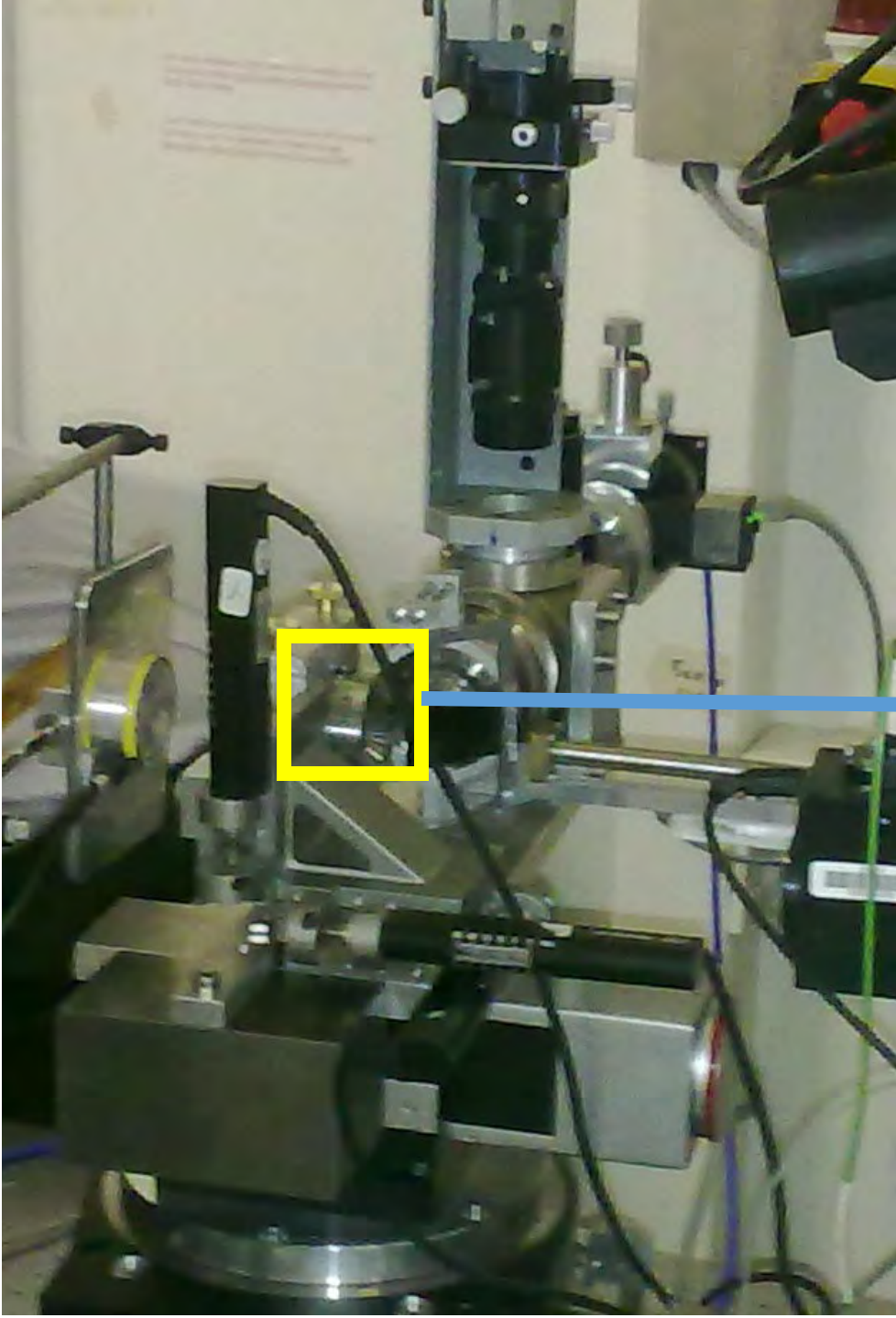
Incoming laser beam



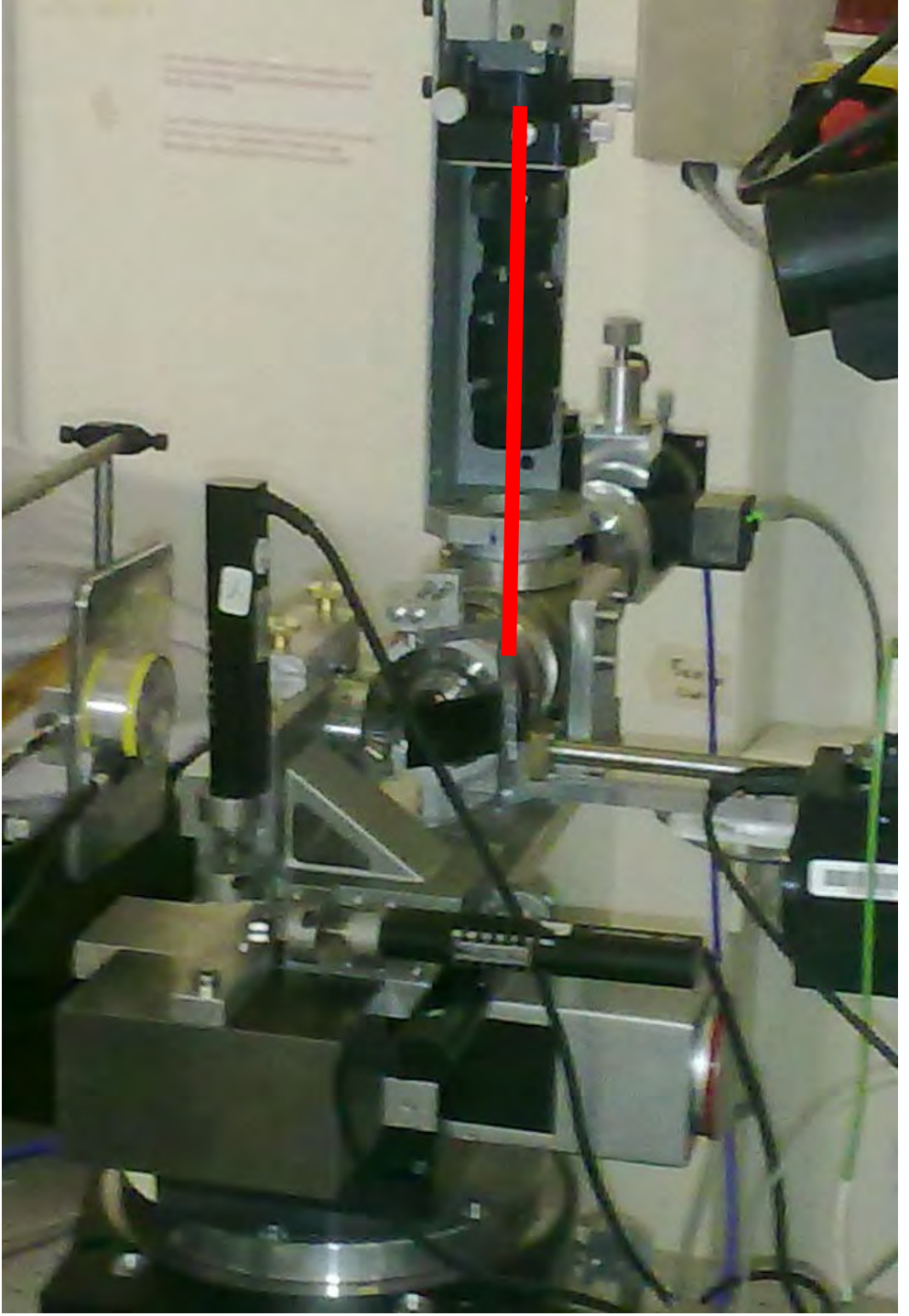
Mirror and lens

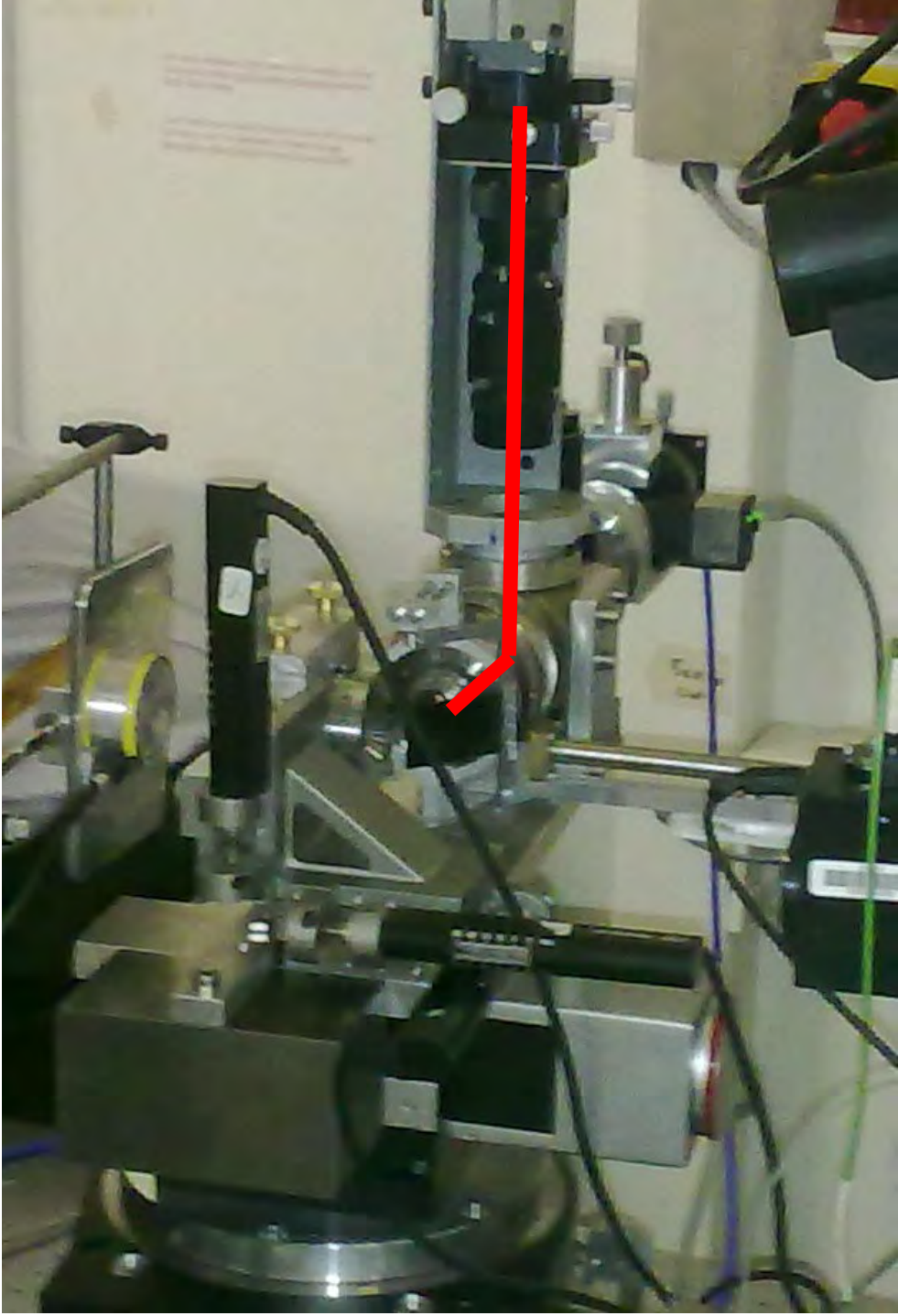


Mirror



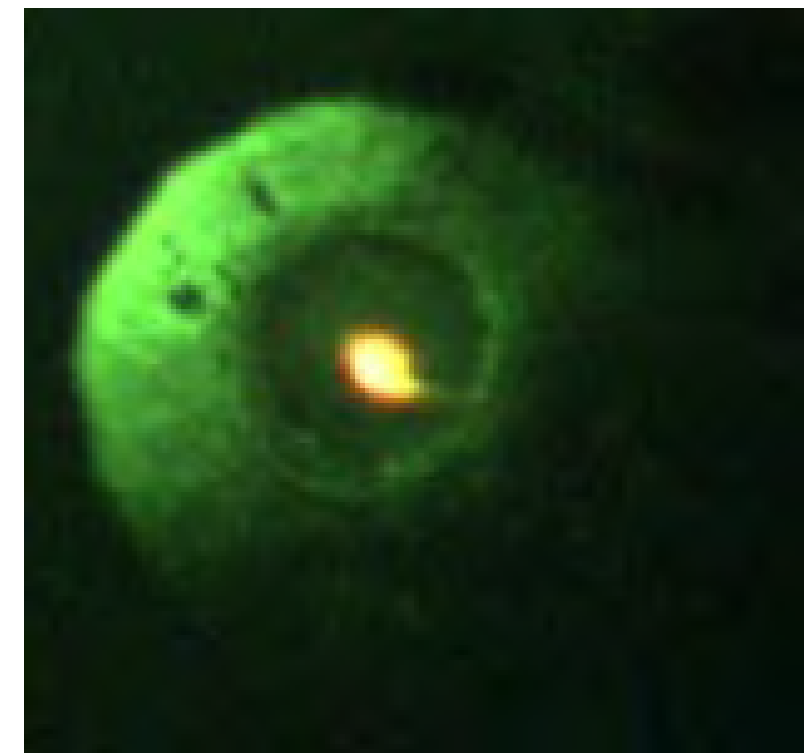
Diamond Anvil Cell

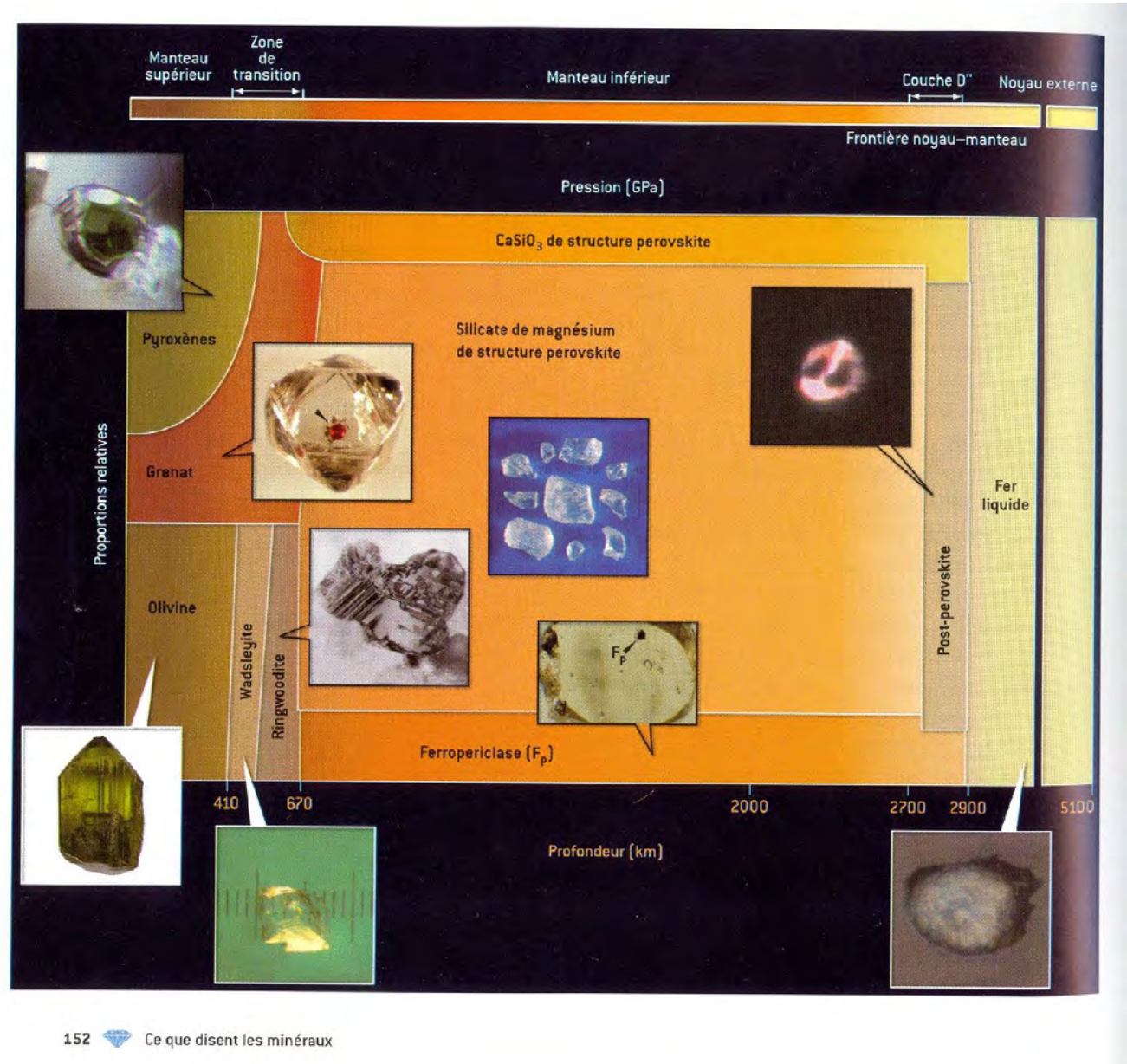






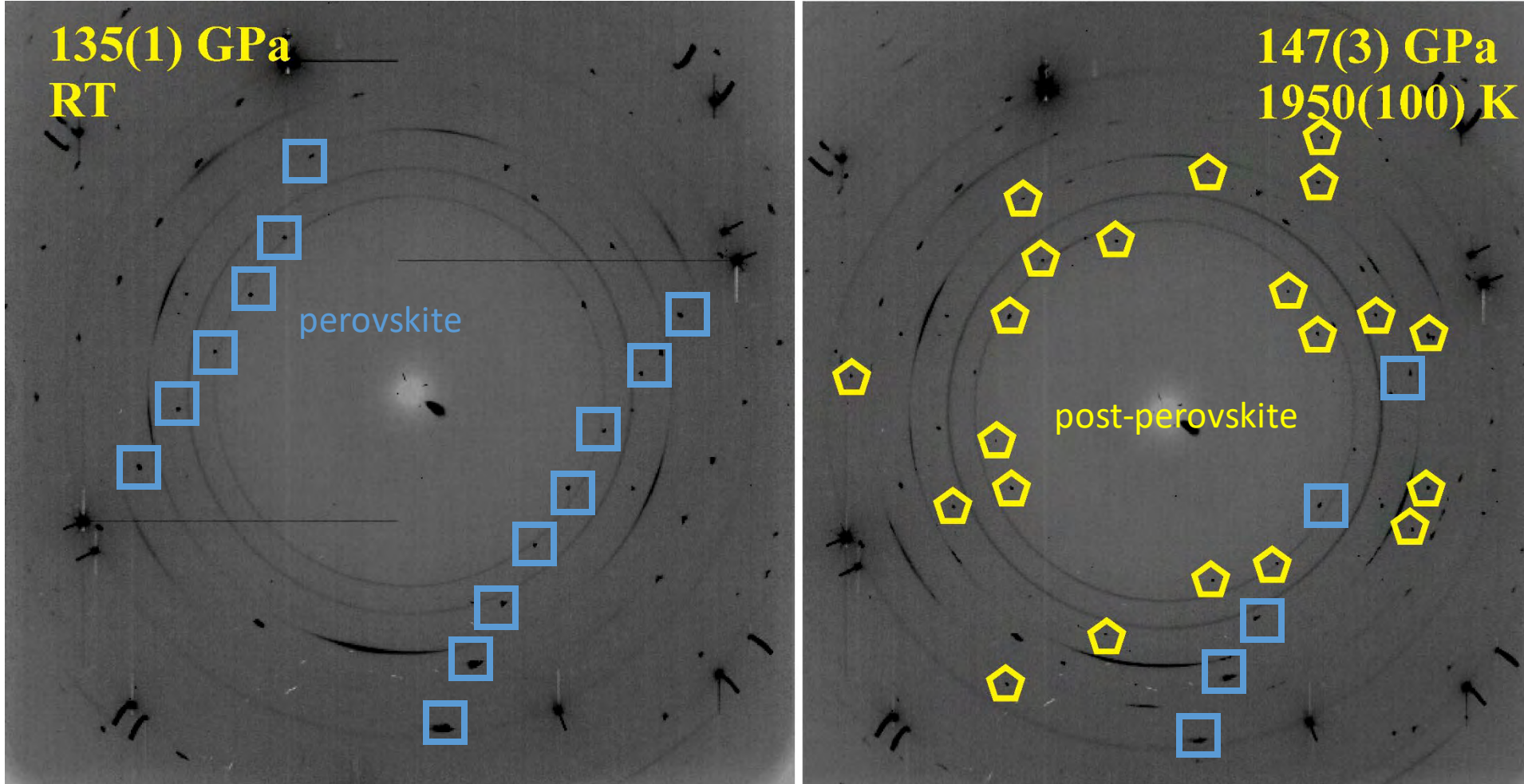
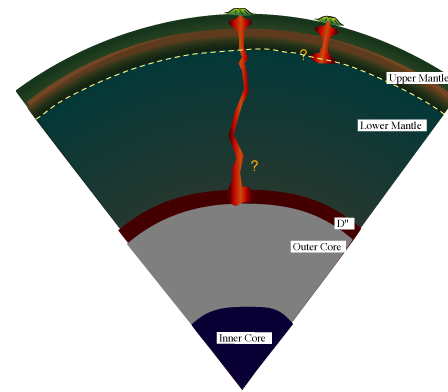
Single crystal laser heating
+ rotation of all the stage
for single crystal diffraction
data collection in situ @
HP/HT

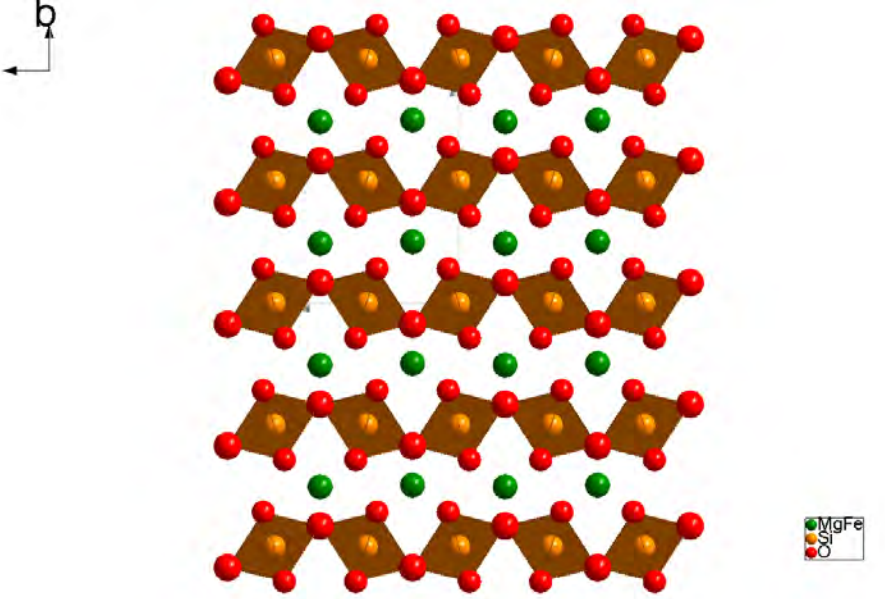




Single crystal diffraction

*In-situ growing of post-perovskite
@ 150 Gpa & 2000 K*





Crystal data

Formula sum $\text{Fe}_1 \text{Mg}_1 \text{O}_1 \text{Si}_1$

Crystal system orthorhombic

Space group $C m c m$ (no. 63)

Unit cell $a = 2.477(7) \text{ \AA}$

$b = 8.03(2) \text{ \AA}$

$c = 6.109(13) \text{ \AA}$

Cell volume $121.51(50) \text{ \AA}^3$

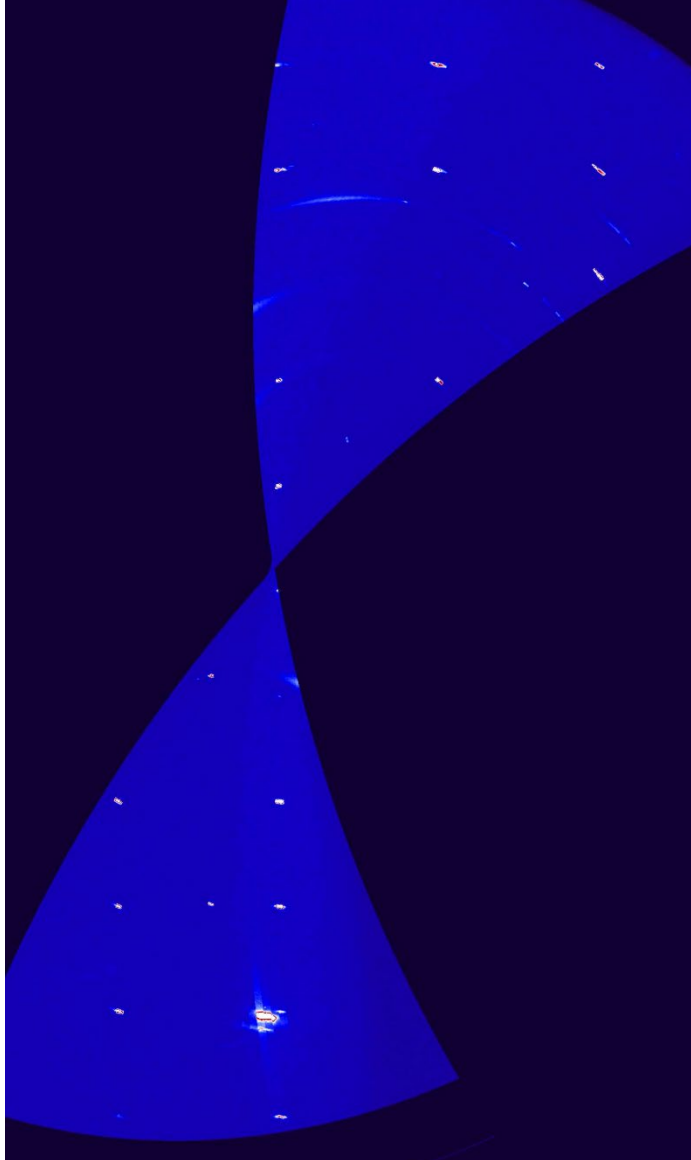
Z 16

Pearson code oC20

**Post-perovskite,
struttura a
140 Gpa e 2000K**

Atomic coordinates and isotropic displacement parameters (in \AA^2)

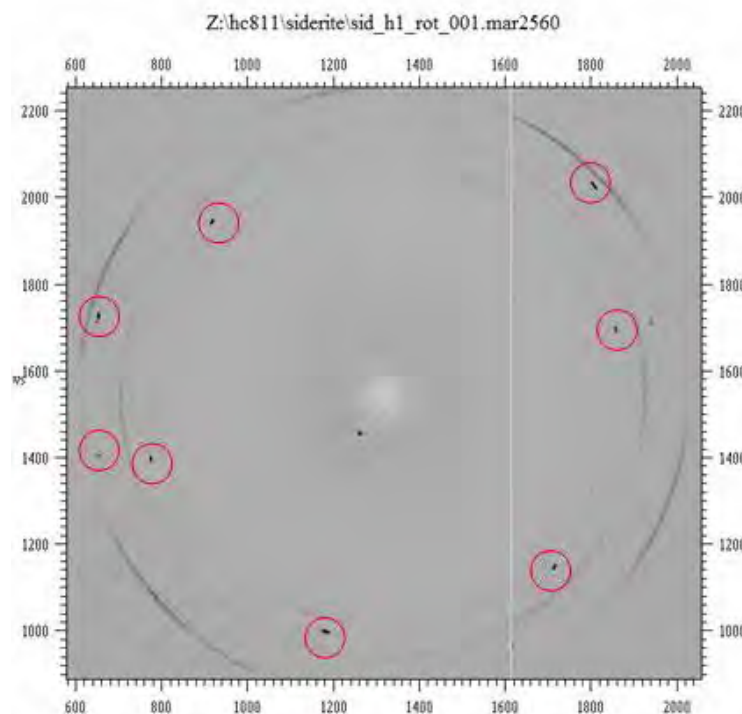
| Atom | Wyck. | Occ. | x | y | z | U |
|------|-------|-------|---|---------|---------|--------|
| Mg1 | 4c | 0.703 | 0 | 0.25346 | 1/4 | 0.0149 |
| Fe1 | 4c | 0.297 | 0 | 0.25346 | 1/4 | 0.0149 |
| Si | 4a | | 0 | 0 | 0 | 0.0126 |
| O1 | 4c | | 0 | 0.91453 | 1/4 | 0.0187 |
| O2 | 8f | | 0 | 0.64244 | 0.44277 | 0.0130 |



FeCO₃

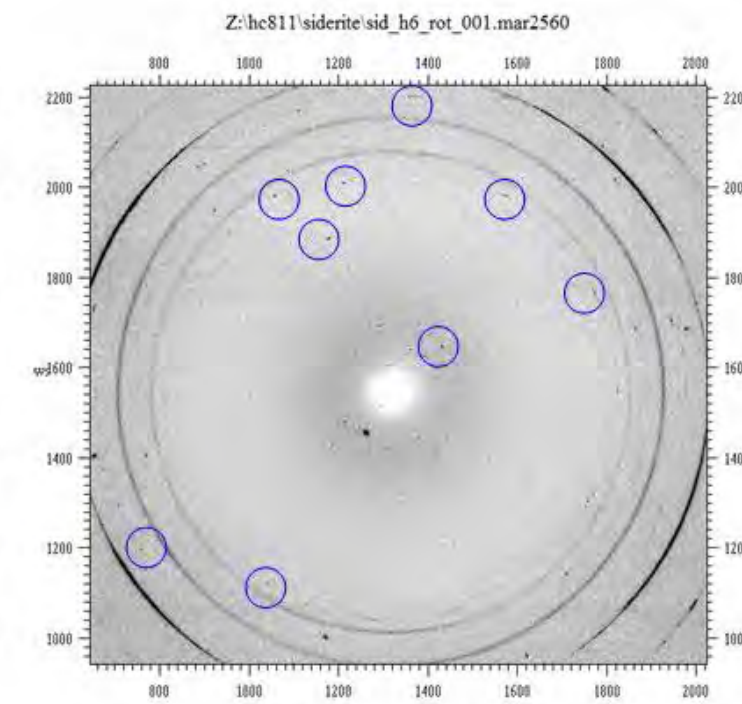
(Experiment with L. Dubrovinsky,
In-situ laser heating single crystal)

1Mbar, start heating



Low pressure FeCO₃

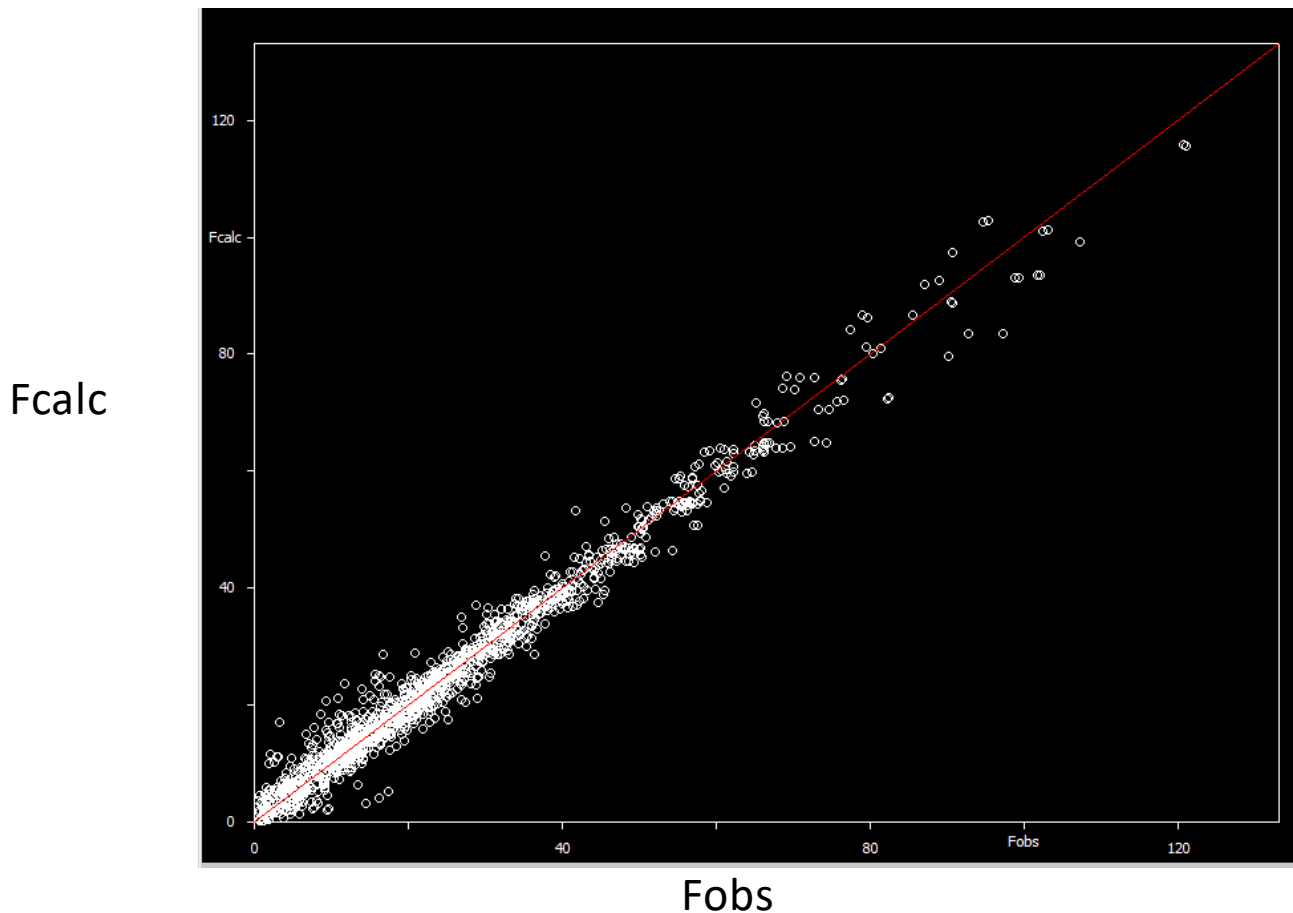
1 Mbar, 2500 K



New single crystal diffraction of
high pressure Fe-carbonate
single crystal

Fe₄C₃O₁₂

Dataset collected at 1Mbar and ambient T

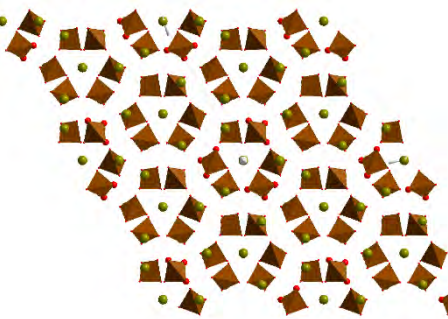


1116 obs

151 refined parameters

R(obs) 7 %

R(all) 8 %



Solved and refined in P1,
pseudo symmetry
elements which suggests
possible HT R3c
symmetry

```
|R factors : [1338=1116+222/151], Damping factor: 0.9000
|GOF(obs)= 4.44 GOF(all)= 4.03
|Number of reflections excluded due to refinement options: 22+0
|R(obs)= 6.94 wR(obs)= 7.22 R(all)= 8.03 wR(all)= 7.27
|Last wR(all): 7.27
|Maximum change/s.u. : 0.0083 for z[C2]
```

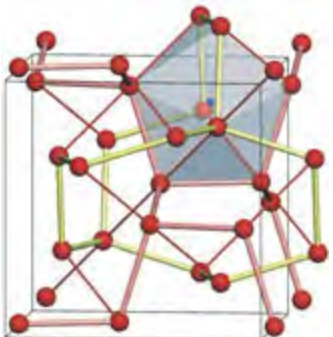
Complex structures of metals @ High Pressure

Letters to Nature

Nature **408**, 174–178 (9 November 2000) | doi:10.1038/35041515; Received 22 May 2000; Accepted 20 September 2000

New high-pressure phases of lithium

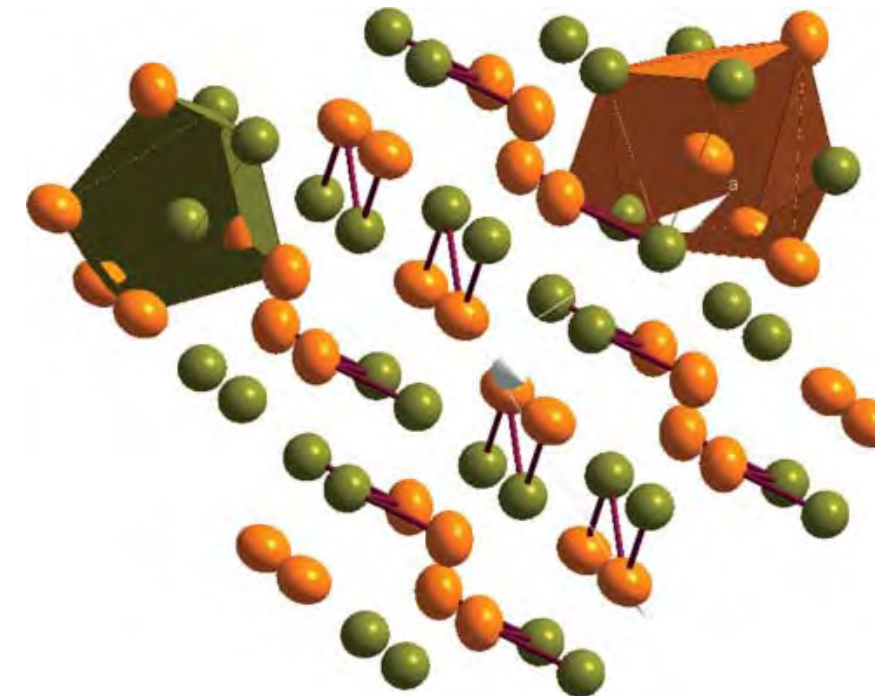
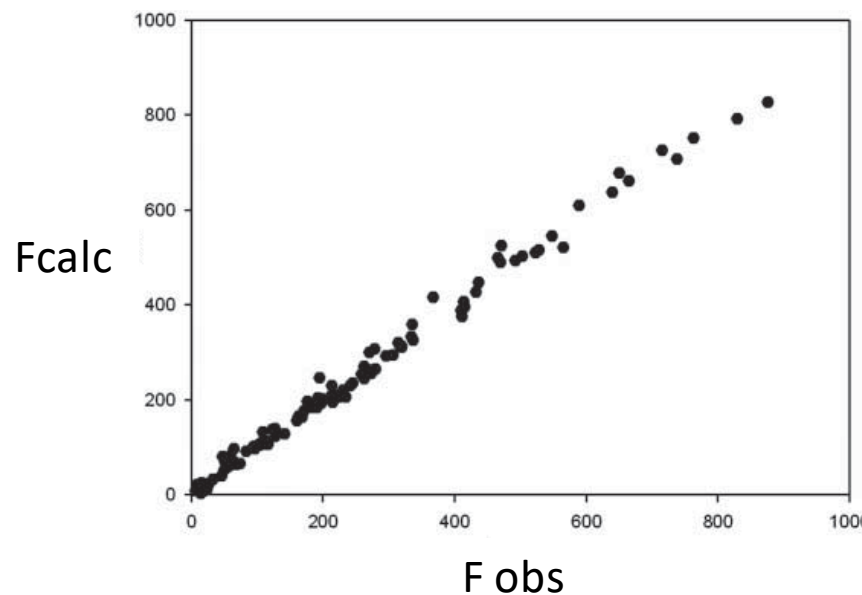
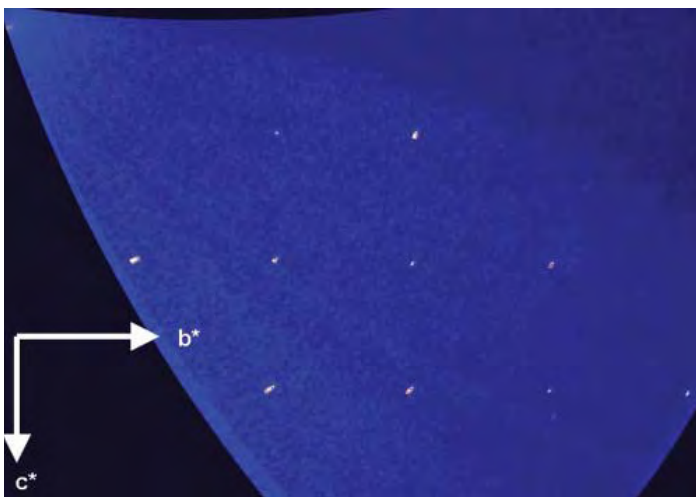
M. Hanfland¹, K. Syassen², N. E. Christensen³ & D. L. Novikov⁴



atomic cores. It was recently predicted¹ that at pressures below 100 GPa, dense Li may undergo several structural transitions, possibly leading to a 'paired-atom' phase with low symmetry and near-insulating properties. Here we report synchrotron X-ray diffraction measurements that confirm that Li undergoes pronounced structural changes under pressure. Near 39 GPa, the element transforms from a high-pressure face-centred-cubic phase, through an intermediate rhombohedral modification, to a cubic polymorph with 16 atoms per unit cell. This cubic phase has not been observed previously in any element; unusually, its

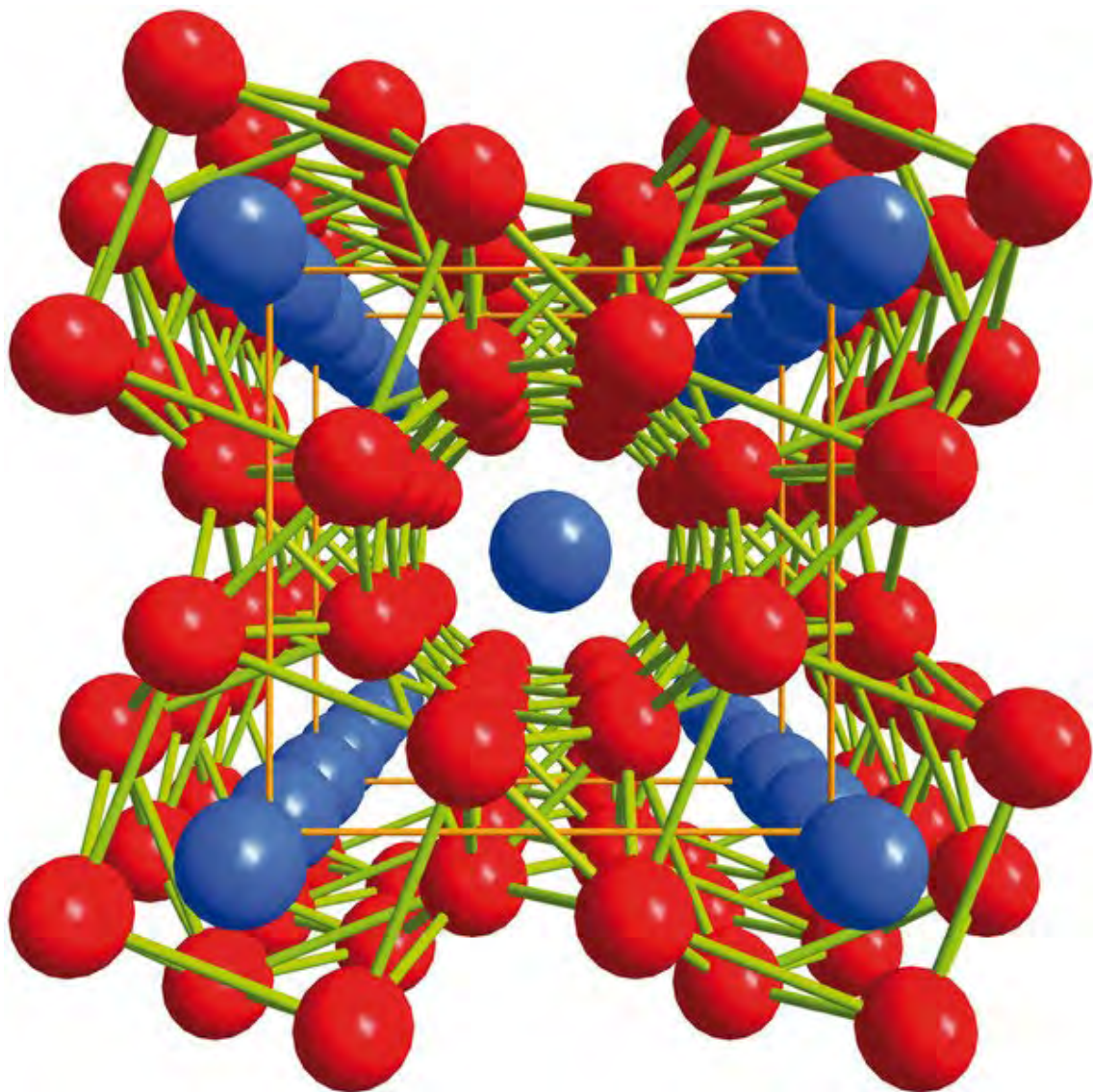
The predictions by Neaton and Ashcroft¹ are in sharp contrast to intuitive expectation that the application of hydrostatic pressure favours high-coordination crystal structures with metallic properties. In their theoretical simulations of dense Li, which are based on first principles band structure theory, they compare the relative stability of a number of crystal structures common among elemental solids. Their results clearly indicate a strong preference of dense Li to form low-symmetry structures. Therefore, experiments aimed at structure determinations of compressed Li are highly desirable. Furthermore, experimental high-pressure studies of Li are of fundamental interest, because they are expected to reveal new aspects relevant for the theoretical modelling of other light elements, including hydrogen², at high density.

Na oP8 structure determined at 118 GPa



MnP type structure

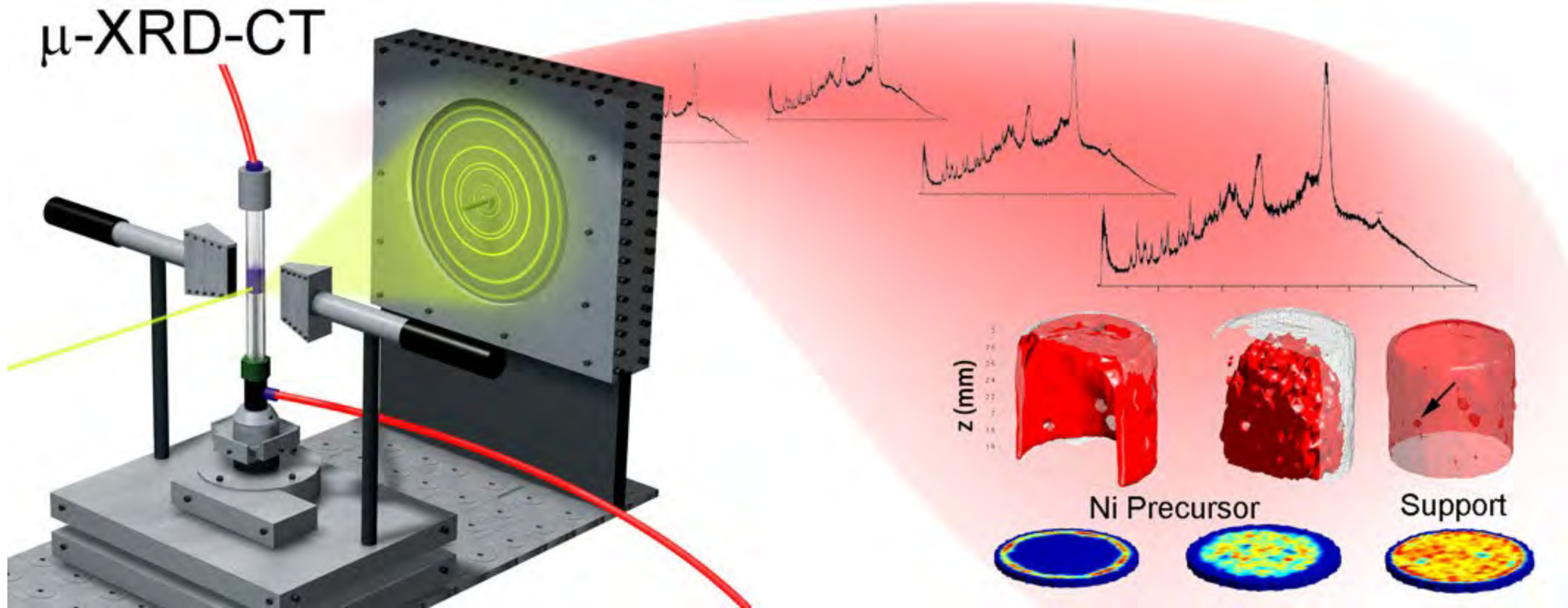
Single atomic species, but
binary compound type
structure



Na – host-guest structure $P > 125$ GPa

- Single crystal diffraction on crystals with size down to $0.005 \times 0.005 \times 0.005$ mm (almost routine) and even less
- Possibility to have structural information from single crystal data at non ambient conditions, not only with static measurements (i.e high pressure) but also during dynamic processes (i.e. variable magnetic field, temperature, etc) on second time scale

3) EXAMPLE: Diffraction tomography



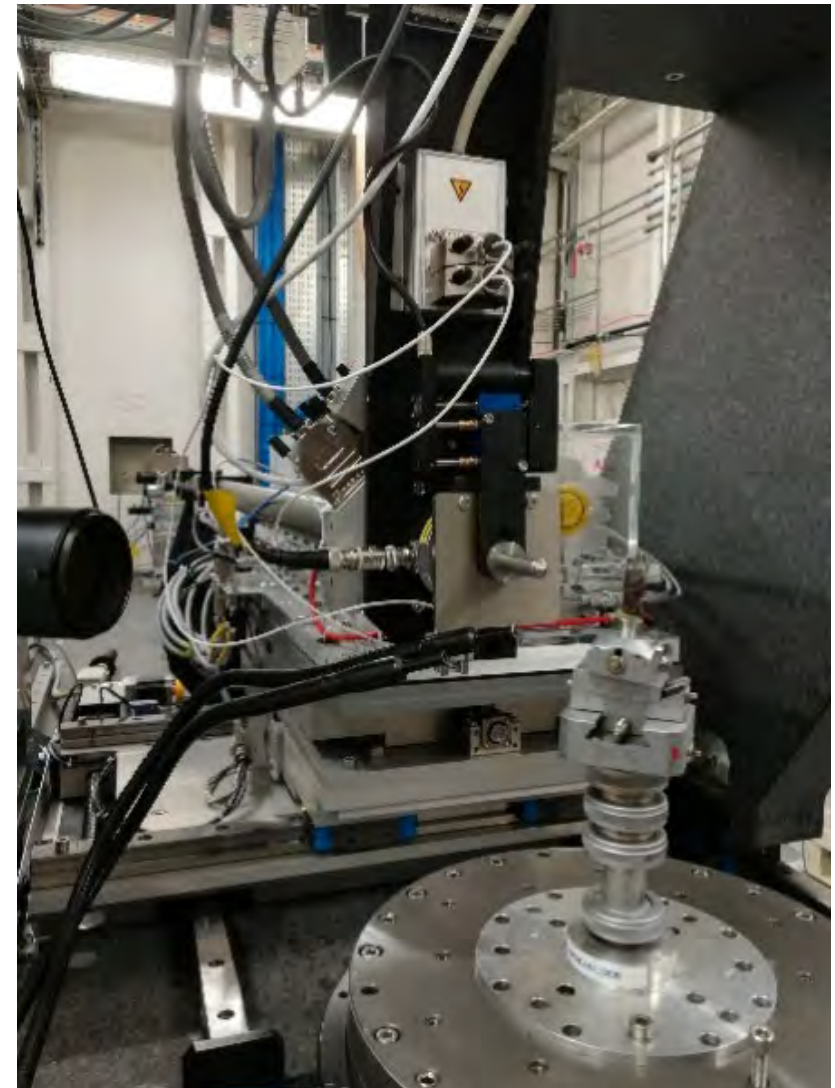
ESRF, ID15A

Courtesy of Marco Di Michiel

Experimental setup

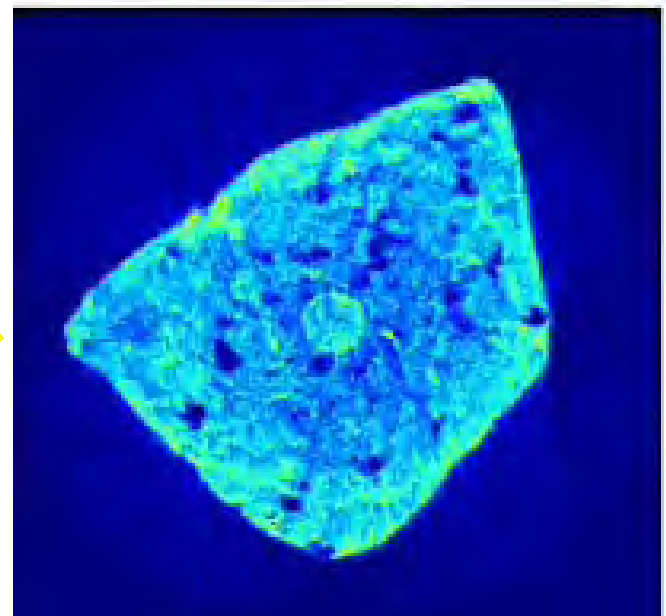
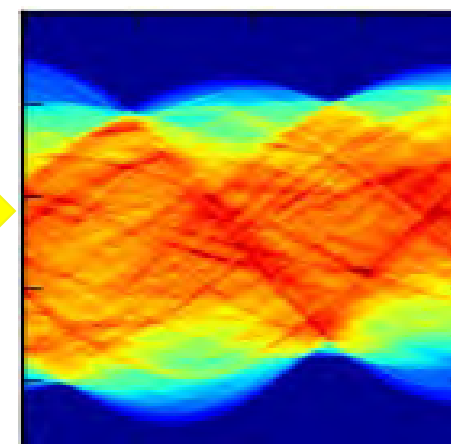
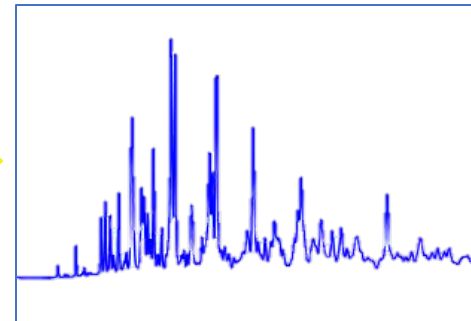
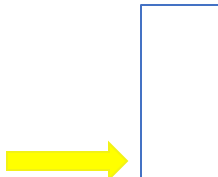
| Energy | 90 KeV |
|-----------------------------|---------------------|
| (λ) | 0.137 Angstrom |
| Sample to detector distance | 1.00/1.40 m |
| Data collection | Continuous rotation |

- Monochromatic beam
- Continuous translation and rotation of the sample
- Diffraction data collection during translation and rotation

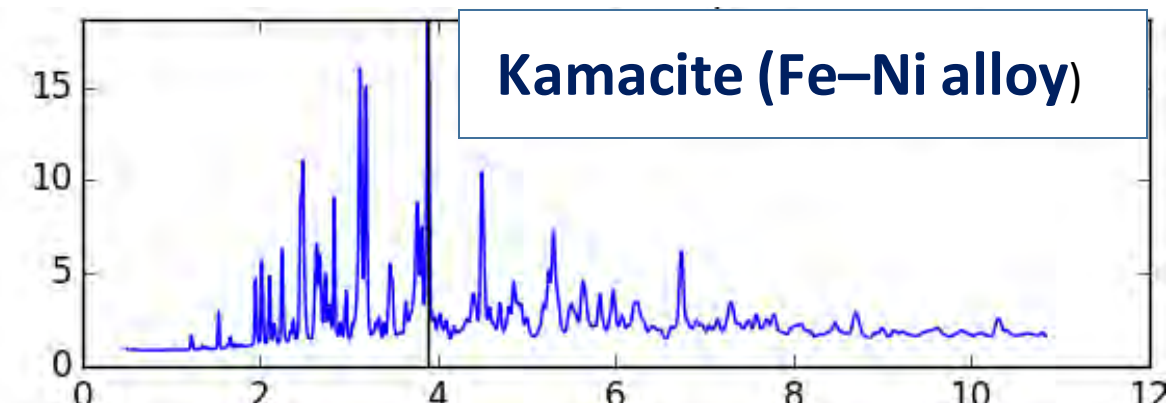
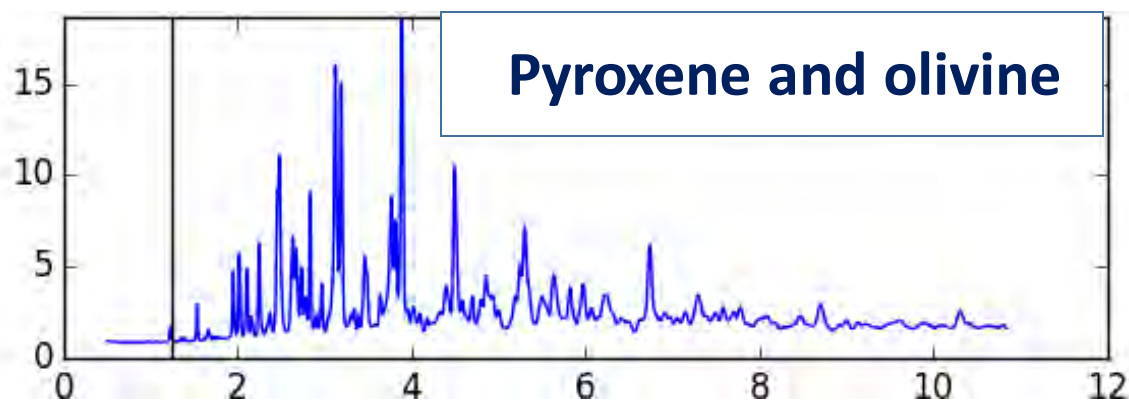
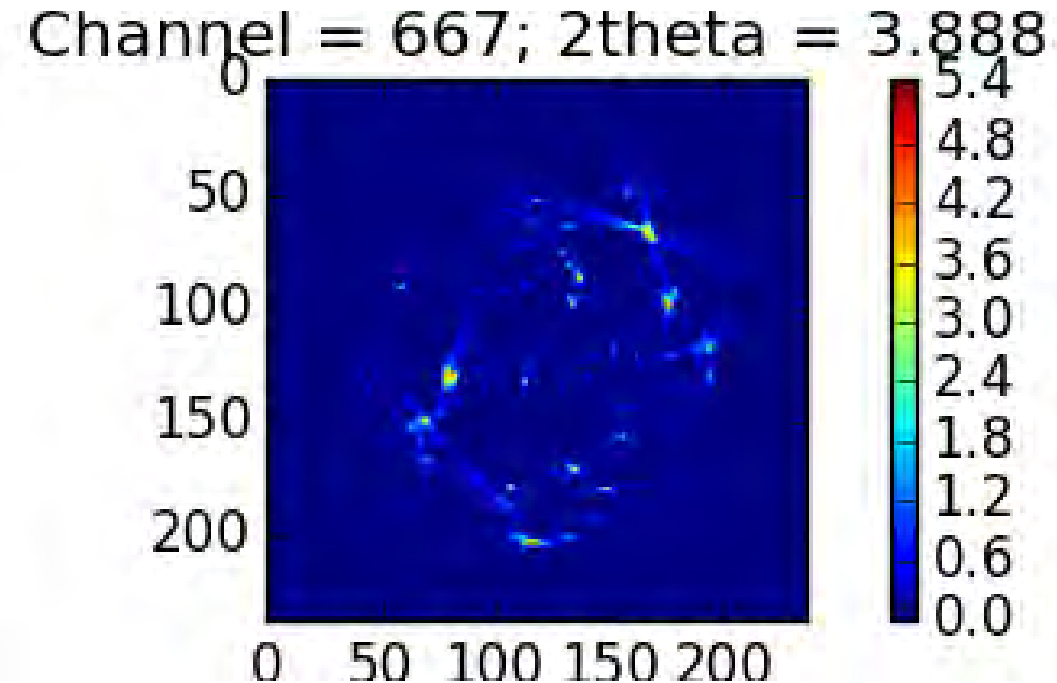
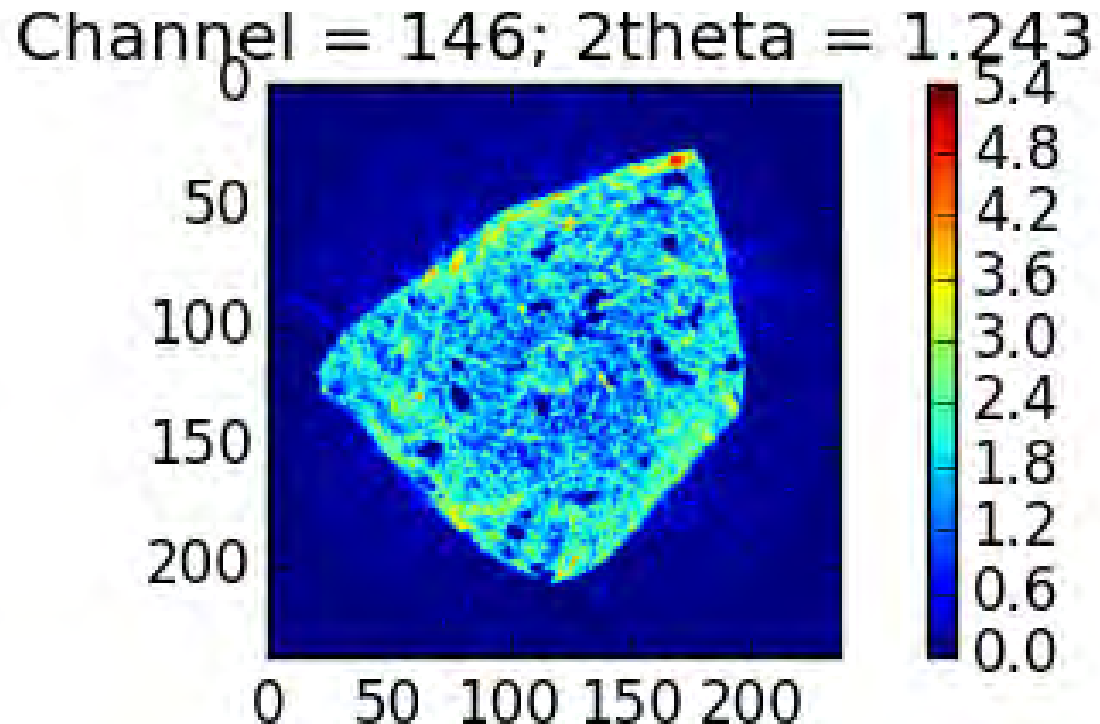


COSA SI OTTIENE?

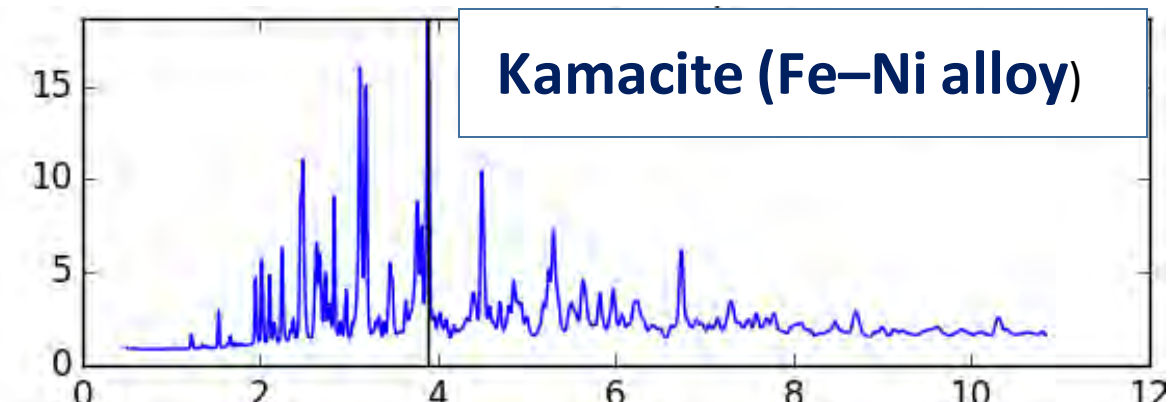
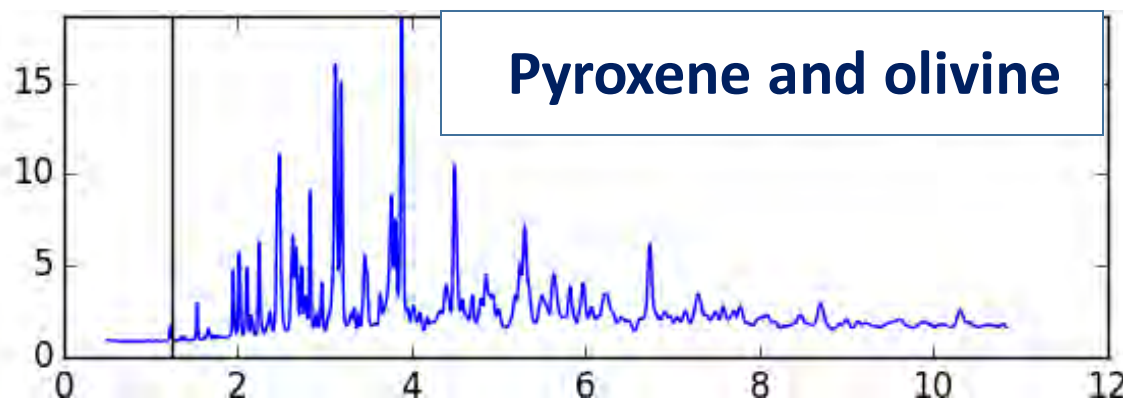
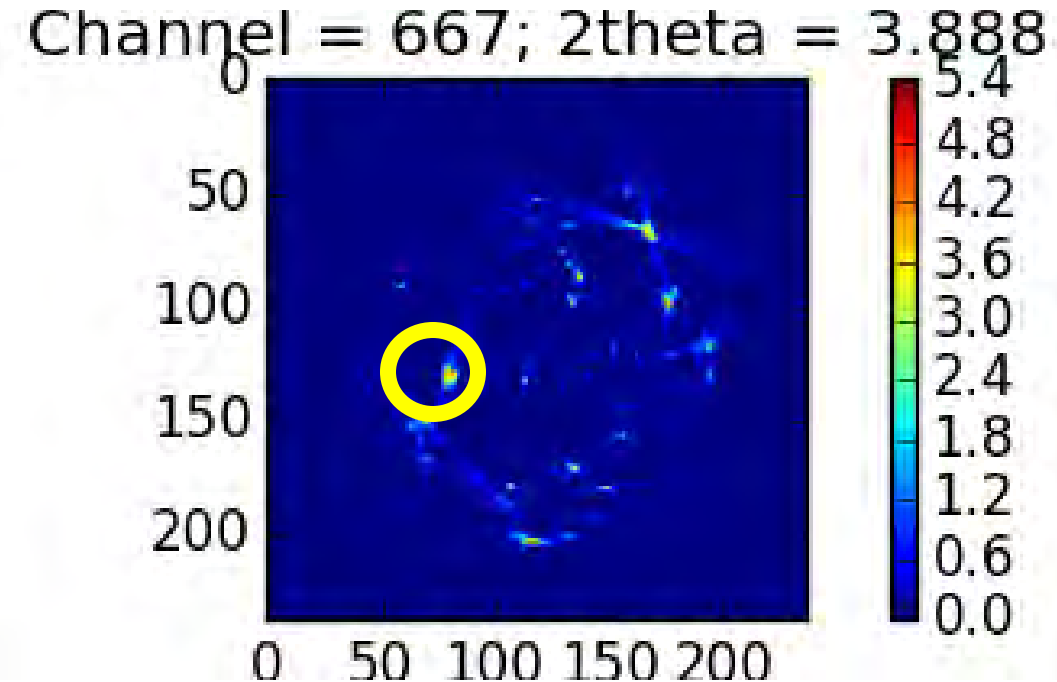
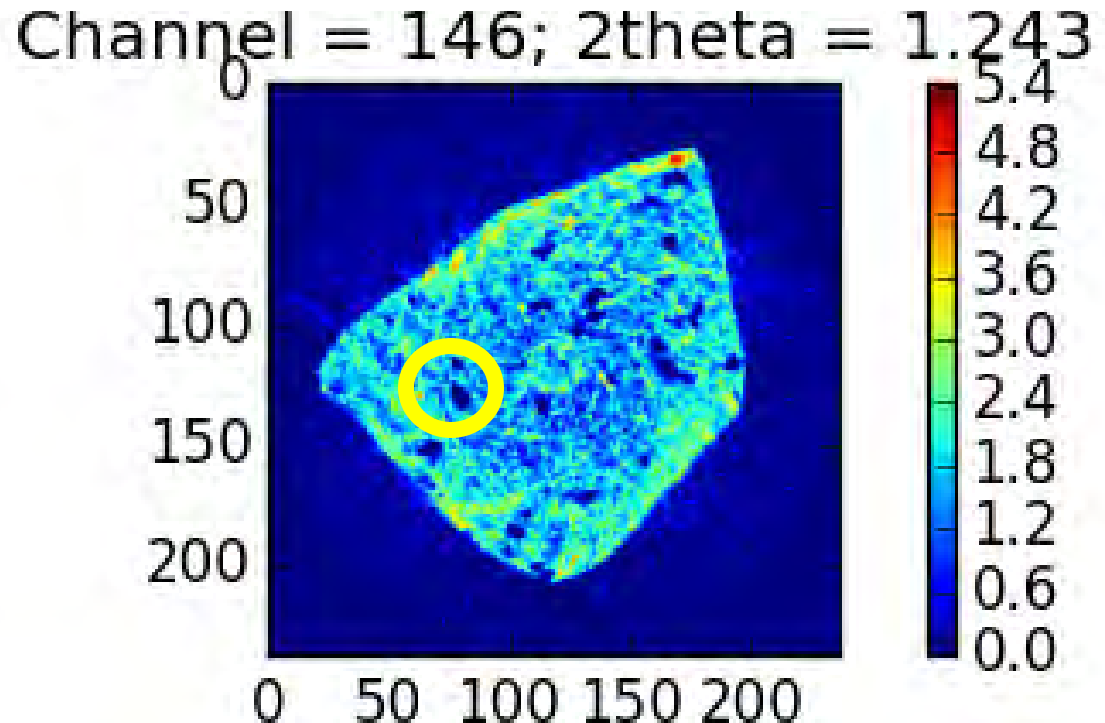
- 2D diffraction
- Integration → from 2D to 1D powder pattern
- «Elaboration» of pattern (synogram)
- «Slices»



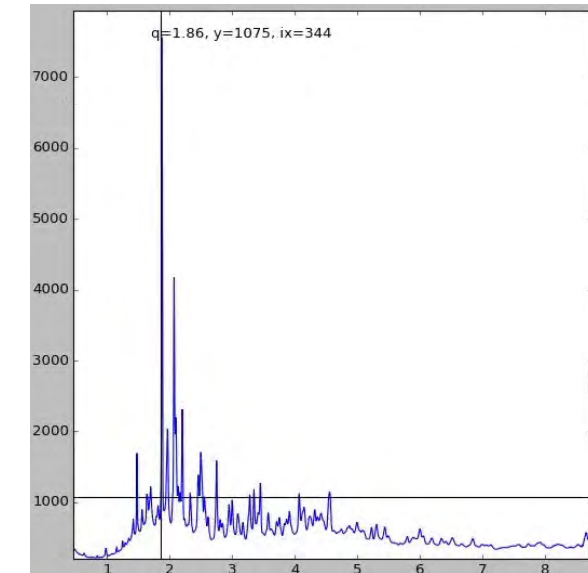
METEORITE from museum collection



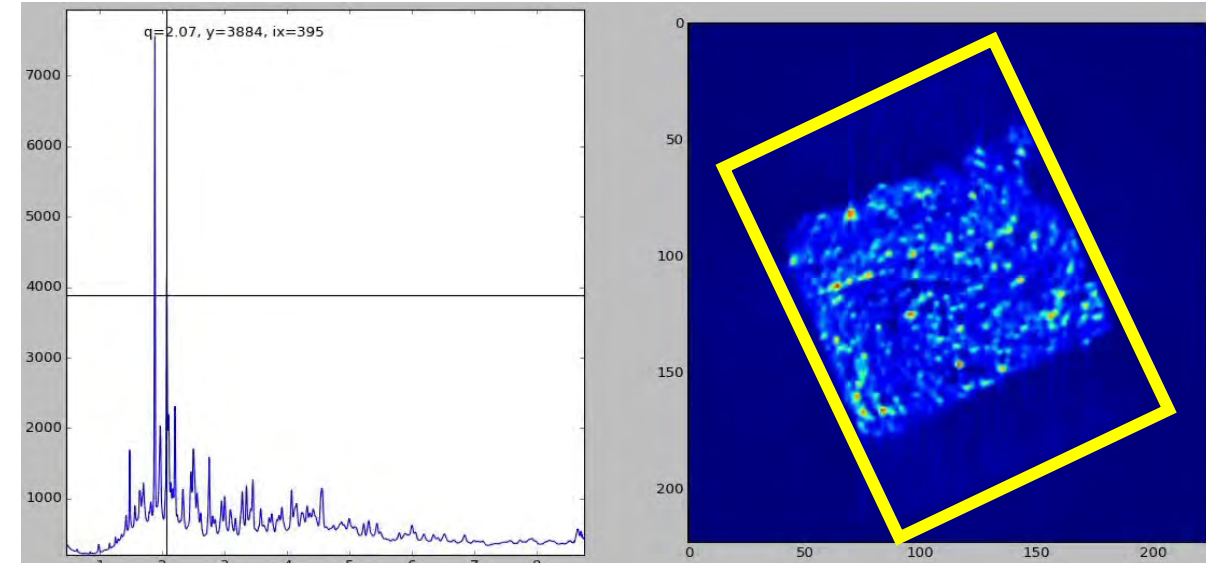
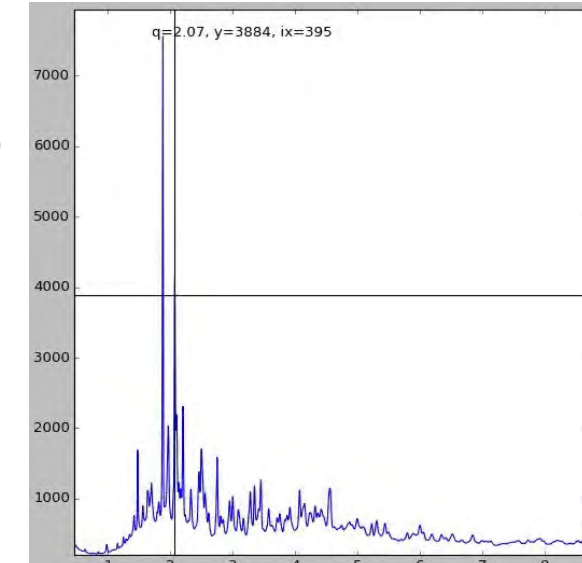
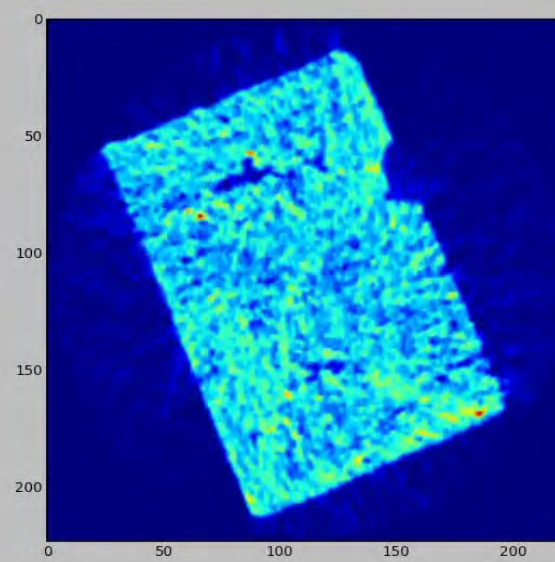
METEORITE from museum collection



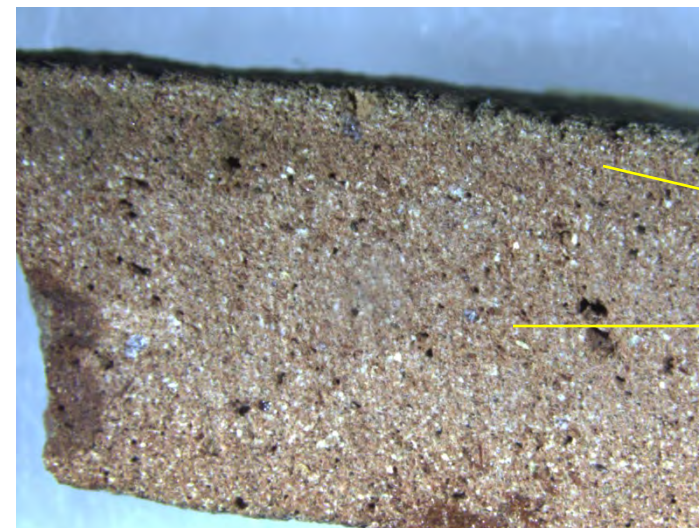
Archaeological sample: ceramic from northern Africa, Roman period (apx. 2000 year ago)



Quartz (SiO_2)

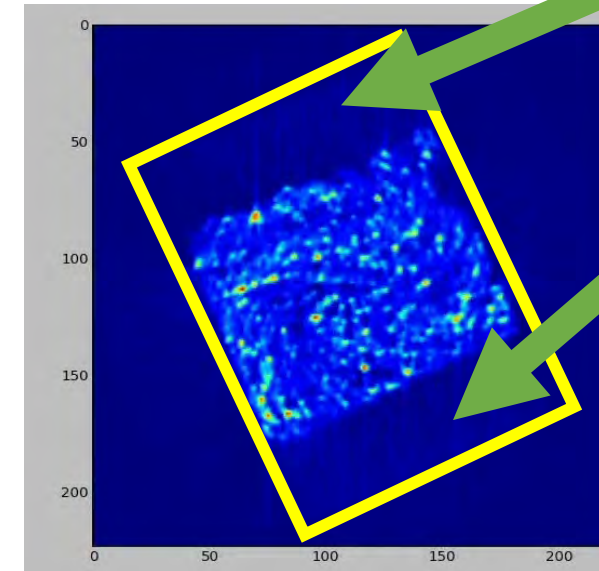
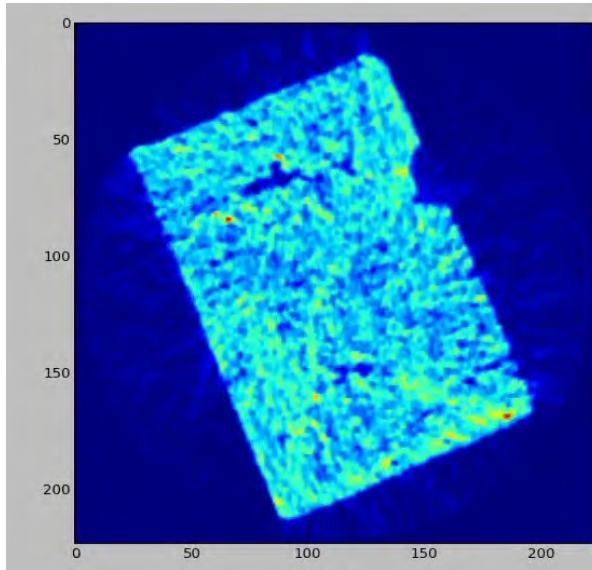


Calcite (CaCO_3)



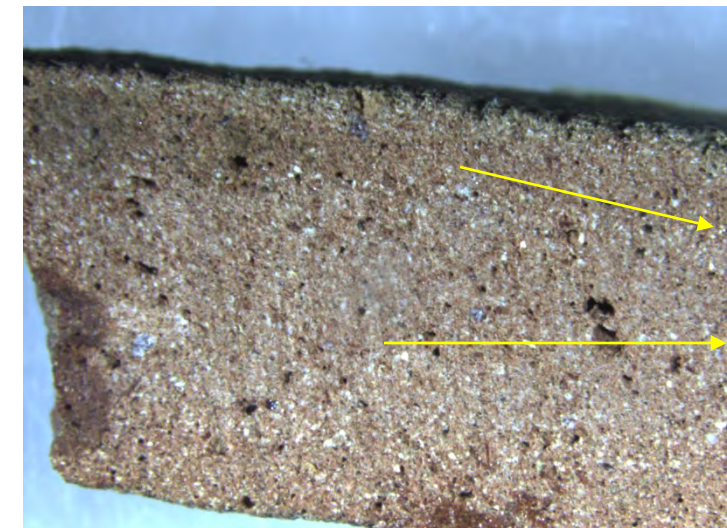
Different
granulometry
and calcite
distribution

Archaeological sample: ceramic from northern Africa, Roman period (apx. 2000 year ago)



Quartz (SiO_2)

Missing calcite in external portion
of ceramic:
«Sandwich» preparation
With different clay composition



Different
granulometry
and calcite
distribution

**Single-crystal diffraction at the Extreme Conditions beamline
P02.2: procedure for collecting and analyzing high-pressure
single-crystal data**

André Rothkirch, G. Diego Gatta, Mathias Meyer, Sébastien Merkel,
Marco Merlini and Hanns-Peter Liermann

Commercial softwares (i.e. scientists and engineer working full time for software development, maintenance and upgrades) for single crystal data reduction from area detectors work much better than in-house written codes

XDS, CrysAlis, etc... are normally available at synchrotron beamlines and universities/research center

J. Synchrotron Rad. (2013). **20**, 711–720

PETRA III, DESY, is presented. A new data image format called ‘Esperanto’ is introduced that is supported by the commercial software package *CrysAlis^{Pro}* (Agilent Technologies UK Ltd). The new format acts as a vehicle to transform the most common area-detector data formats *via* a translator software. Such a conversion tool has been developed and converts tiff data collected on a Perkin Elmer detector, as well as data collected on a MAR345/555, to be imported into the *CrysAlis^{Pro}* software. In order to demonstrate the validity of the new